Molecular Signatures of Zika Virus Infection: Insights into Host Transcriptomic and microRNA Responses in Human Cell Models

Doctoral thesis

to obtain a doctorate (PhD)

from the Faculty of Medicine

of the University of Bonn

Denna Tabari

from Saarbrücken, Germany

2026

Written with authorization of

the Faculty of Medicine of the University of Bonn

First reviewer: Prof. Dr. Julia Stingl

Second reviewer: Prof. Dr. Ulrich Jaehde

Day of oral examination: 02.02.2026

From the Federal Institute for Drugs and Medical Devices

For my parents, Parvin and Amir,

with gratitude for all they made possible

Table of Contents

List of Abbreviations

ADE	Antibody-Dependent Enhancement
ANOVA	Analysis of Variance
ARE	Antioxidant Response Element
AXL	AXL receptor tyrosine kinase
BSA	Bovine Serum Albumin
C	Capsid
CD95	Cluster of Differentiation 95
cDNA	Complementary DNA
CNS	Central Nervous System
Ct	Cycle Threshold
CZS	Congenital Zika Syndrome
DC-SIGN	Dendritic Cell-Specific Intercellular adhesion molecule-3-Grabbing Non-integrin
DENV	Dengue Virus
DICER	Endoribonuclease Dicer
DAPI	4',6-Diamidino-2-Phenylindole
DMEM	Dulbecco's Modified Eagle's Medium
DNP	2,4-Dinitrophenyl
DNPH	2,4-Dinitrophenylhydrazine
DNA	Deoxyribonucleic Acid
DGCR8	DiGeorge Syndrome Critical Region 8
E	Envelope

EGF	Epidermal Growth Factor
EGFR	Epidermal Growth Factor Receptor
ER	Endoplasmic Reticulum
ESCRT	Endosomal Sorting Complex Required for Transport
EV	Extracellular Vesicle
FBS	Foetal Bovine Serum
FGF7	Fibroblast Growth Factor 7
FGFR	Fibroblast Growth Factor Receptor
FOXC1	Forkhead Box C1
FOXO	Forkhead Box O
GAPDH	Glyceraldehyde 3-Phosphate Dehydrogenase
GBS	Guillain-Barré Syndrome
GCL	Glutamate-Cysteine Ligase
GEO	Gene Expression Omnibus
GO	Gene Ontology
GSK3B	Glycogen Synthase Kinase 3 Beta
GST	Glutathione S-Transferase
hNSCs	Human Neural Stem Cells
HCV	Hepatitis C Virus
HESCs	Human Embryonic Stem Cells
HRS	Hepatocyte Growth Factor-Regulated Tyrosine Kinase Substrate
IFN	Interferon
IFIT	Interferon-Induced Protein with Tetratricopeptide Repeats

IFIH1	Interferon-Induced Helicase C-Domain-Containing Protein 1
IFNL	Interferon Lambda
IFI44L	Interferon-Induced Protein 44-Like
IL	Interleukin
iPSC	Induced Pluripotent Stem Cells
ISG	Interferon-Stimulated Gene
JEV	Japanese Encephalitis Virus
JUN	Jun Proto-Oncogene
Keap1	Kelch-like ECH-associated Protein 1
kb	Kilobase pairs
lt-NES®	Long-Term Self-Renewing Neuroepithelial-Like Stem Cells
M	Membrane Protein
MAPK	Mitogen-Activated Protein Kinase
miRNA	MicroRNA
miRISC	miRNA-Induced Silencing Complex
mRNA	Messenger RNA
MOI	Multiplicity of Infection
MVBs	Multivesicular Bodies
mTORC1	Mechanistic Target of Rapamycin Complex 1
mAb	Monoclonal Antibody
NF-kB	Nuclear Factor kappa-light-chain-enhancer of activated B cells
NPC	Neuronal Progenitor Cells
NQO1	NAD(P)H Quinone Dehydrogenase 1

Nrf2	Nuclear Factor Erythroid 2-Related Factor 2
NS	Non-Structural Protein
ORF	Open Reading Frame
OTUD4	OTU Deubiquitinase 4
PBS	Phosphate-Buffered Saline
PCR	Polymerase Chain Reaction
PFU	Plaque Forming Unit
PHEIC	Public Health Emergency of International Concern
Pi3K	Phosphatidylinositol 3-Kinase
PKD1L2	Polycystin 1-Like 2
PLK1	Polo-Like Kinase 1
PPP1R15A	Protein Phosphatase 1 Regulatory Subunit 15A
prM	Precursor Membrane Protein
PRDM16	PR Domain Zinc Finger Protein 16
qRT-PCR	Quantitative Reverse Transcription Polymerase Chain Reaction
RF	Replication Factories
RNA	Ribonucleic Acid
RPL27	Ribosomal Protein L27
ROS	Reactive Oxygen Species
SD	Standard Deviation
SDS	Sodium Dodecyl Sulfate
SDS-PAGE	Sodium Dodecyl Sulfate Polyacrylamide Gel Electrophoresis
SEM	Standard Error of the Mean

SESN2	Sestrin 2
sMaf	Small Musculoaponeurotic Fibrosarcoma Proteins
SLC2A1	Solute Carrier Family 2 Member 1
STAT1	Signal Transducer and Activator of Transcription 1
STAMBP	STAM-Binding Protein
TAM	Tyro3, Axl, and Mer receptor family
TIM-1	T-cell Immunoglobulin and Mucin Domain 1
TRIB3	Tribbles Pseudokinase 3
TUBA1A	Tubulin Alpha 1A
UPR	Unfolded Protein Response
UTR	Untranslated Region
WHO	World Health Organization
WNV	West Nile Virus
XBP1	X-Box Binding Protein 1
YFV	Yellow Fever Virus
ZIKV	Zika Virus

1. Introduction

1.1 Zika Virus: Molecular Virology

Zika virus (ZIKV) is a positive-sense RNA virus with a 10.8 kilobase (kb) genome that comprises a single open reading frame (ORF) flanked by two structured untranslated regions (UTR). The single viral polyprotein encoded by the ORF is processed by host and viral proteases into three structural proteins (capsid (C), precursor of membrane/membrane (prM/M) and envelope (E) and seven non-structural proteins (NS1, NS2A, NS2B, NS3, NS4A, NS4B and NS5). The non-structural proteins are involved in viral replication, assembly, and suppression of the host's antiviral response.

The structural proteins form the virus particle. The C protein builds the nucleocapsid, which protects the viral genome. The outer membrane of the virion consists of a lipid bilayer containing the E and M proteins. The E protein mediates cellular attachment, entry and fusion and serves as the main target of neutralizing antibodies (Dai et al. 2016; Sirohi et al. 2016; Sirohi and Kuhn 2017).

Zika virus exhibits a broad cellular tropism, infecting a wide range of cell types including dermal fibroblasts, epidermal keratinocytes, neuronal progenitor cells, placental and testicular cells, as well as immune cells like dendritic cells and macrophages (Cugola et al. 2016; Hamel et al. 2015a; Mansuy et al. 2016; Miner et al. 2016; Miner and Diamond 2017a). This broad tropism is attributed to ZIKV's interactions with specific cellular receptors that facilitate viral entry (Hamel et al. 2015a; Meertens et al. 2017; Miner and Diamond 2017a; Richard et al. 2017).

The entry of ZIKV into host cells is initiated by the attachment of E protein to specific cellular receptors. The primary receptors identified for ZIKV are members of the Tyro3-AXL-MER (TAM) receptor family, with AXL recognized as a predominant factor (Hamel et al. 2015a). However, studies in mice have shown that ZIKV can infect cells independently of TAM receptors, indicating alternative entry mechanisms (Hastings et al. 2017; Z.-Y. Wang et al. 2017). Additionally, C-type lectins such as Dendritic Cell-Specific Intercellular adhesion molecule-3-Grabbing Non-integrin (DC-SIGN) and the T-cell immunoglobulin mucin (TIM) family are implicated in ZIKV binding (Hamel et al. 2015a). Recent findings indicate a relevant role for the epidermal growth factor receptor (EGFR) in viral entry (Sabino et al. 2021). ZIKV enters the cell through clathrin-mediated endocytosis

(Owczarek et al. 2019). Inside the endosome, the acidic environment triggers conformational changes in the E protein, promoting membrane fusion and release of the nucleocapsid into the cytoplasm (Kaufmann and Rossmann 2010; Persaud et al. 2018). Upon entry, viral RNA translation occurs at the surface of the endoplasmic reticulum (ER), resulting in the formation of a polyprotein, which is then cleaved into structural and non-structural proteins (Barrows et al. 2019; Reid et al. 2018). The replication process involves reorganization of the ER, forming specialized replication factories (RFs) where viral RNA is synthesized. During replication, these RFs also recruit membranous components from other organelles, such as autophagosomes, to optimize viral replication (Chiramel and Best 2018; Cortese et al. 2017; Hamel et al. 2015a). The replication complex synthesizes a complementary RNA strand, serving as a template for generating multiple viral genomes. During the assembly phase, the newly synthesized RNA associates with capsid proteins and prM-E heterodimers, resulting in the budding of immature viral particles into the ER lumen (Barnard et al. 2021; X. Zhang et al. 2019). These particles subsequently mature as they pass through the Golgi apparatus, where a furin protease cleaves the pr peptide. The mechanisms of ZIKV release are less well understood (L. Li et al. 2008; Sager et al. 2018). Evidence suggests that virions leave the cell within vesicular carriers that may contain one or more particles (Sager et al. 2018). These carriers then fuse with the plasma membrane, releasing either free viral particles or virions that are enclosed within secreted vesicles. The presence of ZIKV in extracellular vesicles (EVs) is particularly relevant, as this mode of release can protect the virus from neutralising antibodies and facilitate its spread across restrictive barriers, such as the placenta and the blood-brain barrier (Martínez-Rojas et al. 2025). The origin of these vesicles appears to be heterogeneous and involves secretory autophagy and exosomal pathways. In some cases, there is overlap, such as in amphisome formation. The dominant route of release can vary depending on the infected cell type, highlighting the capacity of ZIKV to exploit different secretory pathways across cell types (Martínez-Rojas et al. 2025; Sager et al. 2018).

1.2 Historical Background and Global Emergence of Zika Virus

Zika virus was first isolated in 1947 from the blood of a rhesus monkey during studies investigating yellow fever transmission in Uganda's Zika Forest, from which the virus

derives its name (G. W. Dick 1953; G. W. A. Dick et al. 1952) . Prior to 2007, Zika virus infection was not considered a significant public health threat, with only 14 documented cases worldwide, including 13 natural infections and one laboratory acquired infection (Wikan and Smith 2016). The virus had been isolated sporadically from mosquitoes and humans in sub-Saharan Africa and Southeast Asia, and interest in it was limited to a small group of specialized researchers. As a result, ZIKV was neglected by the wider scientific community for over 50 years (Jamrozik and Selgelid 2018; Sarkar and Gardner 2016).

This view changed after the 2007 outbreak on the island of Yap in Micronesia, which marked the beginning of increasingly frequent Zika outbreaks (Duffy et al. 2009; Lanciotti et al. 2008). In 2013, the virus caused a significant outbreak in French Polynesia, where it was first linked to severe complications like Guillain-Barré Syndrome (GBS) and neurodevelopmental disorders, including microcephaly (Cao-Lormeau et al. 2014, 2016; Cauchemez, Besnard, Bompard, Dub, Guillemette-Artur, Eyrolle-Guignot, Salje, Kerkhove, et al. 2016; Oehler et al. 2014). Until this point, Zika infections were typically associated with mild symptoms, such as fever, muscle pain, conjunctivitis, headache, and rash, lasting 3–5 days, with no reported hospitalizations or fatalities (Azevedo et al. 2016; Duffy et al. 2009; Lanciotti et al. 2008; Paniz-Mondolfi et al. 2016; Rodriguez-Morales 2015).

By 2013, ZIKV had reached Latin America, and a major outbreak in Brazil in 2015 drew global attention due to its association with microcephaly in newborns (Faria et al. 2016; Schuler-Faccini et al. 2016; Zanluca et al. 2015; Q. Zhang et al. 2017). It is possible that ZIKV had been circulating in Brazil earlier but went undetected, as infections are often asymptomatic and symptomatic cases are typically mild. Moreover, in endemic regions the clinical picture, characterised by fever, rash, arthralgia, and headache, overlaps with that of other arboviral infections like dengue (DENV) and chikungunya virus (CHIKV) (Azevedo et al. 2016; Duffy et al. 2009; Lanciotti et al. 2008; Paniz-Mondolfi et al. 2016; Rodriguez-Morales 2015).

As ZIKV spread across the Americas and beyond, numerous cases were also documented in non-endemic regions, primarily attributed to travelers carrying the virus from affected areas. These cases were reported in several European countries, the United States, and other countries such as Japan, Canada, China, and Australia (Canada 2023b; CDC 2024a; De Smet et al. 2016; Díaz-Menéndez et al. 2018; Duijster et al. 2016;

Kutsuna 2017; Maria et al. 2016; Nicastri, Pisapia, et al. 2016; Pyke et al. 2016; Yin et al. 2016; Zé-Zé et al. 2016).

In response to the growing concern, especially about the risk of birth defects, many countries issued travel advisories specifically warning pregnant women against travel to affected regions (Canada 2023a; CDC 2024b, 2024f).

In February 2016, the World Health Organization (WHO) declared ZIKV a Public Health Emergency of International Concern (PHEIC) as a result of its rapid spread and the severe impact on newborns, particularly in Brazil, where between 440,000 and 1.3 million infections were reported during the outbreak (ECDC 2015; Heymann et al. 2016). Retrospective analysis of the 2013 outbreak in French Polynesia also linked previously unassociated cases of microcephaly to ZIKV infection (Cauchemez, Besnard, Bompard, Dub, Guillemette-Artur, Eyrolle-Guignot, Salje, Van Kerkhove, et al. 2016).

The 2013 and 2015 outbreaks brought the first documented associations between ZIKV and more severe complications like GBS and congenital abnormalities (Calvet et al. 2016; Driggers et al. 2016; Mlakar et al. 2016; Oehler et al. 2014). The 2016 PHEIC lasted for eight months before being lifted due to a decline in reported ZIKV cases (WHO 2016). After the major epidemic, only a few smaller outbreaks occurred in countries such as Cuba and Angola (Grubaugh et al. 2019; Hill et al. 2019). ZIKV transmission continued to decline, with the number of cases decreasing by 2017. However, new cases have continued to appear sporadically, including an increase in India in 2021, where 237 cases were reported by December, mostly in the state of Kerala (Fleiss 2021; WHO 2022). Brazil continues to report ZIKV infections, including both symptomatic and asymptomatic cases, indicating that the virus maintains low level circulation (da Conceição et al. 2022).

Overall, mapping ZIKV transmission has revealed that a total of 92 countries and territories have been affected since it emerged (WHO 2024) (Figure 1).

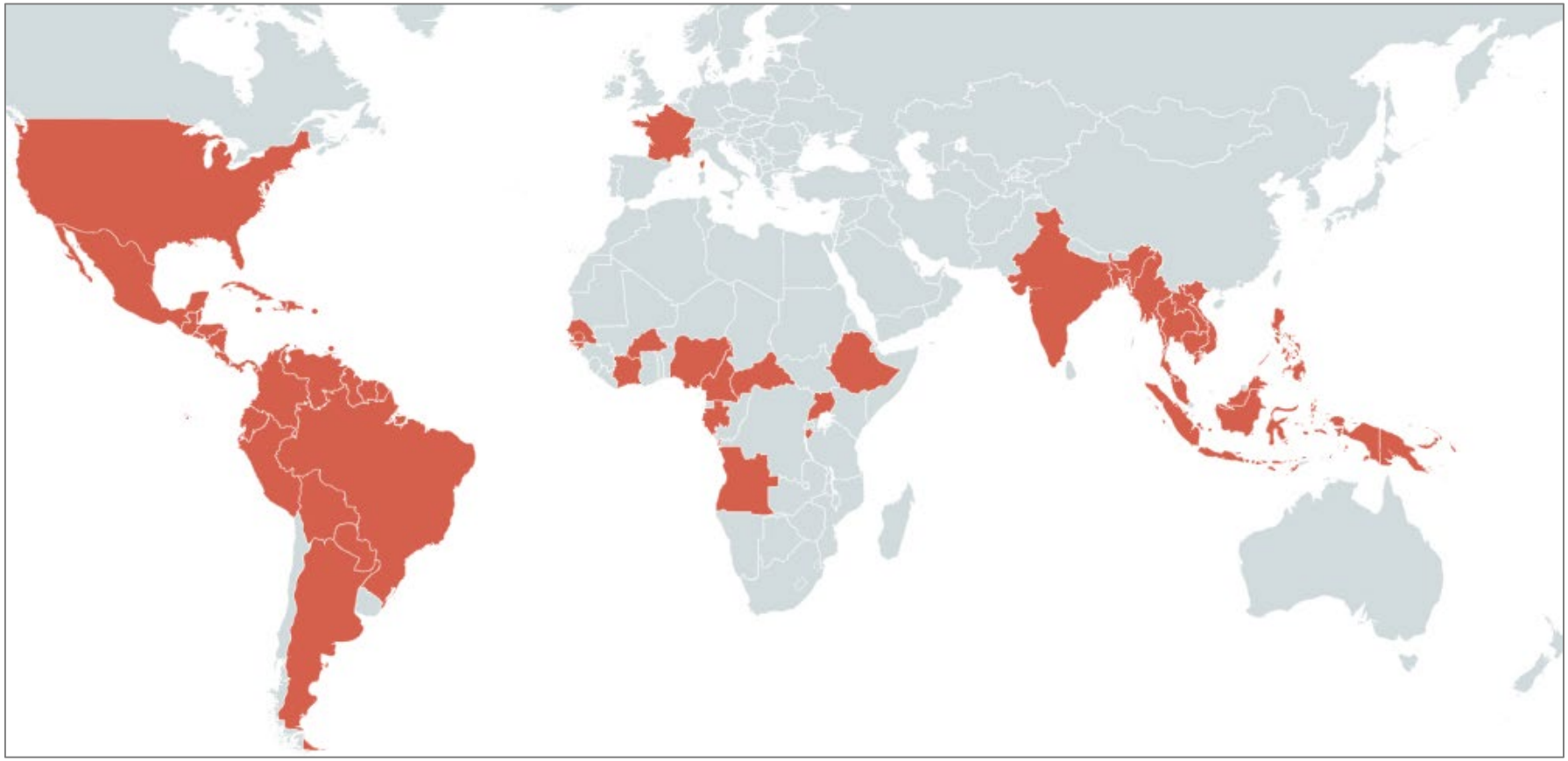

Figure 1. Countries and Territories With Current or Past Zika Virus Transmission.
Countries marked in red indicate documented Zika virus transmission, either through local outbreaks or confirmed cases, from the time of its discovery to recent years. The map reflects the global spread of the virus across Africa, Asia, the Americas, and parts of Europe. Map created with mapchart (mapchart.net 2025).

1.3 Taxonomy and Classification

Zika virus belongs to the family *Flaviviridae* and the genus *Flavivirus*, which includes other highly pathogenic viruses such as dengue (DENV), West Nile (WNV), Japanese encephalitis (JEV) and yellow fever virus (YFV) (Heinz and Stiasny 2017; Simmonds et al. 2017).

As ZIKV spread globally, the virus diversified into two main lineages - African and Asian (Alera et al. 2015; Haddow et al. 2012). The African lineage of ZIKV is divided into two distinct groups: the East African cluster, which includes the original isolated strain (MR766) and its genetic variants, and the West African cluster, comprising strains specific to that region, such as the Nigeria strain (Faye et al. 2014). Meanwhile, the Asian lineage includes all ZIKV strains from Southeast Asia, the Pacific Islands, and the American variants (Lanciotti et al. 2016). This division reflects the geographical and evolutionary divergence observed between these two lineages, with the Asian lineage representing a later spread of the virus outside of Africa. The ZIKV strains from the African and Asian lineages exhibit approximately 89% nucleotide sequence identity and 96.5% amino acid levels similarity (Lanciotti et al. 2008). Despite this high degree of genetic conservation, the African lineage has been rarely associated with human infections and has not been detected outside of Africa. No neurological complications have been reported in connection with this lineage. Notably, the Zika outbreak and cases of Congenital Zika Syndrome reported in Angola in 2016 were linked to the Asian lineage (Hill et al. 2019).

Although ZIKV had circulated in Africa for decades without any documented clinical relevance, it is unclear whether genetic change might have resulted in a greater capacity of neurovirulence or whether ZIKV has always been teratogenic and severe cases have not been documented before 2013 (Jaeger et al. 2019a; Meda et al. 2016; Tabari et al. 2020).

1.4 Transmission Mechanisms

Zika virus is an arbovirus transmitted primarily via two distinct cycles: the sylvatic and urban cycles (Jorge et al. 2020; Weaver et al. 2016). In the sylvatic cycle, ZIKV circulates between non-human primates and *Aedes* mosquitoes, while in the urban cycle, humans

are the primary hosts, with transmission mainly through *Aedes aegypti* and *Aedes albopictus*, which are adapted to urban environments (Chouin-Carneiro et al. 2016).

Transmission begins when an infected mosquito, typically *Aedes aegypti*, bites a human and introduces the virus through its saliva. During this process, keratinocytes, the predominant cells in the outer layer of the skin, are an early target of ZIKV. The virus replicates within the mosquito, accumulating in its salivary glands before being transmitted to new hosts through subsequent bites (Azar and Weaver 2019; Kim et al. 2019; Kramer and Ciota 2015). While *Aedes albopictus* can also transmit ZIKV and is widespread in temperate regions like North America and Europe, it plays a lesser role compared to *Aedes aegypti*, the principal vector in tropical and subtropical regions such as Africa, Asia, the Americas, and Oceania. *Aedes aegypti* is particularly prevalent in densely populated urban areas, making it a significant vector for ZIKV transmission (Gutiérrez-Bugallo et al. 2019; Kraemer et al. 2015; Vazeille et al. 2019). Other species, such as *Aedes polynesiensis*, have been linked to localized outbreaks, notably in French Polynesia (Oliveira Melo et al. 2016). However, *Aedes aegypti* remains the most important vector globally. As climate change and urbanization expand the habitats of these mosquitoes, the likelihood of future ZIKV outbreaks increases.

In addition to vector-borne transmission, several cases of direct human-to-human transmission of ZIKV have been documented. Maternal-foetal transmission during pregnancy, through the placenta, is well-documented and associated with Congenital Zika Syndrome (CZS) (Oliveira Melo et al. 2016). Perinatal transmission during childbirth has also been reported, and while ZIKV RNA has been detected in breast milk, transmission via breastfeeding remains unconfirmed (D'Ortenzio et al. 2016; Dupont-Rouzeyrol et al. 2016). Sexual transmission is another notable route, primarily male-to-female, likely due to prolonged viral persistence in semen. ZIKV can remain in semen for up to six months post-infection, distinguishing it from other arboviruses. However, sexual transmission accounts for a small fraction of cases (Barzon et al. 2016; Nicastri, Castilletti, et al. 2016; Paz-Bailey et al. 2018). Blood transfusion and organ transplantation are additional transmission routes, though less common (M. Aubry et al. 2015; Nogueira et al. 2017). These routes pose a risk due to the asymptomatic nature of many ZIKV infections, complicating donor screening (Gallian et al. 2017). An overview of the main modes of ZIKV transmission is summarized in Figure 2.

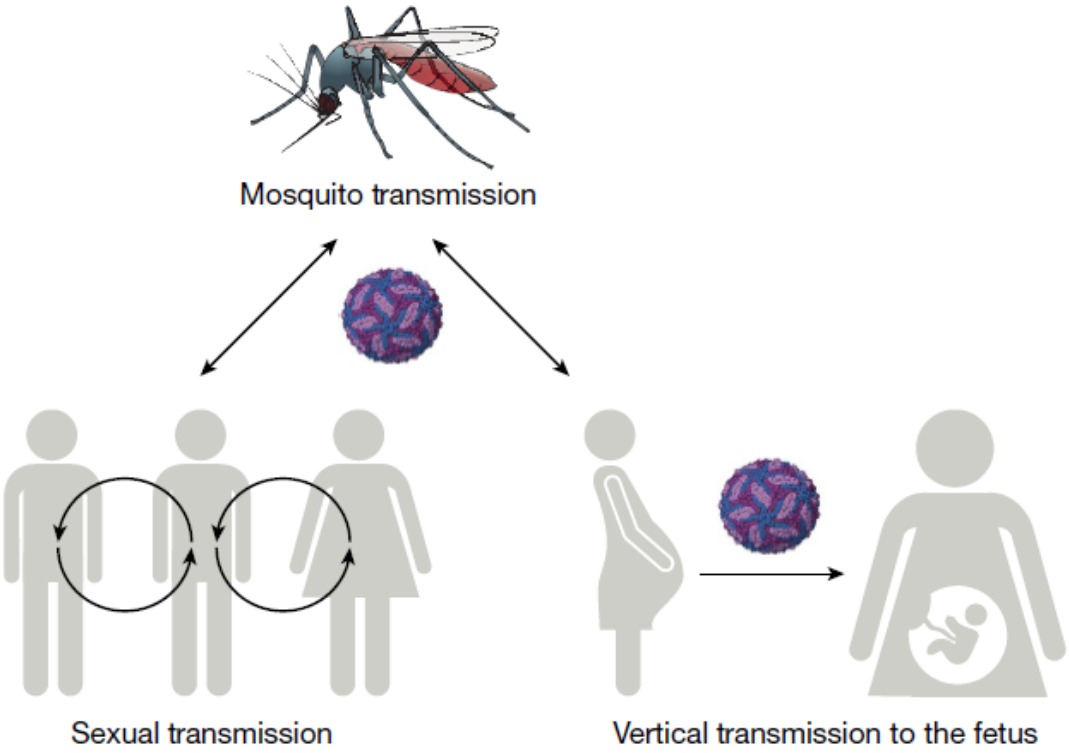

Figure 2. Transmission Routes of ZIKV.
ZIKV is primarily transmitted through *Aedes* mosquitoes, though it can also be transmitted via sexual contact and vertical transmission from mother to foetus during pregnancy. Reproduced from Pierson et al., Nature 560, 573–581 (2018), with permission from Springer Nature (Pierson and Diamond 2018).

1.5 Clinical Manifestations and Pathogenesis

Zika virus infections are predominantly asymptomatic; however, when clinical manifestations do occur, they typically include mild fever, maculopapular rash, arthralgia, conjunctivitis, myalgia, fatigue, and headache (Halani et al. 2021). The incubation period is typically between 3 and 14 days, with symptoms generally persisting for 2 to 7 days (Baud et al. 2017; Duffy et al. 2009; Musso and Gubler 2016). Despite its generally mild presentation, ZIKV has been associated with serious neurological and congenital complications (Figure 3).

Pregnant women infected with ZIKV are at higher risk of adverse outcomes, including miscarriage, preterm birth, and stillbirth (Brasil et al. 2016; Meaney-Delman et al. 2016). Furthermore, ZIKV is strongly linked to a spectrum of congenital anomalies collectively termed Congenital Zika Syndrome (CZS). CZS primarily affects the nervous system, but can also involve musculoskeletal, ophthalmological, and auditory defects (Brasil et al.

2016; Freitas et al. 2020; Ventura et al. 2016). One of the most notable manifestations of CZS is microcephaly, a condition characterised by a significantly smaller head size in a newborn compared to what would be expected for their age. This condition is frequently associated with an underdeveloped brain, which can result in impaired motor and cognitive functions, extra cranial malformations, and facial deformities (Passemard et al. 2013; von der Hagen et al. 2014). ZIKV preferentially infects neuronal progenitor cells (NPCs), leading to disruption of their proliferation, differentiation, and migration (J. Dang et al. 2016; Tang et al. 2016). This leads to impaired brain development, resulting in cortical thinning, structural brain abnormalities, and microcephaly (Cugola et al. 2016; Garcez et al. 2016). Neurological damage, including motor impairments, has also been observed in children who did not exhibit abnormalities at birth, particularly in those exposed to ZIKV during the later stages of gestation (López-Medina et al. 2021).

Moreover, ZIKV infection has been linked to the development of Guillain-Barré syndrome (GBS) in adults. GBS is an acute immune-mediated polyneuropathy affecting the peripheral nervous system, resulting in progressive muscle weakness and, in severe cases, paralysis. While the majority of GBS cases resolve without significant sequelae, approximately 20% result in severe disability, respiratory failure or death. The mechanism behind ZIKV-induced GBS is thought to involve molecular mimicry, whereby the immune system mistakenly attacks nerve cells, causing damage (Acosta-Ampudia et al. 2018; Parra et al. 2016).

Other neurological complications associated with ZIKV include meningoencephalitis and acute myelitis, highlighting the potential of the virus to cause severe nervous system damage (Carteaux et al. 2016; Halani et al. 2021; Mécharles et al. 2016). Moreover, recent evidence suggests a connection between ZIKV infection and the development of inflammatory demyelinating diseases affecting the central nervous system, including conditions with clinical features similar to multiple sclerosis (MS) (Alves-Leon et al. 2019, 2021; da Silva et al. 2023). Transcriptomic studies have shown that ZIKV infection and MS share molecular signatures, particularly in oxidative stress and immune-inflammatory pathways (da Silva et al. 2023).

Taken together, although the clinical spectrum of ZIKV-associated neurological disease is well documented, the precise mechanisms through which ZIKV causes neurological complications and congenital disorders have not yet been fully elucidated.

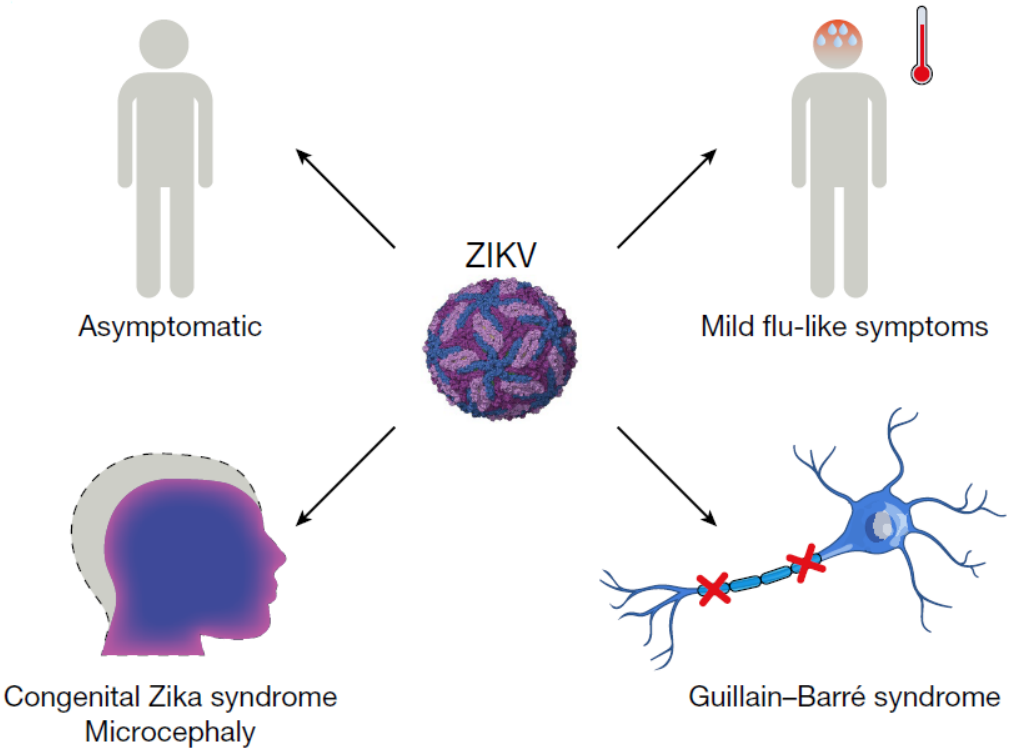

Figure 3. Clinical Manifestations of ZIKV Infection.
The majority of ZIKV infections are asymptomatic. In cases where symptoms do occur, patients often present with mild flu-like symptoms. When infection occurs during pregnancy, it may lead to microcephaly, CZS, or foetal death. In some adults, ZIKV infection has been associated with GBS. Reproduced from Pierson et al., Nature 560, 573–581 (2018), with permission from Springer Nature (Pierson and Diamond 2018).

1.6 Treatment and Prevention

At present, there are no approved treatments or vaccines for ZIKV, and the primary focus of management is on relieving symptoms (CDC 2024c). Several potential ZIKV vaccines are currently undergoing clinical trials, including mRNA and DNA-based candidates. Among the most advanced candidates, an mRNA-based vaccine (mRNA-1893) has shown neutralizing antibody responses in early trials, with a sustained response for up to one year. The vaccine has now progressed to Phase 2 trials (Bollman et al. 2023). Similarly, a purified inactivated vaccine (PIZV/TAK-426) has demonstrated favourable safety and immunogenicity profiles, with high-dose regimens producing immune responses comparable to those observed in individuals who have recovered from ZIKV infection (Baldwin et al. 2018; Han et al. 2021). Concurrently, monoclonal antibodies

(mAbs) such as ZIKV-117 are being tested in preclinical studies (Erasmus et al. 2020; Nkolola et al. 2024).

Despite this progress, significant barriers remain. The decline in ZIKV cases has made it difficult to test clinical efficacy, while unresolved questions about the mechanisms of immunity and the risk of antibody-dependent enhancement (ADE), add further complexity. ADE occurs when antibodies from a previous ZIKV or DENV infection enhance, rather than neutralize, subsequent viral infections. The cross-reactivity between ZIKV and DENV has the potential to complicate immune responses and may contribute to an increase in the severity of illness. It has been demonstrated that pre-existing immunity to one virus affects the immune response and disease outcome of the other. This interaction poses significant difficulties in designing vaccines that can safely and effectively protect against ZIKV, particularly in regions where both viruses co-circulate (Halstead and O'Rourke 1977; Littaua et al. 1990; Miner and Diamond 2017b; Rodrigo et al. 2006; Woodson and Morabito 2024).

In the absence of specific antiviral treatments or vaccines, prevention through vector control measures, including mosquito bite avoidance and safe sexual practices, remains the most effective strategy to mitigate ZIKV transmission and its associated risks, particularly for pregnant women (CDC 2024d, 2024e; Staples et al. 2016).

1.7 microRNAs

Zika virus can cause irreversible neurological damage, and, in this context, it becomes of great importance to explore the underlying molecular pathways that contribute to this neurodevelopmental disruption. One such pathway involves microRNAs (miRNAs), which are key regulators of various physiological processes including those critical for neurodevelopment. These small, non-coding RNA molecules play a crucial role in controlling gene expression by modulating protein translation. Functionally, miRNAs regulate their target mRNAs by binding to the 3′ UTR or ORF, leading to either mRNA degradation or inhibition of translation (Bartel 2018; Mendell 2005).

miRNA biogenesis begins with the transcription of primary miRNA (pri-miRNA) by RNA polymerase II (Gregory et al. 2004, 2005). These long transcripts are then cleaved by the RNase III enzyme Drosha and DGCR8, forming precursor miRNAs (pre-miRNAs), which are hairpin-shaped structures. Pre-miRNAs are exported from the nucleus to the

cytoplasm via the exportin-5-Ran-GTP complex. Once in the cytoplasm, the enzyme DICER further cleaves the pre-miRNAs into mature miRNA duplexes of approximately 22 nucleotides in length. From the mature miRNA duplex, one strand, known as the guide strand, is incorporated into the Argonaute (AGO) proteins, forming the miRNA-induced silencing complex (miRISC). This complex targets mRNA molecules by binding to complementary sequences in their 3' UTR, resulting in either the repression of protein production or the degradation of the mRNA itself. Though the passenger strand of the miRNA duplex is also produced, it is less frequently involved in the miRISC (Gregory et al. 2004, 2005).

miRNAs are involved in a wide range of biological processes, including cell proliferation, differentiation, metabolism, and host responses to viral infection (Barbu et al. 2020; Fu et al. 2013; Liu et al. 2019; Yao 2016). They are estimated to regulate over 60% of protein-coding genes post-transcriptionally (Friedman et al. 2009). Dysregulation of miRNAs has been implicated in various diseases, including neurological diseases (S. Li et al. 2022). In viral infections, interference with miRNA biogenesis has been reported. The ZIKV core protein has been shown to bind and inhibit Dicer, impairing the processing of pre-miRNAs into mature miRNAs (Zeng et al. 2020). More recently, however, it has also been shown that host factors such as ILF3 and DHX9 can enhance Dicer processing of ZIKV-derived small RNAs, thereby contributing to antiviral defence (Lei et al. 2025). These findings highlight the complex interplay between ZIKV and the host RNA interference machinery, in which the virus can both suppress and be targeted by Dicer-dependent pathways. miRNA-mediated regulation has emerged as an important mechanism in ZIKV pathogenesis, but the specific changes induced by infection and their impact on cellular processes are still poorly characterised (Mousavi et al. 2024).

1.8 microRNAs and Extracellular Vesicle-Mediated Communication

miRNAs can be incorporated into extracellular vesicles (EVs) and mediate cell-to-cell communication (Gurunathan et al. 2019). EVs are classified into three main types: exosomes (30–150 nm), microvesicles (100–1000 nm), and apoptotic bodies (1 μm) (Borges et al. 2013; Yáñez-Mó et al. 2015; Zaborowski et al. 2015). These vesicles differ based on their size, biogenesis, release mechanisms, and cargo. Exosomes originate from the inward budding of endosomal membranes, forming multivesicular bodies (MVBs),

which then fuse with the plasma membrane to release the enclosed exosomes into the extracellular space (Bebelman et al. 2018; Raposo and Stoorvogel 2013; Simons and Raposo 2009; Yáñez-Mó et al. 2015). Microvesicles form directly from the outward budding of the plasma membrane (Zaborowski et al. 2015). Apoptotic bodies are released during programmed cell death and contain cellular fragments, such as organelles and nuclear material (Borges et al. 2013).

EVs protect their cargo from degradation, including miRNAs, which are otherwise vulnerable to the extracellular environment, where RNases would typically degrade unprotected RNAs. The stability of miRNAs in biological fluids such as blood, urine, and saliva is enhanced by their encapsulation within EVs, ensuring their functional delivery to target cells (Caby et al. 2005; Grigor'eva et al. 2016; Hornick et al. 2015; Street et al. 2012; Vojtech et al. 2014).

The release of miRNAs through EVs plays important roles in both normal physiological and pathological processes, including viral infections. The cargo packaged within EVs can be altered under diseased and infected states (Chahar et al. 2015; Salomon et al. 2013; Vora et al. 2018). For example, in the context of viral diseases, exosomal miRNAs can modulate host immune responses and contribute to viral pathogenesis. Viruses may exploit these EVs to transfer viral RNA or proteins to uninfected cells, thereby aiding in the spread of infection (Chahar et al. 2015). This ability to manipulate the host's cellular environment highlights the importance of miRNA-EV interactions in intercellular communication and disease development.

1.9 Oxidative Stress and Nrf2 Signalling

Oxidative stress is a condition in which the balance between the production of reactive oxygen species (ROS) and the body's ability to detoxify them through antioxidant defences is disrupted. This imbalance leads to the accumulation of ROS, which can cause damage to essential cellular components such as lipids, proteins, and DNA (Pizzino et al. 2017; Sies 2015). ROS encompass superoxide anions ($O_2^{\bullet -}$), hydroxyl radicals ($OH^{\bullet}$), and hydrogen peroxide (H_2O_2) and are byproducts of cellular metabolic processes. They play key roles in various intracellular signalling pathways, including the regulation of cytokines, growth factors, and the immune response to pathogens (Geiszt and Leto 2004). Also, ROS are highly reactive and unstable, and elevated levels can lead to cellular damage

affecting DNA, lipids, and proteins (Halliwell and Cross 1994). Maintaining ROS levels is essential for cellular balance, with the antioxidant system serving as a protective mechanism against oxidative stress.

During viral infections, an increase in ROS production can trigger the host cell's antiviral inflammatory response, thereby influencing viral pathogenesis (Z. Zhang et al. 2019). Several viruses, including DENV and hepatitis C virus (HCV), induce oxidative stress as part of their infection strategy. This process can help viruses to manipulate host cellular pathways to promote viral replication or evade immune detection (Valadão et al. 2016).

In response to oxidative stress, cells activate several defence mechanisms, with one of the most critical being the nuclear factor erythroid 2-related factor 2 (Nrf2) / antioxidant response element (ARE) signalling pathway. Nrf2 is a transcription factor that regulates the expression of genes involved in detoxification and antioxidant defence, helping to maintain cellular redox balance (Kobayashi et al. 2009). Under unstressed conditions, Nrf2 is bound by the actin-binding protein Keap1 (Kelch-like ECH-associated protein 1), which promotes its ubiquitination and subsequent degradation. Upon exposure to oxidative stress, Nrf2 is released from Keap1, translocates to the nucleus, and forms a complex with small Maf proteins. This complex then binds to antioxidant response elements (AREs) within the promoter regions of target genes, driving the expression of antioxidant and cytoprotective genes (Yamamoto et al. 2018). These genes include those encoding detoxifying enzymes such as NAD(P)H oxidoreductase 1 (NQO1), glutathione S-transferases (GSTs), and glutamate-cysteine ligase (GCL), which are involved in the synthesis of glutathione, a major cellular antioxidant. Activation of these genes enhances the cell’s ability to neutralize ROS and maintain redox balance (Jaiswal 2004; Kobayashi and Yamamoto 2005).

In addition to its role in regulating antioxidant defences, Nrf2 is also involved in other protective cellular processes, including the regulation of autophagy, which helps remove damaged cellular components (Komatsu et al. 2010). Several flaviviruses exploit this pathway; for example, in HCV infection, viral suppression of Nrf2 activity leads to elevated oxidative stress and triggers autophagy, which in turn facilitates viral particle release (Medvedev et al. 2017). Taken together, Nrf2 plays a critical role in the regulation of cytoprotective genes during oxidative stress and in autophagy-related pathways.

1.10 Relevance and Aim of this Study

Zika virus poses a persistent and unpredictable threat to global public health due to its potential to cause severe neurological complications, such as microcephaly in newborns and Guillain-Barré syndrome in adults. Despite a decline in incidence following the 2015-2016 outbreak, the risk of ZIKV re-emergence remains high, particularly in regions where *Aedes* mosquito vectors are prevalent or expanding due to climate change (Woodson and Morabito 2024).

For prevention and improved management of ZIKV infection, molecular insights into virus-host interactions are crucial. A better understanding of how ZIKV alters host miRNA profiles may provide a foundation for developing biomarkers, improving neurodevelopmental risk assessment, and informing future therapeutic or prevention strategies.

The aim of this study was therefore to characterise ZIKV-induced changes in host miRNA and mRNA expression. To gain representative results for the situation in humans, two relevant human cell lines were selected that reflect key sites of infection and pathology. Long-term neuroepithelial stem cells (lt-NES®) were used as a model of early neural development, which is especially vulnerable to ZIKV-associated disruption. HaCaT keratinocytes served as a model of skin epithelium, the likely initial site of viral entry following mosquito transmission (Hamel et al. 2015a).

By profiling host miRNA and mRNA transcriptomes and conducting integrative analyses, this work seeks to identify ZIKV-associated molecular signatures and regulatory networks. The objective is to uncover specific miRNA signatures and associated gene expression changes that may contribute to neurodevelopmental disruption during ZIKV infection and that could serve as a basis for future biomarker and therapeutic development.

2. Materials and Methods

2.1 Cell Culture

2.1.1 lt-NES® Cells

Long-term self-renewing neuroepithelial-like stem cells (lt-NES®) utilized in this study serve as a reductionist in vitro model for investigating early human neural stem cell differentiation (Koch et al. 2009). These cells, derived from both hESCs (Koch et al. 2009) and iPSCs (Falk et al. 2012), maintain stable neurogenic and gliogenic potential even after long-term proliferation. lt-NES® cells used in this study were generated from the iPSC line iLB-C-31f (Rehbach et al. 2019), which originated from a female donor in her mid-20s through retroviral reprogramming. Both the generation and cultivation of these cells were performed by the research group of Prof. Oliver Brüstle at the Life & Brain Center.
The generation of lt-NES® cells followed a previously established protocol (Koch et al. 2009) with minor modifications. The lt-NES® cells were maintained on 6-well plastic cell culture dishes coated with 1× poly-L-ornithine and 10 µg/mL laminin (Merck, Darmstadt, Germany). Cells were cultured in Dulbecco's Modified Eagle's/F12 medium (DMEM/F12; Thermo Fisher Scientific, Waltham, MA, USA) supplemented with N2 Supplement (PAA Laboratories, Pasching, Austria), 10 ng/mL basic fibroblast growth factor 2 (FGF2), 10 ng/mL epidermal growth factor (EGF) (both from R&D Systems, Minneapolis, MN, USA), and B-27 Supplement (1:1000; Thermo Fisher Scientific, Waltham, MA, USA).
Passaging was performed every 2–3 days at a 1:2 split ratio. For enzymatic dissociation, cells were incubated with 0.125% trypsin (Thermo Fisher Scientific, MA, USA) for 5–10 minutes at room temperature. Trypsin activity was neutralized by adding trypsin inhibitor (Thermo Fisher Scientific, MA, USA). The cell suspension was centrifuged at 300 x g for 3 minutes. The supernatant was discarded, and the cell pellet was resuspended in fresh maintenance medium for continued culture.

2.1.2 HaCaT Cells

Human adult low-calcium high-temperature (HaCaT) keratinocytes were cultured in 75 cm² tissue culture flasks (TPP, Trasadingen, Switzerland) designed for adherent cell growth. Cells were maintained in high-glucose Dulbecco's Modified Eagle Medium

(DMEM; Thermo Fisher Scientific, Waltham, USA), supplemented with 10% foetal bovine serum (FBS Superior; Biochrom, Merck, Berlin, Germany), 1% L-glutamine (Thermo Fisher Scientific, Waltham, USA), and 1% penicillin-streptomycin (Pen/Strep; Biowest, Nuaillé, France). The culture medium was exchanged twice weekly by aspirating the spent medium and replacing it with fresh, pre-warmed medium under sterile conditions.

Cell confluency was routinely monitored, and subculturing was performed when cultures reached approximately 75% confluency, typically every 5–7 days. For enzymatic dissociation, the medium was aspirated, and the cells were washed with 10 ml phosphate-buffered saline (PBS; Biowest, Nuaillé, France). After removal of PBS, 2 ml of TrypLE Express (Thermo Fisher Scientific, Waltham, USA) was added per flask and incubated at 37 °C for 5–10 minutes. Cell detachment was assisted by gently tapping the bottom of the flask.

Once detached, 10 ml of fresh complete medium was added to stop enzymatic activity, and the cells were resuspended by gentle pipetting. The suspension was transferred to a 50 ml conical tube and centrifuged at 600 × g for 5 minutes. After centrifugation, the supernatant was discarded, and the cell pellet was washed with 10 ml PBS (Biowest, Nuaillé, France). Cells were then resuspended in 1 ml of complete medium, and a 10 µl aliquot of the suspension was used for cell counting using an automated cell counter (Bio-Rad, Hercules, USA). Cells were subsequently seeded into new 75 cm² tissue culture flasks (TPP, Trasadingen, Switzerland) at a density of 4 × 10^5 cells per flask and maintained under standard culture conditions.

2.2 Infection

2.2.1 ZIKV Infection of lt-NES® Cells

This study employed two Zika virus (ZIKV) strains: ZIKV Uganda 976, obtained from the European Virus Archive, and ZIKV PF13/251013-18 from French Polynesia, kindly provided by Professor Musso (Institute Louis Malardé, Tahiti) and the European Virus Archive (Figure 5). The Uganda strain is not known to be associated with severe clinical outcomes, whereas the French Polynesian strain has been linked to neurological complications and congenital Zika syndrome (Cauchemez, Besnard, Bompard, Dub, Guillemette-Artur, Eyrolle-Guignot, Salje, Van Kerkhove, et al. 2016). Virus stocks were

prepared and titrated by collaborators at the Paul-Ehrlich-Institut (Langen, Germany), as described in the virus stock production section.

lt-NES® cells were seeded into 6-well plates at a density of 1 × 10^6 cells per well. Infections were performed using serum-free virus stocks at a multiplicity of infection (MOI) of either 0.1 or 1. The higher MOI (1) was selected in some experiments to enhance the likelihood of observing more pronounced cellular effects. Both infected and uninfected control cells received daily medium changes at 24, 48, and 72 hours post-infection. Supernatants were collected 8 hours after each medium change for subsequent analysis by plaque assay. In parallel, cells were harvested at 24, 48, and 72 hours post-infection.

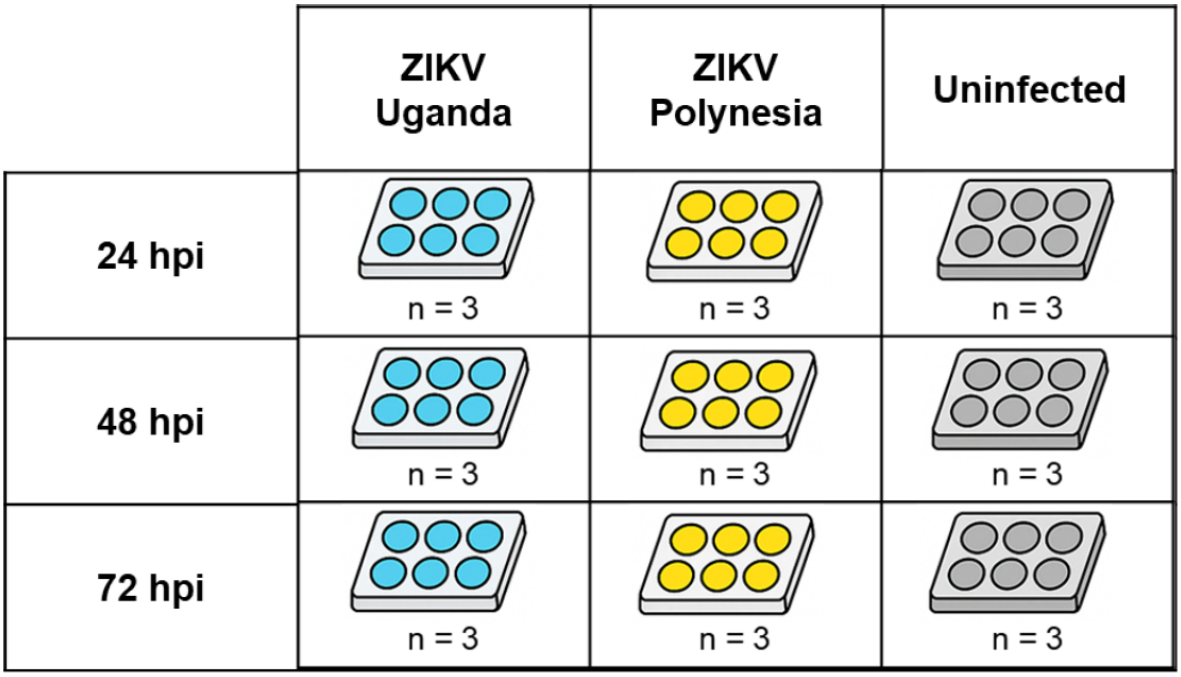

Figure 4. Experimental Design for ZIKV Infection and Sampling Time Points.
Overview of experimental setup showing infection conditions (ZIKV Uganda, ZIKV French Polynesia, and uninfected controls) across 24, 48, and 72 hours post-infection. Each condition was performed in triplicate.

2.2.2 ZIKV Infection of HaCaT Cells

HaCaT cells were seeded into 6-well plates and infected with ZIKV Uganda (976) or ZIKV French Polynesia (PF13/251013-18) at a multiplicity of infection (MOI) of 0.1. The viral inoculum was prepared in serum-free medium and incubated with the cells for 16 hours. After incubation, the inoculum was removed, and cells were gently washed once with pre-

warmed PBS (Biowest, Nuaillé, France). Fresh complete medium (3 mL per well) was then added. Two hours post-infection, cells were treated with 20 ng/mL recombinant human fibroblast growth factor 7 (FGF7) or left untreated as controls. The culture medium containing FGF7 (or control medium) was replaced every 24 hours.
Cells were harvested for total RNA extraction at 24, 48, and 72 hours post-infection.

2.3 Virus Stock Production and Titration

ZIKV virus stocks used in this study were generated and titrated by colleagues at the Paul-Ehrlich-Institut (Langen, Germany), as described below.
For virus stock production, Vero cells were infected with the respective ZIKV strain in Dulbecco's Modified Eagle Medium (DMEM) high glucose (BioWest, Nuaillé, France) supplemented with 10% foetal bovine serum superior (FBS; "DMEM complete", Biochrom GmbH, Berlin, Germany), 2 mM L-glutamine (Biochrom GmbH), and 100 U/mL penicillin with 100 µg/mL streptomycin (Paul-Ehrlich-Institut, Langen, Germany). Three days post-infection, cells were washed once with PBS (Biowest, Nuaillé, France). For virus stocks intended for HaCaT cell infections, cultures were maintained in DMEM complete. For virus stock intended for lt-NES® cell infections, the FBS-containing medium was replaced with DMEM containing 10% KnockOut™ Serum Replacement (Thermo Fisher Scientific, Waltham, USA) to ensure compatibility with stem cell culture conditions. On day 7 post-infection, the supernatant was harvested, clarified by centrifugation at 1000 × g for 5 minutes to remove cellular debris, and stored at –80 °C until further use in plaque assays.
To determine viral titers, plaque assays were performed on Vero cells. Cells were seeded in 6-well plates at a density of 3×10^5 cells per well. Serial 10-fold dilutions of viral supernatants were prepared, and 100 µL of each dilution was added per well. After 2 hours of incubation at 37 °C the inoculum was removed and cells were overlaid with 0.4% SeaPlaque™ agarose (Lonza, Basel, Switzerland) in complete DMEM. Following a five-day incubation, the agarose overlay was removed, and cells were fixed with 4% formaldehyde (Carl-Roth, Karlsruhe, Germany) in PBS for 20 minutes at room temperature. Plaques were visualized by staining with 0.1% crystal violet in 20% ethanol (Merck, Darmstadt, Germany) for 15 minutes, washed with distilled water, air-dried, and counted. Viral titers were calculated as plaque-forming units per millilitre (PFU/mL).

2.4 miRNA: Sequencing and Data Analysis

2.4.1 RNA Isolation

For the analysis of intracellular miRNAs, total RNA was extracted from previously infected and uninfected lt-NES® cell samples at 24, 48, and 72 hours post-infection (hpi) using the miRNeasy Mini Kit® (Cat. No. 217004, Qiagen, Hilden, Germany) following the manufacturer's protocol (Figure 5). Cells were lysed in QIAzol Lysis Reagent, followed by chloroform-mediated phase separation. The aqueous phase was combined with ethanol and transferred to a silica membrane spin column to bind total RNA, including small RNAs. After washing, RNA was eluted in RNase-free water and stored at -80 °C until further use. Biological triplicates had been established during the infection setup, with three replicates per condition and time point (i.e., uninfected controls and cells infected with either ZIKV Uganda or ZIKV French Polynesia, each at 24, 48, and 72 hpi).

For the analysis of extracellular vesicle (EV)-derived miRNAs, cell culture supernatants from previously established infected and uninfected lt-NES® cell samples were collected at 24, 48, and 72 hours post-infection. EV-associated miRNAs were extracted using the exoRNeasy Serum/Plasma Kit (Cat. No. 77064, Qiagen, Hilden, Germany) following the manufacturer's instructions. Briefly, 1 mL of cell-free supernatant was mixed with a binding buffer and applied to a membrane affinity spin column to capture extracellular vesicles. After washing, EVs were lysed on-column, and total RNA was eluted for downstream applications.

As with intracellular RNA samples, three biological replicates per condition and time point were processed, corresponding to uninfected controls and cells infected with either ZIKV Uganda or ZIKV French Polynesia at 24, 48, and 72 hpi.

RNA concentrations were quantified using the Qubit RNA High Sensitivity Assay Kit (Thermo Fisher Scientific, Waltham, USA) according to the manufacturer's instructions.

2.4.2 miRNA Library Preparation and Size Selection

To prepare libraries for miRNA sequencing, the NEBNext® Multiplex Small RNA Library Prep Set for Illumina (E7300S, New England Biolabs, Frankfurt, Germany) was used. The protocol includes the ligation of 3′ and 5′ adapters specifically designed for small RNA

molecules, followed by reverse transcription and polymerase chain reaction (PCR) amplification using indexed primers to enable multiplexing.

After PCR amplification, the resulting double-stranded complementary DNA (cDNA) was quantified using the Qubit dsDNA High Sensitivity Assay Kit (Thermo Fisher Scientific, Waltham, USA) according to the manufacturer's protocol. The libraries were then purified using the QIAquick PCR Purification Kit (Cat. No. 28104, Qiagen, Hilden, Germany) to remove excess primers and buffer components.

Purified libraries from 12 indexed samples were pooled, mixed with 6× loading dye, and separated on a 10% denaturing polyacrylamide gel in 1× TBE buffer. Electrophoresis was performed for 1 hour and 20 minutes at 100 V. Gels were stained with ethidium bromide, and the ~147 bp band corresponding to adapter-ligated miRNAs was excised. To avoid UV-induced degradation, only one reference lane containing a marker was exposed to UV light, and this was used to guide the cutting of corresponding bands in the other gel lanes. Excised gel pieces were shredded by centrifugation and incubated twice with gel elution buffer at room temperature to extract the cDNA. The eluate was purified via gel filtration columns, ethanol-precipitated in the presence of sodium acetate and linear acrylamide, and the resulting pellet was resuspended in TE buffer. Library size and concentration were assessed using the Agilent 2100 Bioanalyzer and the High Sensitivity DNA Kit (5067-4626, Agilent, Santa Clara, CA, USA). The assay allows accurate quantification and sizing of DNA fragments within the range of 50–7000 bp. Only libraries displaying a distinct peak at approximately 147 bp were considered of sufficient quality and submitted for sequencing.

2.4.3 miRNA Sequencing

Prepared miRNA libraries were sequenced using the Illumina® MiSeq system with the MiSeq Reagent Kit v2 (50 cycles) (MS-102-2001, Illumina, CA, USA), following the manufacturer’s protocol for small RNA libraries.

Prior to sequencing, libraries were denatured and diluted to the required loading concentration. Indexed sample libraries were first diluted with TE buffer to a final concentration of 2 nM. Then, 10 µL of the 2 nM libraries were mixed with 10 µL of freshly prepared 0.2 N NaOH, vortexed briefly, and centrifuged at 280 x g for 1 minute. After 5 minutes of incubation at room temperature to achieve complete denaturation, 20 µL of

denatured libraries were diluted in 980 µL pre-chilled HT1 buffer, yielding a 20 pM library. A final dilution to 15 pM was prepared by mixing 10 µL of the 20 pM library with 750 µL HT1 buffer. A denatured PhiX control library was spiked into the sequencing mix as an internal control. For this, 2 µL of PhiX were diluted with 8 µL of 10 mM Tris-Cl (pH 8.5) containing 0.1% Tween-20. The mixture was denatured by adding 10 µL of 0.2 N NaOH, followed by a 5-minute incubation at room temperature. The denatured PhiX was diluted in two steps to a final concentration of 12.5 pM: first, 20 µL PhiX was added to 980 µL HT1 buffer, then 625 µL of that mixture was further diluted with 375 µL HT1. To prepare the final loading mix, 10 µL of 12.5 pM PhiX library was combined with 990 µL of 15 pM denatured sample libraries. From this, 600 µL was loaded into the sample reservoir of a new sequencing cartridge, which included all required reagents. A new flow cell was rinsed with RNase-free water, followed by 100% ethanol, and allowed to dry before insertion into the MiSeq instrument along with the loaded cartridge and a fresh bottle of wash buffer. The MiSeq was programmed for 36 cycles to generate single-end reads, which is sufficient for sequencing adapter-ligated miRNAs.

2.4.4 miRNA Data Analysis

Following the completion of the sequencing run, raw sequencing data were extracted as FASTQ files using the MiSeq® Reporter Software (Illumina, San Diego, CA, USA). Each FASTQ file contained single-end reads corresponding to individual miRNA-derived cDNA fragments.

To ensure high-quality data, raw reads were first processed using Cutadapt, a tool for trimming adapter sequences. The 3′ adapter, which had been ligated during library preparation, was removed to enable accurate alignment. Additionally, sequencing reads shorter than 15 nucleotides after trimming were discarded to minimize false-positive alignments and improve mapping specificity. Trimmed reads were then aligned to the human reference genome (hg38) using the alignment tool Bowtie2, allowing identification of genomic origin. Initially, alignment was performed across the entire genome to capture all potentially relevant loci. Successfully mapped reads were then used to identify precursor (hairpin) and mature miRNAs based on annotations from miRBase.

Count data for all detected miRNAs were compiled and imported into the R statistical environment for differential expression analysis using the DESeq2 package.

Within DESeq2, read counts were normalized to account for differences in sequencing depth across samples. Differential expression was calculated using the Wald test, and p-values were adjusted for multiple testing using the Benjamini-Hochberg method. To focus on miRNAs with higher biological relevance and reduce the influence of technical variability, miRNAs with fewer than 100 read counts across all samples were excluded from further analysis (tenOever 2013).

To interpret the potential biological functions of differentially expressed miRNAs, gene ontology (GO) and pathway enrichment analyses were conducted using the DIANA-miRPath v3 tool (Kanehisa and Goto 2000; Vlachos et al. 2015). This platform allowed for the identification of enriched biological processes and signaling pathways using the Kyoto Encyclopedia of Genes and Genomes (KEGG) database and GO annotations. Predicted gene targets were obtained using the microT-CDS algorithm with a threshold score of 0.8, ensuring high-confidence predictions. Additionally, experimentally validated interactions were included from the TarBase database (Reczko et al. 2012). For both sources, only targets with a p-value below 0.05 were considered for enrichment analysis.

All miRNA sequencing datasets generated in this study have been deposited in the Gene Expression Omnibus (GEO) under the accession number GSE157532.

2.5 Microarray-Based Gene Expression Analysis

Gene expression analysis was performed using the SurePrint G3 Human Gene Expression 8x60K Microarray Kit (Agilent Technologies, Santa Clara, CA, USA), following Agilent's one-color microarray protocol. For each sample, 100 ng of total RNA (extracted using the miRNeasy Mini Kit, Qiagen) was used as input. Amplification and labeling with Cyanine-3 (Cy3) were performed using T7 promoter-based in vitro transcription, according to the manufacturer’s instructions.

Labelled complementary RNA (cRNA) was purified using the RNeasy Mini Kit (Qiagen, Hilden, Germany), and dye incorporation and RNA concentration were assessed using a NanoDrop spectrophotometer (Thermo Fisher Scientific, Waltham, USA). Samples with a specific activity of at least 6 pmol Cy3 per µg cRNA were considered suitable and used for hybridization. Labelled samples were hybridized to microarray slides, incubated for 17 hours at 60 °C, washed, and scanned using the Agilent SureScan Microarray Scanner. Raw image data were extracted with Agilent Feature Extraction Software (v10).

Data analysis was conducted using GeneSpring GX 14.9.1 (Agilent Technologies). After background correction and normalization, signal intensities below 50 were excluded. Differential expression was determined using a two-way analysis of variance (ANOVA) with Benjamini–Hochberg correction for multiple testing.

Differentially expressed genes were cross-referenced with predicted miRNA targets from PiCTar, TarBase, TargetScan, and miRDB (Agarwal et al. 2015; Krek et al. 2005; Sethupathy et al. 2006; X. Wang 2008). Pathway and network enrichment analysis was performed using Reactome (version 73) (Croft et al. 2014).

Gene expression profiling was conducted using three biological replicates per condition and time point. This included lt-NES® cells and HaCaT cells that were either uninfected or infected with ZIKV Uganda or ZIKV French Polynesia at 24, 48, and 72 hours post-infection (Figure 5). Additionally, for HaCaT cells, three biological replicates were analysed for cells infected with ZIKV French Polynesia and treated with FGF7, as well as for uninfected HaCaT cells treated with FGF7 at each corresponding time point.

The microarray data sets are deposited in GEO (GSE157532).

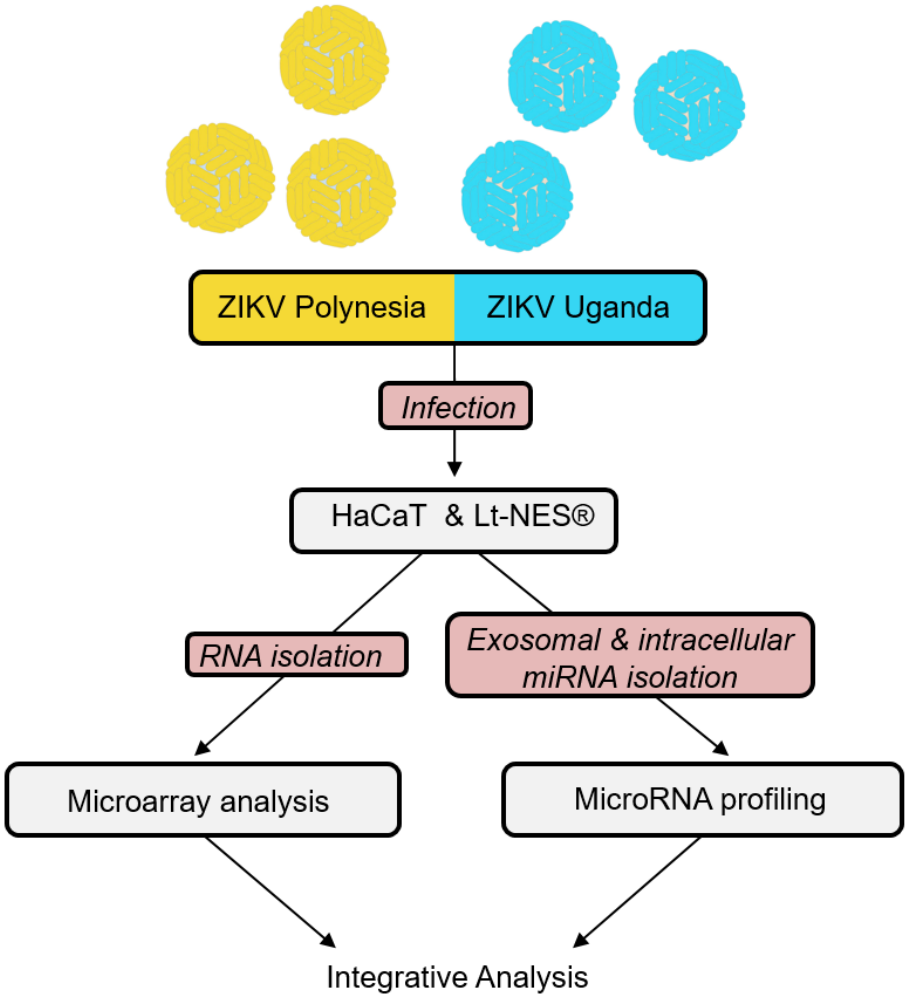

Figure 5. Schematic Overview of the Experimental Workflow.
lt-NES® cells and HaCaT keratinocytes were infected with ZIKV strains from French Polynesia or Uganda. Following infection, RNA was isolated for transcriptome analysis. Gene expression profiling in both cell types was performed using microarrays, while intracellular and exosomal miRNA profiling was conducted in lt-NES® cells using next-generation sequencing. An integrative analysis of mRNA and miRNA datasets was performed to identify ZIKV-associated molecular changes.

2.6 Real-Time Quantitative PCR

Quantitative real-time PCR (qRT-PCR) was used to validate selected miRNAs and mRNAs identified in the sequencing and microarray analyses. Complementary DNA (cDNA) was synthesized from total RNA using the miScript II RT Kit (Cat. No. 218161, Qiagen, Hilden, Germany) for miRNA validation and the QuantiTect Reverse Transcription Kit (Cat. No. 205311, Qiagen) for mRNA analysis, following the respective manufacturer's protocols. For miRNA analysis, 500 ng of total RNA per sample was reverse transcribed

using the HiFlex Buffer. For mRNA validation, 1000 ng of total RNA was used, and an integrated genomic DNA elimination step was included prior to reverse transcription, as recommended by the QuantiTect protocol.

qPCR reactions were carried out using the SYBR Green PCR Kit (Cat. No. 204145, Qiagen) on a LightCycler 480 Real-Time PCR System (Roche, Basel, Switzerland). qPCR reactions were carried out using the SYBR Green PCR Kit (204145, Qiagen, Hilden, Germany) on a Roche LightCycler 480 instrument (Roche, Basel, Switzerland). The amplification program was identical for both miRNA and mRNA analyses and consisted of an initial activation step at 95 °C for 15 minutes, followed by 40 amplification cycles of 94 °C for 15 seconds (denaturation), 55 °C for 30 seconds (annealing), and 70 °C for 30 seconds (extension). A final melting curve analysis was performed from 60 °C to 95 °C with a gradual temperature increase of 0.1 °C/second to verify amplification specificity.

miScript Primer Assays were used for the detection of miRNAs (Hs_miR-205_1, Hs-miR-182_2, Hs_miR-4792_1, Hs-miR-16_2; Qiagen). miR-16 served as the reference gene for normalization of miRNA expression. For mRNA validation, expression levels of selected genes (ASNS, FOXC1, SESN2) were quantified using QuantiTect Primer Assays (Hs_ASNS_1_SG, Hs_FOXC1_2_SG, Hs_SESN2_1_SG, and Hs_GAPDH_1_SG; Qiagen). Glyceraldehyde 3-phosphate dehydrogenase (GAPDH) was used as the reference gene. Fold changes in expression were calculated using the comparative ΔΔ cycle threshold (Ct) method, where Ct values for target RNAs were first normalized to those of the respective internal control (miR-16 for miRNAs or GAPDH for mRNAs), resulting in ΔCt values. These were then compared to the corresponding control samples to determine ΔΔCt, and relative expression levels were calculated using the formula $2^{-\Delta\Delta Ct}$ (Schmittgen and Livak 2008).

2.7 Oxyblot

Carbonylation of proteins, an indicator of oxidative protein damage, was analysed using the OxyBlot™ Protein Oxidation Detection Kit (Merck, Darmstadt, Germany) following the manufacturer's protocol. This assay is based on the detection of carbonyl groups that are introduced into protein side chains by reactive oxygen species (ROS). These carbonyl groups are derivatized by reaction with 2,4-dinitrophenylhydrazine (DNPH), resulting in

the formation of stable 2,4-dinitrophenyl (DNP) hydrazone adducts, which can be detected by immunoblotting using anti-DNP antibodies (Figure 6).

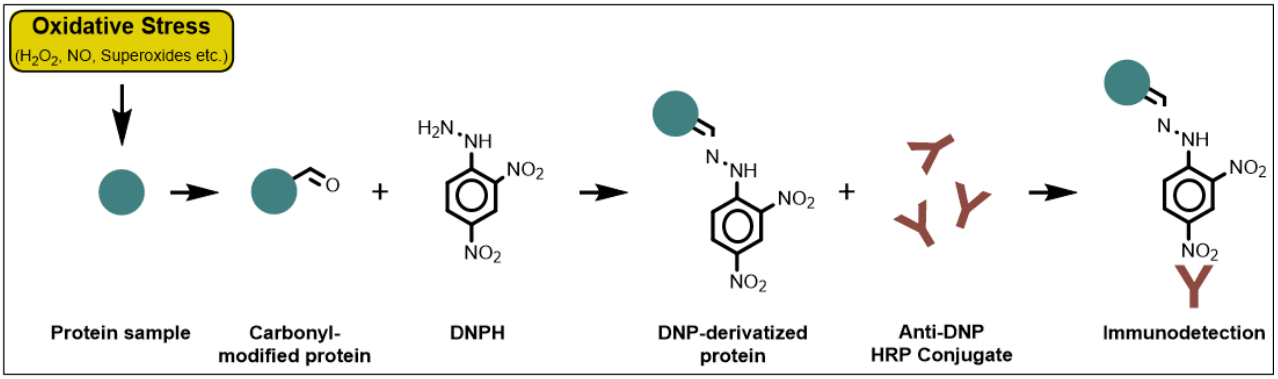

Figure 6. Principle of the OxyBlot™ Protein Carbonylation Assay.
Proteins oxidized under conditions of oxidative stress are derivatized with DNPH, converting carbonyl groups into DNP adducts. These are subsequently detected by anti-DNP antibodies via Western blotting.

ZIKV-infected and uninfected control lt-NES® cells were harvested at 24, 48, and 72 hours post-infection and washed with PBS. Cells were lysed in radioimmunoprecipitation assay buffer (50 mM Tris-HCl pH 7.2, 150 mM NaCl, 0.1% sodium dodecyl sulfate (SDS), 1% sodium deoxycholate, 1% Triton X-100) supplemented with protease inhibitors including aprotinin (serine protease inhibitor), leupeptin (serine and cysteine protease inhibitor), pepstatin (aspartic protease inhibitor), and phenylmethylsulfonylfluoride (serine and cysteine protease inhibitor), all from Applichem (Darmstadt, Germany).
Equal amounts of total protein (15 µg per sample) were derivatized with DNPH according to the kit protocol. Samples were denatured by mixing 1:1 with 10% SDS solution and separated by SDS-polyacrylamide gel electrophoresis (SDS-PAGE) using manually prepared stacking and separating gels composed of standard components (all from Carl Roth, Karlsruhe, Germany; see Table 1 for compositions).

Table 1. Composition of SDS-PAGE Gels

Component	Separation Gel (80 ml)	Stacking Gel (30.5 ml)
4 x Gel Buffer	20 mL (1.5 M Tris-HCl, pH 8.8, 0.4% SDS)	7.5 mL (0.5 M Tris-HCl, pH 6.7, 0.4% SDS)
Rotiphorese® Gel 40	24 mL	3 ml
ddH_2O	36 ml	20 ml
Ammonium persulfate	800 µL	300 µL
TEMED	80 µL	30 µL

After polymerization, samples were loaded onto the gel, and SDS-PAGE was run at 80 V through the stacking gel and at 120 V through the separating gel. Proteins were then transferred onto nitrocellulose membranes for subsequent detection. After protein transfer, membranes were blocked for 1 hour at room temperature using the blocking buffer provided in the OxyBlot™ kit, according to the manufacturer's instructions. Following blocking, membranes were incubated with primary anti-DNP antibodies and corresponding secondary antibodies for chemiluminescent detection. Band intensities were quantified using Image Studio Lite Software Version 5.2 (LI-COR Biosciences, Lincoln, NE, USA), enabling the comparative analysis of protein oxidation levels between samples.

2.8 Immunofluorescence Microscopy

To investigate the localization of proteins within the cells and assess potential colocalization of viral and host proteins, immunofluorescence staining followed by confocal microscopy was performed. Cells were cultured on sterile glass coverslips under standard conditions and fixed at 24, 48, or 72 hours post-infection using 4% formaldehyde (Carl-Roth, Karlsruhe, Germany) in phosphate-buffered saline (PBS) for 20 minutes at room temperature. After three washes with PBS (5 minutes each), cells were permeabilized with 0.5% Triton X-100 for 10 minutes and washed again three times. To reduce nonspecific antibody binding, cells were blocked with 1% bovine serum albumin (BSA) in PBS for 30 minutes. Cells were incubated for 1 hour at room temperature with the following primary antibodies diluted in PBS: anti-ZIKV NS1 (1:1000; Biofront Technologies, Tallahassee, FL, USA) and anti-MafG (1:300; Abcam, Cambridge, UK).

After three additional PBS washes, cells were incubated for 1 hour in the dark with the corresponding fluorophore-conjugated secondary antibodies: anti-mouse IgG-Alexa 488 (1:1000; Thermo Fisher Scientific, MA, USA) and anti-rabbit-Cy3 (1:400; Jackson Immunoresearch,West Grove, PA, USA). Cell nuclei were stained with 4′,6-diamidino-2-phenylindole (DAPI; Carl Roth, Karlsruhe, Germany). Coverslips were mounted onto glass slides using Mowiol mounting medium (Merck, Darmstadt, Germany) and stored at 4 °C until imaging. Fluorescence imaging was performed using the confocal laser scanning microscope LSM 510 Meta and ZEN 2009 software (Carl Zeiss, Oberkochen, Germany).

2.9 Data Analysis and Tools

Statistical analyses were conducted using R - statistical computing environment (version 4.2.2), GraphPad Prism 8 (GraphPad Software, San Diego, USA), and analysis tools provided by sequencing and microarray platforms as follows:

For miRNA sequencing, differential expression was analysed using the DESeq2 package in R. Read counts were normalized to account for differences in library size, and miRNAs with fewer than 100 reads across all samples were excluded to minimize background noise. The Wald test was used for statistical comparison, and p-values were adjusted for multiple testing using the Benjamini–Hochberg method. miRNAs with an adjusted p-value ≤ 0.05 were considered significantly differentially expressed.

Microarray gene expression data were analysed using a two-way ANOVA to assess differences across infection conditions and time points. As with the miRNA data, multiple testing correction was applied using the Benjamini-Hochberg method, and genes with an adjusted p-value ≤ 0.05 were considered significant.

For qRT-PCR validation experiments, expression levels were calculated using the ΔΔCt method, with GAPDH (for mRNA) and miR-16 (for miRNA) used as internal reference genes. Comparisons between groups were made using two-tailed, unpaired Student’s t-tests.

Results are shown as mean ± standard deviation (SD) with significance defined at $p \leq 0.05$.

Schematic illustrations were created using ChemDraw (PerkinElmer, version 20.0).

3. Results

3.1 Strain-Specific Differences in Gene Expression Modulation by ZIKV Uganda and Polynesia in HaCaT and It-NES® Cells

To investigate strain-specific effects of Zika virus (ZIKV) on host gene expression, two human cell models were used, chosen for their relevance to infection and pathogenesis: It-NES® cells, representing the developing neural environment, and HaCaT keratinocytes, modelling the skin's epithelial barrier as the primary site of viral entry following a mosquito bite (Hamel et al. 2015b). Both cell lines were infected with either the African-lineage ZIKV Uganda strain (MP-976) or the Asian-lineage ZIKV French Polynesia strain (PF13/251013-18) at a multiplicity of infection (MOI) of 0.1. Total RNA was extracted at 24, 48, and 72 hours post-infection (hpi) for transcriptomic profiling. The experiment aimed to capture temporal and strain-specific differences in host gene expression dynamics.

In It-NES® cells, the ZIKV Uganda strain exhibited a higher impact on gene expression compared to ZIKV Polynesia (Figure 7a). By more than 2-fold, ZIKV Uganda significantly upregulated 1,280 genes and downregulated 1,208 genes at 72 hpi, whereas only 258 genes were upregulated, and 12 genes were downregulated by ZIKV Polynesia at the same time point. Plaque-forming assays confirmed the production of a significantly higher number of infectious particles by ZIKV Uganda at 24 and 48 hpi, though no significant difference was observed between the two strains by 72 hpi (Figure 8).

In HaCaT cells, a similar trend was observed with ZIKV Uganda showing an overall greater influence on gene expression compared to ZIKV Polynesia. At 24 hpi, both strains upregulated over 2,500 genes, while ZIKV Uganda downregulated nearly 1,000 genes, almost twice as many as ZIKV Polynesia. By 48 hpi, the Uganda strain upregulated 2,209 genes, whereas ZIKV Polynesia upregulated 1,889. In contrast, downregulation was more pronounced in ZIKV Polynesia-infected cells. At 72 hpi, upregulation was comparable between the strains, while downregulation was higher in ZIKV Uganda-infected cells (Figure 7b).

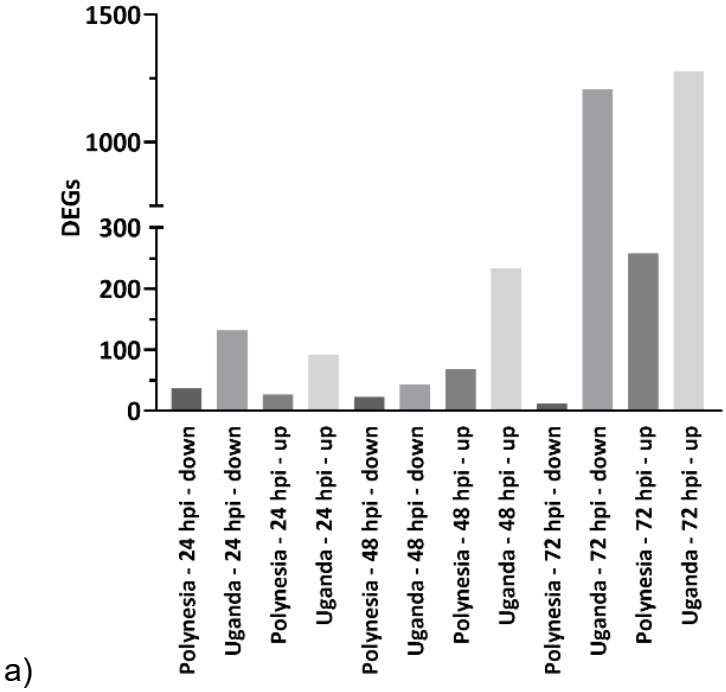

a)

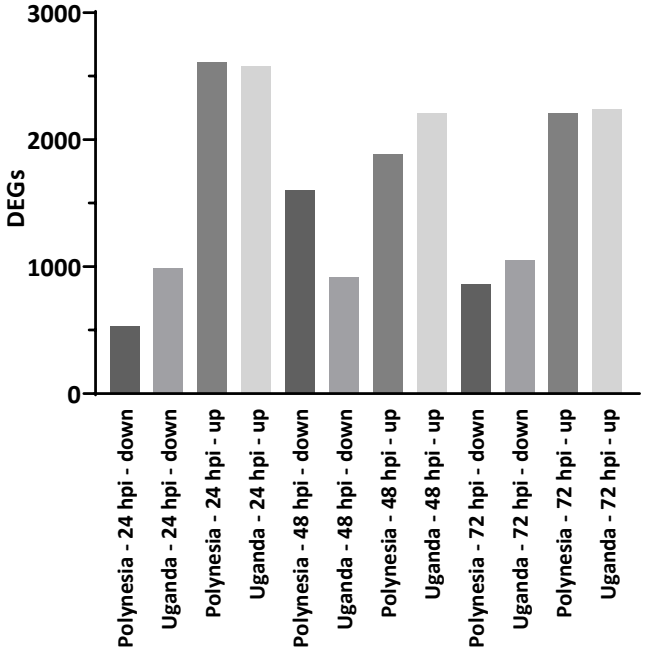

b)

Figure 7. Differentially Expressed Genes Following ZIKV Infection.
Number of ≥ 2-fold, significantly (p-value ≤ 0.05) differentially expressed genes at 24, 48, 72 hours post infection with ZIKV Polynesia and ZIKV Uganda in a) It-NES® cells (Tabari et al. 2020) and b) HaCaT cells.

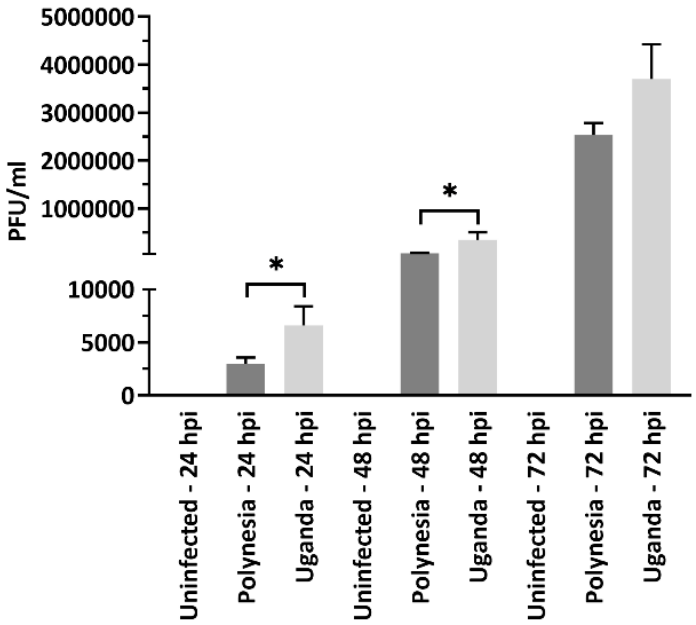

Figure 8. Plaque Forming Assays.
Quantification was performed in Vero cells by plaque-forming assays and the number of infectious viral particles is expressed in plaque forming units per mL (PFU/mL). Error bar represents the mean ± SEM of n = 3 biological replicates; *p < 0.05. Quantification of the number of extracellular infectious viral particles from It-NES® cells infected with either the Polynesia or the Uganda strain at 24, 48 and 72 hpi at MOI of 0.1 (Tabari et al. 2020).

3.2 FGF7-Mediated Modulation of Innate Immune Response in ZIKV-Infected HaCaT Cells

ZIKV transmission through mosquito bites introduces the virus directly into the skin, where local injury occurs and wound-healing pathways are activated. Fibroblast growth factor 7 (FGF7) is a key mediator of epithelial repair and is known to be upregulated during skin regeneration, acting primarily through FGFR2b and, to a lesser extent, FGFR1b (Maddaluno et al. 2020). To investigate whether FGF7 modulates the host response to ZIKV infection, HaCaT keratinocytes were treated with FGF7 after infection. This model aimed to simulate the local wound-healing environment potentially present during natural ZIKV transmission.

HaCaT cells were infected with ZIKV Uganda or ZIKV French Polynesia (MOI = 0.1), and FGF7 (20 ng/mL) was added 2 hours post-infection. Transcriptomic profiling was

conducted at 24, 48, and 72 hpi and compared to untreated infected and uninfected controls.

Gene ontology analysis of differentially expressed genes in ZIKV-infected HaCaT cells revealed a significant enrichment of immune-related processes in response to ZIKV infection, including type I interferon signalling, viral defence, and cytokine-mediated signalling pathways (Figure 9). Overall, a significant upregulation of immune response genes following ZIKV infection was observed. Notably, bone marrow stromal antigen 2 (*BST2*, also known as tetherin), a viral restriction factor, exhibited elevated expression. In addition, several interferon-stimulated genes (ISGs), including those with antiviral functions, were significantly upregulated.

In FGF7-treated ZIKV-infected HaCaT cells, ISG expression remained elevated compared to uninfected controls but was consistently lower than in untreated ZIKV-infected cells. For example, interferon-induced protein 44-like (*IFI44L*) showed a 41.4-fold increase in ZIKV Polynesia + FGF7-treated cells at 72 hpi, versus 69.2-fold in ZIKV Polynesia-infected cells without FGF7 treatment. Similarly, MX dynamin-like GTPase 2 (*MX2*) was upregulated 24.6-fold in FGF7-treated cells at 72 hpi, compared to 54.4-fold in untreated cells. This pattern of reduced ISG upregulation with FGF7 treatment was consistently observed across multiple genes at 72 hpi (Table 2). Taken together, ZIKV infection led to an upregulation of innate immune response genes in HaCaT cells, particularly ISGs, while FGF7 treatment mitigated the extent of this upregulation.

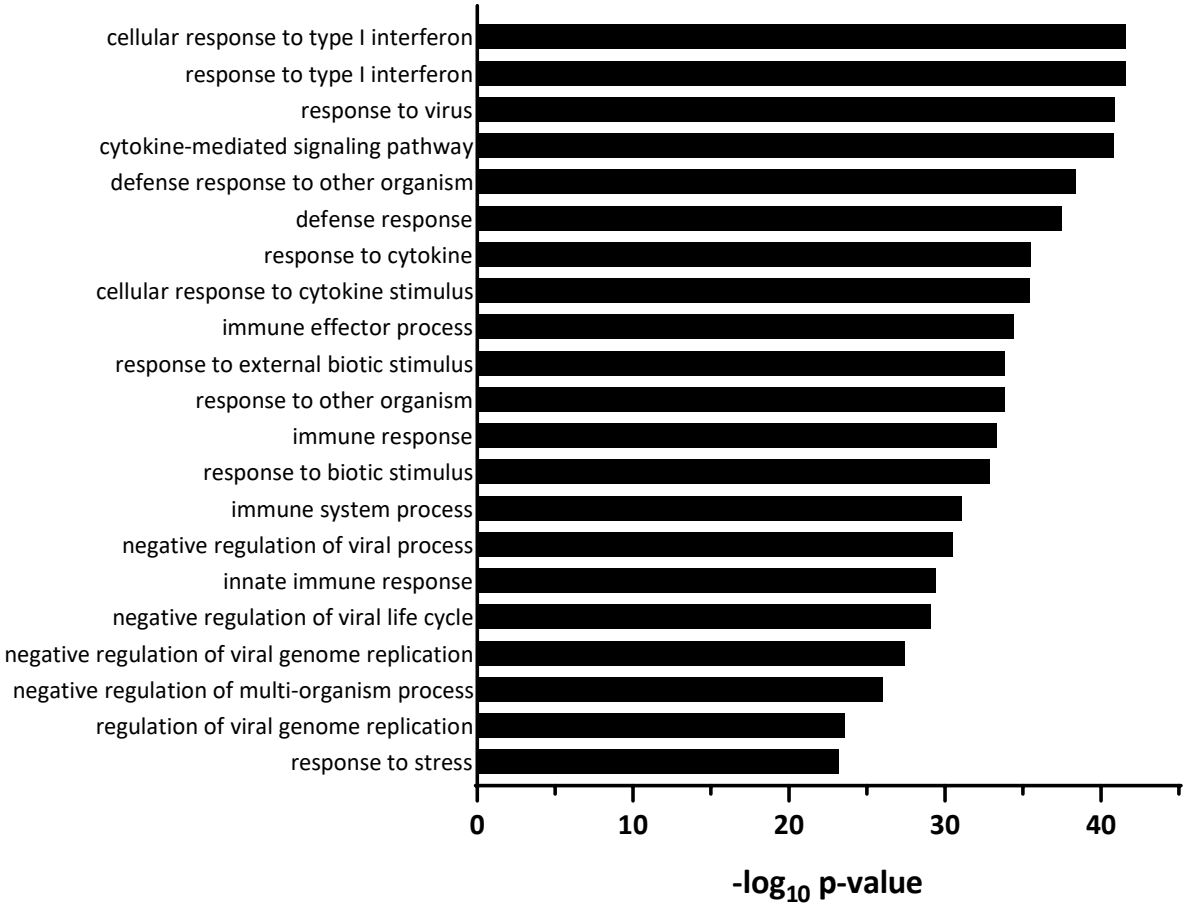

Figure 9. Gene Ontology Enrichment of Upregulated Genes in ZIKV-Infected HaCaT Cells at 72 hpi.
Top enriched biological processes identified by Gene Ontology analysis of ≥ 2-fold upregulated genes in HaCaT cells infected with ZIKV Polynesia and ZIKV Uganda at 72 hpi. Pathways ranked by significance based on -log10 p-values.

Table 2. Top Upregulated Genes in HaCaT Cells.

GeneSymbol	FC ZIKV Polynesia 24 hpi	FC ZIKV Poly + FGF7 24 hpi	FC ZIKV Uganda 24 hpi	FC ZIKV Polynesia 48 hpi	FC ZIKV Poly + FGF7 48 hpi	FC ZIKV Uganda 48 hpi	FC ZIKV Polynesia 72 hpi	FC ZIKV Poly + FGF7 72 hpi	FC ZIKV Uganda 72 hpi
IFI44L	2.3	3.1	19.1	144.2	172.8	640.4	69.2	41.4	128.8
IFNB1	-1.1	1.6	2.0	11.2	11.1	21.3	20.8	15.9	84.9
CXCL10	1.6	2.8	5.2	4.1	4.6	17.1	35.5	24.4	82.8
IFNL1	-1.2	1.8	2.8	8.2	6.6	19.5	19.1	16.0	77.7
CMPK2	1.0	1.0	2.0	9.9	9.6	20.9	51.2	30.1	76.1
MX2	2.9	2.3	14.2	250.3	193.0	758.2	54.4	24.6	74.4
IFNL2	1.5	1.6	3.5	7.1	8.5	16.8	15.8	13.4	64.2
BST2	2.7	2.3	6.4	30.8	23.7	183.0	34.4	18.3	51.4
CXCL11	1.3	1.3	1.7	4.1	2.7	14.6	23.9	14.6	48.5
BATF2	1.7	1.6	2.9	11.6	8.2	27.8	21.3	11.3	46.8
BST2	3.3	1.9	6.8	28.0	21.6	157.0	29.5	15.8	45.5
RSAD2	1.4	1.3	3.2	24.3	19.6	57.4	36.1	17.6	43.4
MX1	2.6	2.2	8.1	42.8	42.7	85.2	35.2	22.1	41.4

Top upregulated genes in HaCaT cells following infection with ZIKV Polynesia and ZIKV Uganda at 24, 48, and 72 hpi, with and without treatment with FGF7.

3.3 Dysregulation of Genes Involved in Antiviral Responses and Cell Cycle Processes in It-NES® Cells Following ZIKV Infection

In It-NES® cells, pathway analysis using the Reactome Pathway Database revealed significant alterations in gene expression following infection with both ZIKV Uganda and ZIKV Polynesia strains. Both strains primarily affected pathways related to antiviral responses, with a focus on interferon signalling and innate immune responses (Figure 11). These pathways included the upregulation of genes associated with the interferon-stimulated gene (ISG) network, antiviral defence mechanisms, and cellular stress responses. Specifically, genes involved in the ER stress response and the unfolded protein response (UPR) were notably upregulated across both strains, consistent with previous reports (J. W. Dang et al. 2019; Kozak et al. 2017). The majority of downregulated genes were related to signal transduction, cell cycle regulation, and gene expression (Figure 12, Figure 13, Table 3, Table 4). Among the most significantly affected processes by ZIKV Uganda were cell cycle-related pathways, including G1/S-specific transcription (Figure 13).

A detailed analysis of differentially expressed genes using the Comparative Toxicogenomics Database (Davis et al. 2017) identified five genes associated with microcephaly that were exclusively dysregulated in ZIKV Uganda-infected cells (Table 5). One gene, *ASNS* (asparagine synthetase), was upregulated by both ZIKV Uganda and ZIKV Polynesia strains, as confirmed by RT-qPCR (Figure 10). The five microcephaly-associated genes dysregulated only by ZIKV Uganda included *COL4A1*, *MIR17HG*, *TUBA1A*, *SLC2A1*, and *STAMBP*, all of which exhibited ≥ 2-fold changes in expression level (Table 5). These genes are known to play crucial roles in neural development and cell division.

An overall increase in innate immune response-related genes was observed over time, with *BST2* showing substantial upregulation, exhibiting a 10.2-fold increase in ZIKV Polynesia-infected cells and a 26.6-fold increase in ZIKV Uganda-infected cells by 48 hours (Table 6 and Table 7).

In summary, the data demonstrate that both ZIKV Uganda and Polynesia strains modulate gene expression in It-NES® cells, primarily dysregulating genes involved in interferon signalling and cell cycle processes, potentially contributing to ZIKV pathogenesis.

Table 3. Downregulated Genes by ZIKV Polynesia at 72 hpi.

GeneSymbol	Fold Change ZIKV Polynesia 72 hpi
YBX1	-2.6
PIAS1	-2.2
RAD1	-2.1
AGPAT9	-2.1
ADAMTS8	-2.0
LRP2	-2.0

Table 4. Top Downregulated Genes by ZIKV Uganda at 72 hpi.

GeneSymbol	Fold Change ZIKV Uganda 72 hpi
LSP1	-7.4
COL9A1	-5.6
MIR670HG	-5.1
CTSC	-4.6
HES5	-4.4
CCDC177	-4.4
SMOC1	-4.2
HES3	-4.2
KCNS3	-4.0
RNASE4	-4.0
AGPS	-3.9
LIX1	-3.9
L3MBTL3	-3.8
GAL3ST3	-3.8
TRHDE-AS1	-3.8
OVOS2	-3.8
TPM3	-3.8
TARDBP	-3.7

Table 5. Comparative Toxicogenomics Database Screening.

GeneSymbol	Fold Change ZIKV Uganda	p-value ZIKV Uganda	Fold Change ZIKV Polynesia	p-value ZIKV Polynesia
COL4A1	-2.1	0.0093	-1.2	0.635
MIR17HG	-2.3	0.0497	-1.3	0.749
TUBA1A	-2.2	2.56E-04	-1.5	0.256
SLC2A1	-2.3	0.0239	1.0	0.806
ASNS	9.6	0.0314	2.9	0.006
STAMBP	2.5	1.07E-04	1.4	0.975

Genes dysregulated by ZIKV Uganda > 2-fold and by ZIKV Polynesia, which are associated with microcephaly according to Comparative Toxicogenomics Database (Davis et al. 2017; Tabari et al. 2020).

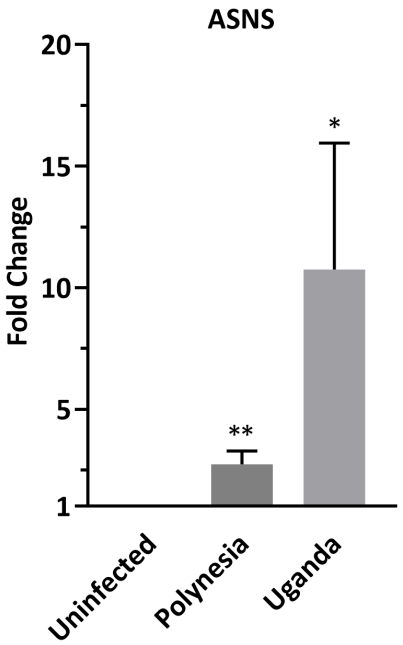

Figure 10. Dysregulation of *ASNS* by ZIKV Uganda and Polynesia in It-NES® Cells. Relative *ASNS* mRNA levels measured by qRT-PCR presented as fold change compared to uninfected control cells at 72 hpi at MOI of 0.1. Error bar represents the mean ± SEM of n = 3 biological replicates; *p < 0.05; **p < 0.01 (Tabari et al. 2020).

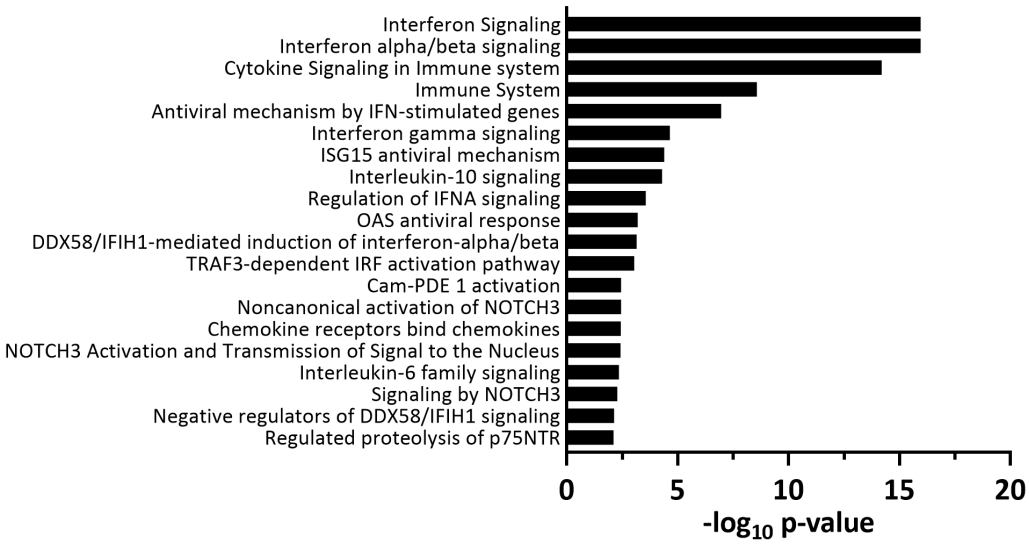

(a)

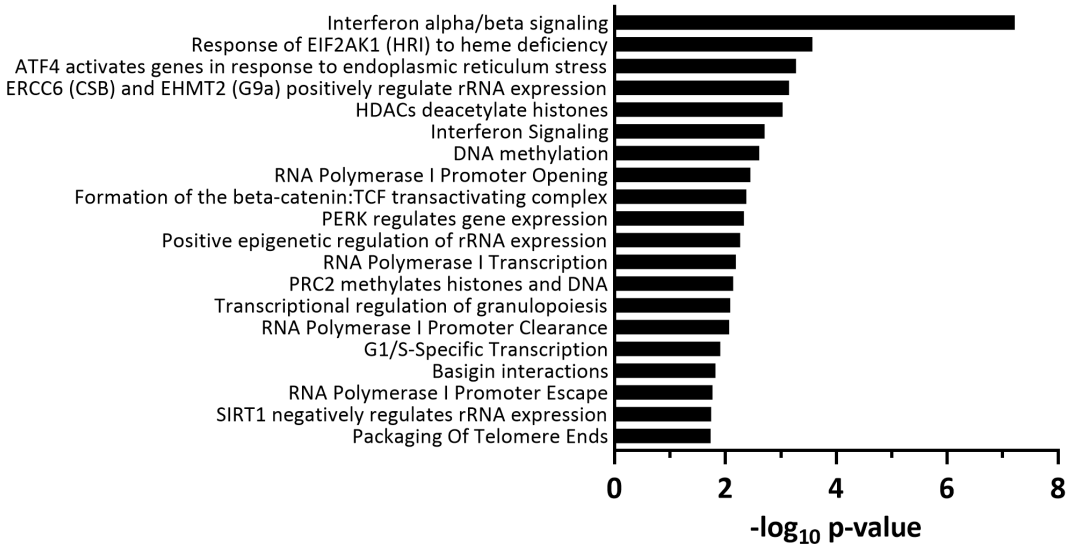

(b)

Figure 11. Top 20 Enriched Pathways Identified by Functional Reactome Analysis. Pathway analysis of ≥ 2-fold up- and downregulated genes upon infection with either (a) ZIKV Polynesia or (b) ZIKV Uganda. Pathways ranked according to -log$_{10}$ p-value (Tabari et al. 2020).

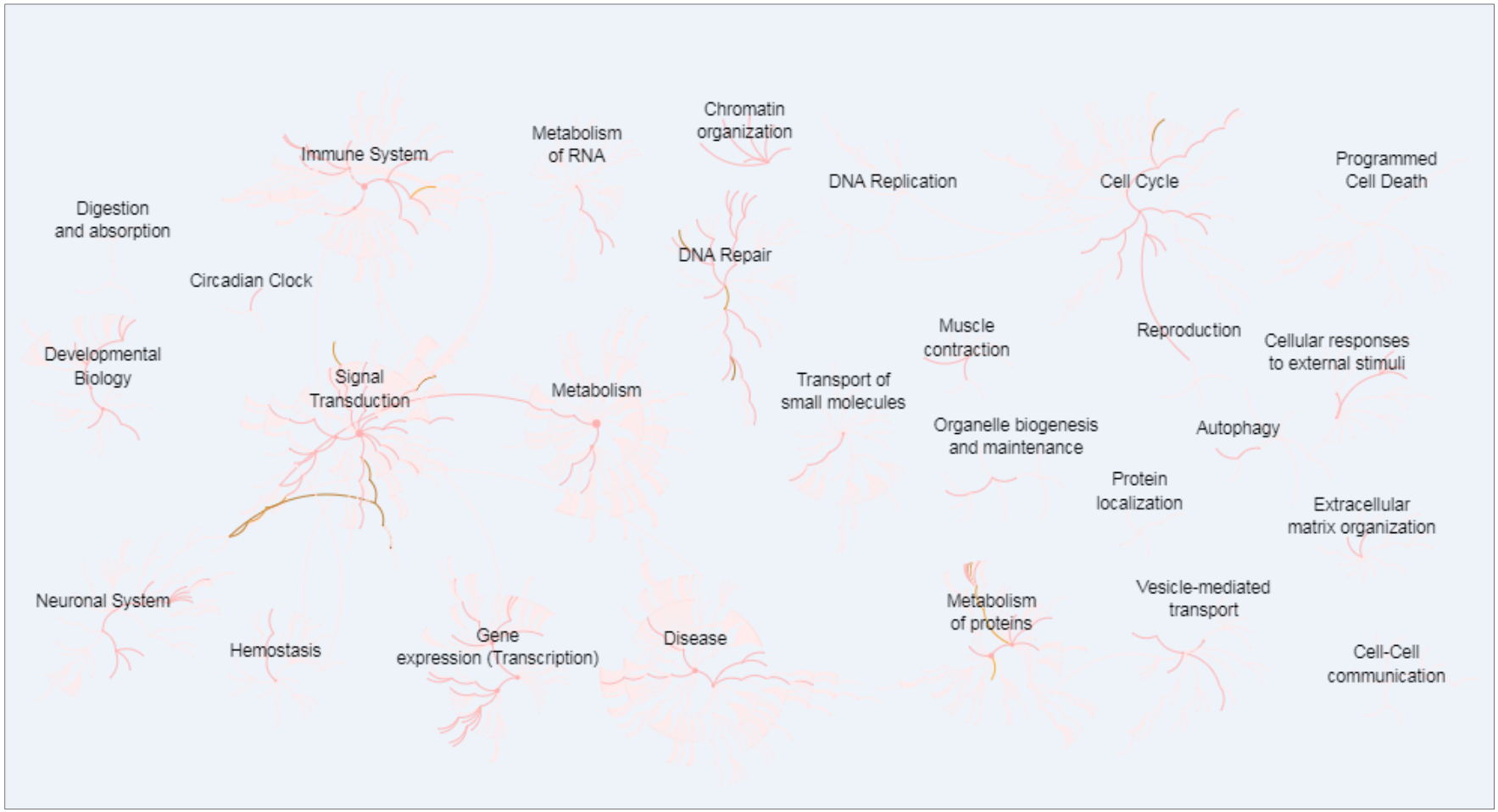

Figure 12. Pathway Enrichment Network of Downregulated Genes in ZIKV Polynesia-Infected It-NES® Cells. Genome-wide overview pathway analysis of ≥ 2-fold downregulated genes for ZIKV Polynesia. Pathway over-representation is indicated by increased line intensity within the network structure (Tabari et al. 2020).

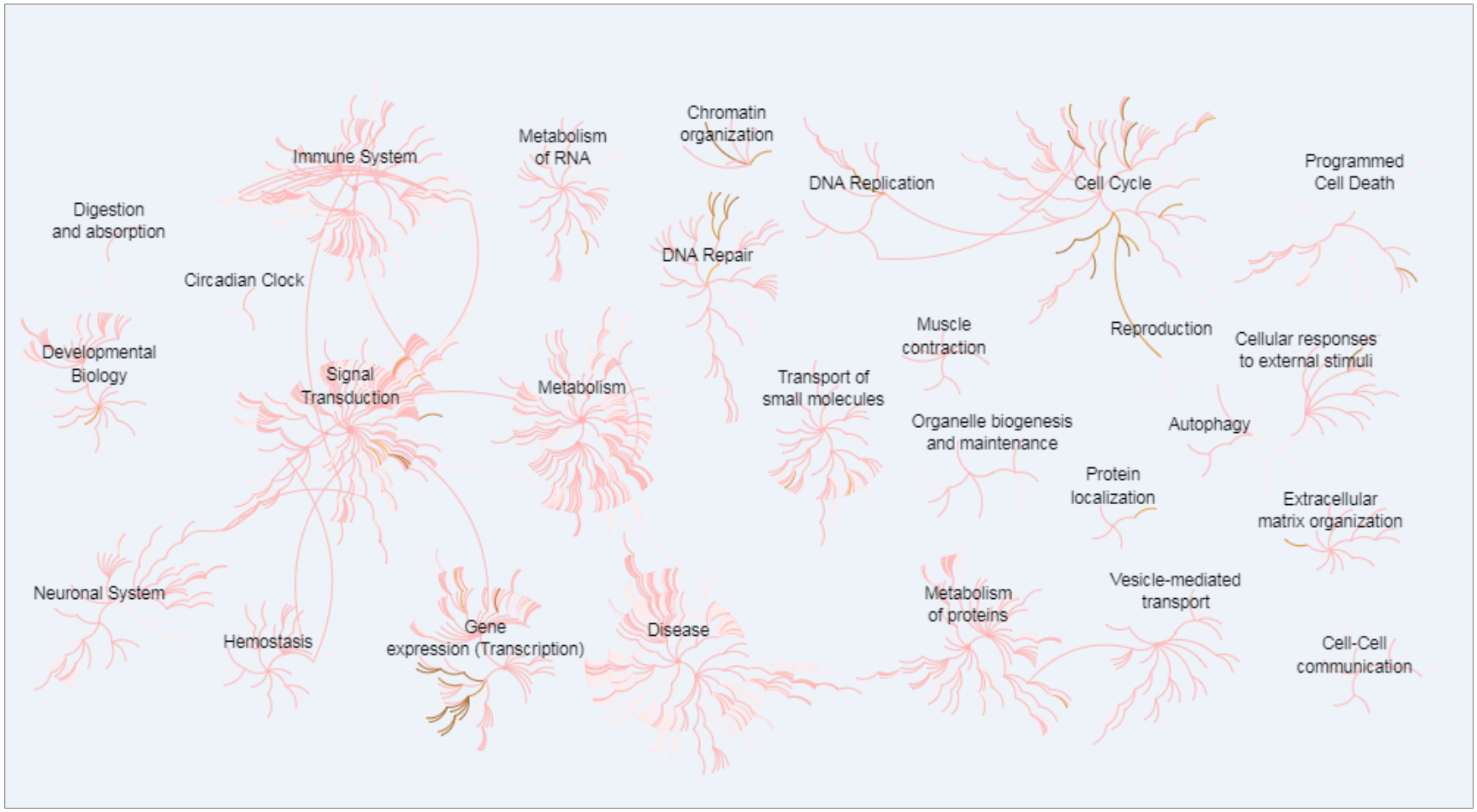

Figure 13. Pathway Enrichment Network of Downregulated Genes in ZIKV Uganda-Infected It-NES® Cells.
Genome-wide overview pathway analysis of ≥ 2-fold downregulated genes for ZIKV Uganda. Pathway over-representation is indicated by increased line intensity within the network structure (Tabari et al. 2020).

Table 6. Top Upregulated Genes by ZIKV Uganda.

GeneSymbol	Fold Change ZIKV Uganda 24 hpi	Fold Change ZIKV Uganda 48 hpi	Fold Change ZIKV Uganda 72 hpi
OASL	1.6	49.9	766.7
CH25H	2.5	46.8	611.3
IFNB1	2.3	37.9	554.3
CXCL10	-1.3	40.8	521.3
IFIT2	1.0	30.7	218.8
IFIH1	2.1	38.1	176.4
PRDM16	8.1	23.5	141.9
CCL5	-1.3	10.3	117.1
CXCL11	1.1	12.8	104.1
GSC	1.2	9.0	60.4
BST2	1.8	26.6	59.0
IFI44	2.4	20.8	55.5
PKD1L2	2.8	9.6	49.9
DHX58	1.3	8.3	46.3
ATP4A	1.1	3.7	38.3
TMEM71	2.5	8.7	35.8
CEACAM1	1.4	6.8	35.8
NEURL3	1.2	10.5	34.0
IFI6	1.0	9.1	33.8

Table 7. Top Upregulated Genes by ZIKV Polynesia.

GeneSymbol	Fold Change ZIKV Polynesia 24 hpi	Fold Change ZIKV Polynesia 48 hpi	Fold Change ZIKV Polynesia 72 hpi
BST2	1.2	10.2	459.5
OAS1	-1.0	2.7	261.2
IFIH1	1.5	11.8	219.1
IFNB1	1.4	4.3	211.2
OASL	-1.1	6.3	193.1
CXCL10	1.0	4.2	147.1
IFITM1	1.4	4.8	133.1
HERC6	1.1	3.2	130.7
CH25H	1.5	3.0	126.7
IFI44	2.1	11.6	124.7
IFI6	-1.0	3.7	118.3
SAMD9L	-1.0	6.2	105.6
IFIT2	1.3	5.1	96.8
MX1	1.1	4.3	90.2
ISG15	-1.0	5.1	67.5
OAS2	-1.1	2.4	54.4
DDX60	1.0	4.3	52.0

3.4 miRNA Dysregulation and Neurodevelopmental Implications in ZIKV-Infected lt-NES® Cells

Following the transcriptomic analysis to investigate ZIKV's effects on gene expression, miRNA regulation was also profiled in lt-NES® cells infected with ZIKV strains from Uganda and French Polynesia at 24, 48, and 72 hpi at an MOI of 0.1. Both ZIKV strains induced widespread miRNA dysregulation, with a greater number of miRNAs being upregulated than downregulated (Figure 14a). A notable overlap was observed between the two strains, with both dysregulating the same 70 miRNAs (Figure 14b, Table 8). Of these, 69 miRNAs were upregulated, and only one, miR-182-5p, was consistently downregulated by both strains.

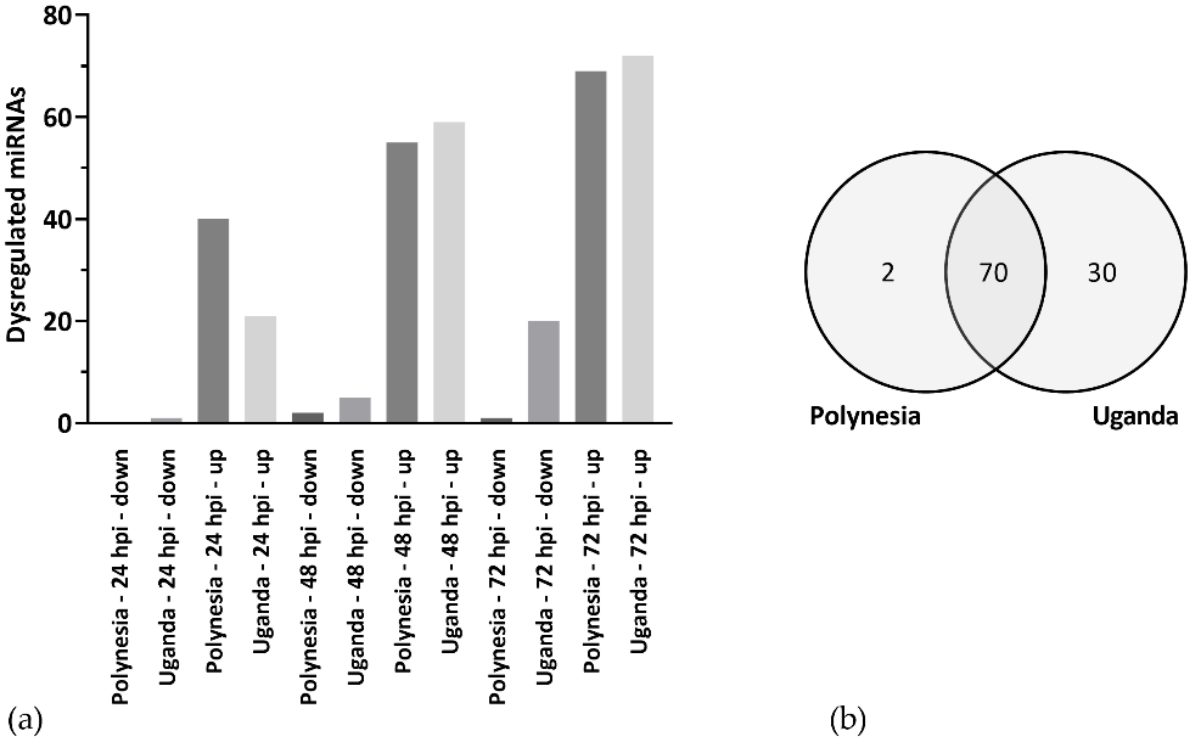

Figure 14. Overview of Dysregulated miRNAs in ZIKV-Infected lt-NES® Cells.
(a) Number of more than 2-fold, significantly (p-value ≤ 0.05) dysregulated miRNAs by ZIKV Polynesia and Uganda at 24, 48, 72 hpi. (b) Significantly more than 2-fold dysregulated miRNAs by ZIKV Polynesia and Uganda including all time points (Tabari et al. 2020).

To further investigate the role of these differentially regulated miRNAs, potential target genes were predicted using the microRNA Target prediction in Coding DNA Sequences (microT-CDS, v5.0) database, followed by Gene Ontology analysis, which focused on biological processes. The dysregulated miRNAs shared between the two strains were implicated in pathways such as the neurotrophin tropomyosin receptor kinase receptor signalling pathway, synaptic transmission, and the mitotic cell cycle (Figure 15a). These pathways were also enriched among the 30 miRNAs dysregulated only by ZIKV Uganda (Table 9, Figure 16).
One miRNA of particular interest, miR-7704, was upregulated by both ZIKV strains and was associated with developmental processes, including neural tube formation (Figure 15b). An integrative analysis cross-referencing differentially expressed mRNAs with miRNA target predictions revealed several downregulated genes, such as *EPHB4* (Ephrin Receptor B4) and *CNP* (2',3'-Cyclic Nucleotide 3' Phosphodiesterase), which are involved in neurodevelopment and may be regulated by the upregulated miRNAs. Thus, multiple miRNAs could potentially affect the same mRNA targets.

Additionally, miRNA profiling identified two miRNAs, miR-433-5p and miR-205-5p, that were significantly downregulated only by ZIKV Polynesia (Figure 17). Notably, miR-205-5p was predicted to target the upregulated gene *ASNS* (Asparagine Synthetase). However, further experiments are necessary to validate the interaction between miR-205-5p and *ASNS* in It-NES® cells.

Overall, these findings indicate that ZIKV infection significantly alters miRNA regulation in It-NES® cells, with both ZIKV Uganda and ZIKV Polynesia showing similar patterns of miRNA dysregulation. The dysregulated miRNAs may play key roles in neurodevelopmental and cell cycle-related pathways and could be involved in ZIKV pathogenesis.

Table 8. Intracellular mature miRNAs dysregulated by ZIKV Polynesia and Uganda.

miRNA ID	log2 Fold Change ZIKV Polynesia	log2 Fold Change ZIKV Uganda
hsa-miR-6786-5p	9.20	11.32
hsa-miR-6090	8.58	10.18
hsa-miR-6746-3p	8.02	9.67
hsa-miR-5690	7.96	9.55
hsa-miR-6075	7.93	10.32
hsa-miR-718	7.78	9.55
hsa-miR-6084	7.55	9.75
hsa-miR-3195	7.08	9.20
hsa-miR-4667-5p	6.88	9.86
hsa-miR-6126	6.75	9.53
hsa-miR-3659	6.56	8.21
hsa-miR-4763-5p	6.48	8.94
hsa-miR-3621	6.47	8.68
hsa-miR-211-5p	6.46	9.56
hsa-miR-4634	6.37	8.46
hsa-miR-887-3p	6.36	7.92
hsa-miR-4800-5p	6.27	8.47
hsa-miR-638	6.23	9.04
hsa-miR-7161-3p	6.21	8.05
hsa-miR-4787-5p	6.18	8.09
hsa-miR-186-3p	6.07	7.36
hsa-miR-3614-3p	5.99	8.94
hsa-miR-4459	5.95	8.82
hsa-miR-6088	5.88	8.40
hsa-miR-6087	5.77	8.32
hsa-miR-4662a-5p	5.74	6.52
hsa-miR-3692-5p	5.70	7.67
hsa-miR-4449	5.69	7.33
hsa-miR-4516	5.57	8.12
hsa-miR-6509-5p	5.54	8.19
hsa-miR-6724-5p	5.46	8.30
hsa-miR-1181	5.41	7.39
hsa-miR-3960	5.37	7.62
hsa-miR-611	5.36	6.87
hsa-miR-3656	5.27	7.22
hsa-miR-1343-5p	5.25	8.61
hsa-miR-3141	5.24	7.15
hsa-miR-4792	5.14	7.60
hsa-miR-5787	5.07	7.16
hsa-miR-4743-5p	5.06	6.69
hsa-miR-6836-3p	5.01	7.30
hsa-miR-4654	4.98	7.41
hsa-miR-6510-5p	4.67	6.38

Table 8. Intracellular mature miRNAs dysregulated by ZIKV Polynesia and Uganda.

miRNA ID	log2 Fold Change ZIKV Polynesia	log2 Fold Change ZIKV Uganda
hsa-miR-6089	4.65	7.09
hsa-miR-759	4.47	6.47
hsa-miR-874-5p	4.21	7.92
hsa-miR-6836-5p	4.09	6.74
hsa-miR-6873-3p	4.08	6.19
hsa-miR-4800-3p	4.07	5.77
hsa-miR-1469	4.00	5.60
hsa-miR-6793-5p	3.93	6.67
hsa-miR-875-5p	3.86	6.57
hsa-miR-6876-3p	3.84	5.14
hsa-miR-4508	3.81	5.71
hsa-miR-6861-5p	3.78	6.99
hsa-miR-663a	3.78	5.99
hsa-miR-6870-5p	3.69	6.39
hsa-miR-6790-3p	3.56	5.91
hsa-miR-5585-5p	3.53	7.04
hsa-miR-4739	3.49	4.95
hsa-miR-4497	3.24	4.94
hsa-miR-183-5p	3.01	4.63
hsa-miR-7641	2.84	6.26
hsa-miR-4771	2.76	5.86
hsa-miR-589-5p	2.06	4.22
hsa-miR-92a-1-5p	1.88	3.12
hsa-miR-1261	1.20	3.59
hsa-miR-125b-1-3p	1.19	3.90
hsa-miR-7704	3.91	6.14
hsa-miR-182-5p	-1.51	-1.40

Table 9. Intracellular mature miRNAs dysregulated by ZIKV Uganda.

miRNA ID ZIKV Polynesia	log2 Fold Change ZIKV Uganda
hsa-miR-5701	6.15
hsa-miR-619-5p	3.48
hsa-miR-212-5p	2.82
hsa-miR-99b-3p	1.69
hsa-miR-99b-5p	1.35
hsa-let-7e-5p	1.28
hsa-miR-181a-2-3p	1.18
hsa-miR-125a-5p	1.09
hsa-miR-21-5p	1.00
hsa-miR-1180-3p	-1.13
hsa-miR-92b-3p	-1.16
hsa-miR-127-3p	-1.18
hsa-miR-493-5p	-1.21
hsa-miR-543	-1.21
hsa-miR-4652-3p	-1.26
hsa-miR-335-3p	-1.26
hsa-miR-654-3p	-1.27
hsa-miR-92a-3p	-1.30
hsa-miR-30c-5p	-1.33
hsa-miR-431-5p	-1.34
hsa-miR-28-5p	-1.40
hsa-miR-301a-5p	-1.44
hsa-miR-328-3p	-1.47
hsa-miR-1260b	-1.49
hsa-miR-4456	-1.56
hsa-miR-411-3p	-1.59
hsa-miR-484	-1.68
hsa-miR-151a-5p	-1.76
hsa-miR-4473	-2.15
hsa-miR-4455	-3.12

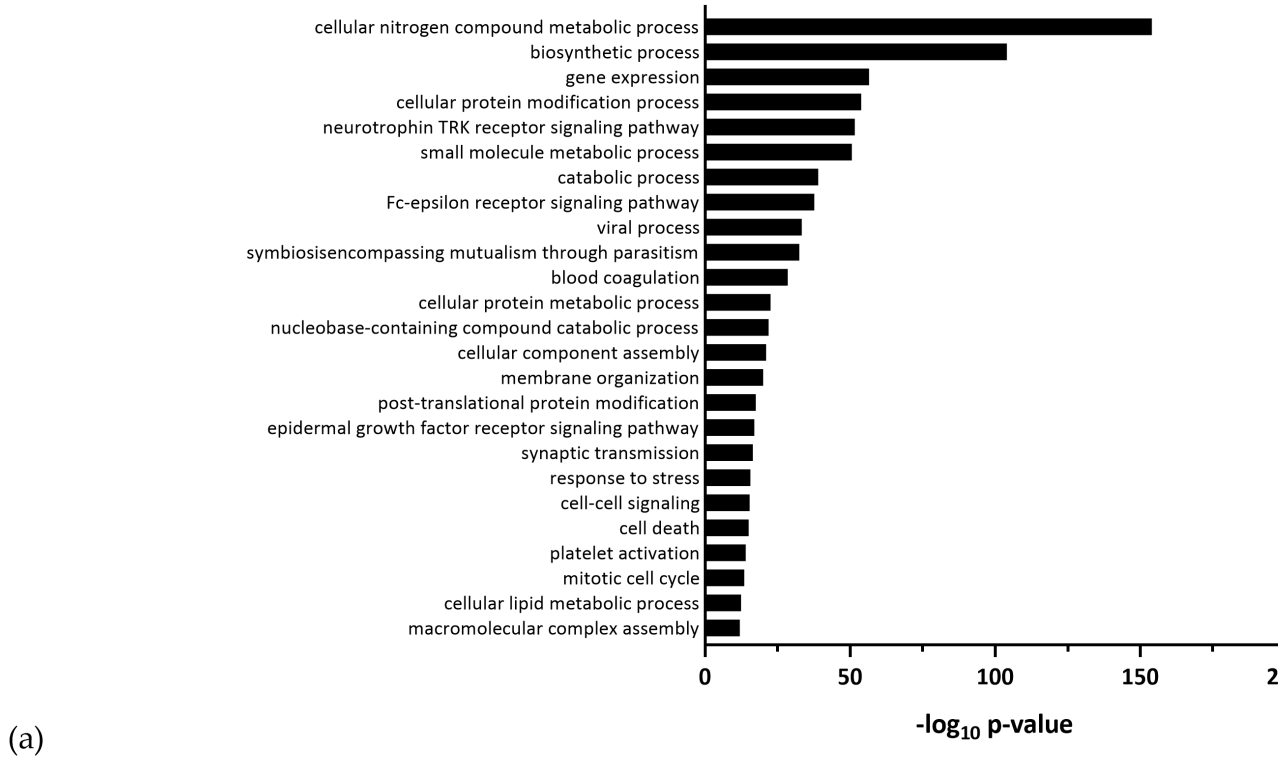

(a)

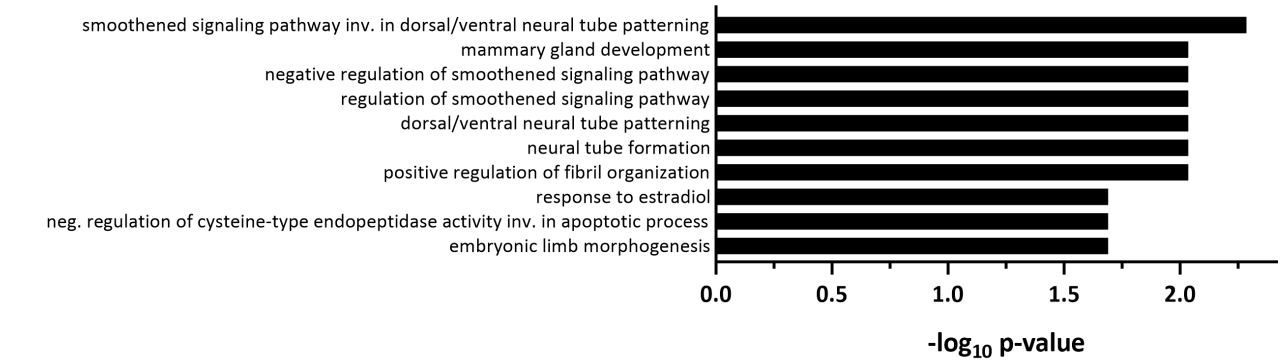

(b)

Figure 15. Gene Ontology Analysis of Potential Target Genes of miRNAs Altered by ZIKV Polynesia and Uganda.
(a) GO analysis of biological processes of putative targets of miRNAs which were dysregulated in lt-NES® cells during infection with ZIKV Polynesia and Uganda. (b) GO analysis of biological processes of putative targets of miR-7704, which was upregulated by ZIKV Polynesia and Uganda (Tabari et al. 2020).

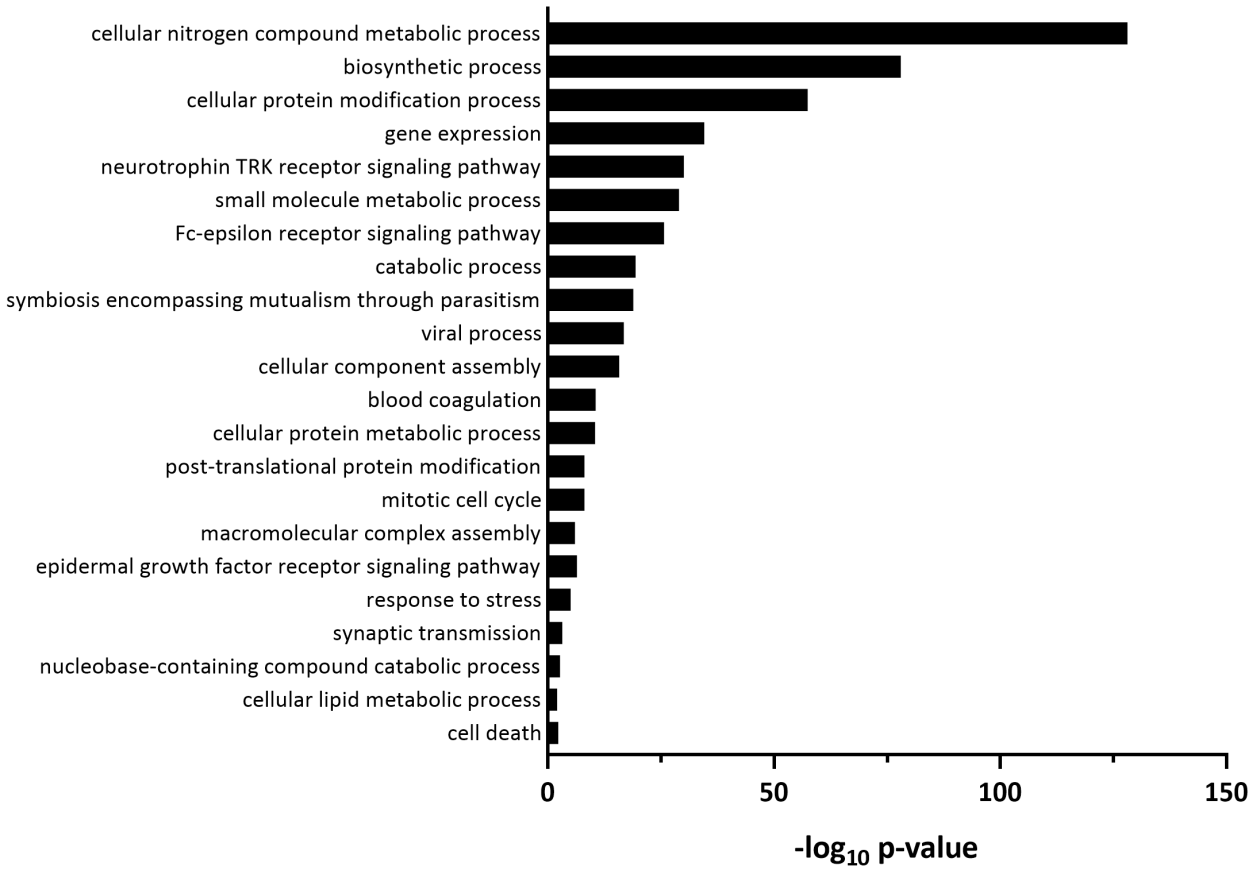

Figure 16. Gene Ontology Analysis of Potential Target Genes of miRNAs Altered by ZIKV Uganda**.**
GO analysis of biological processes of potential target genes of miRNAs, which were dysregulated in lt-NES® cells only during infection with ZIKV Uganda (Tabari et al. 2020).

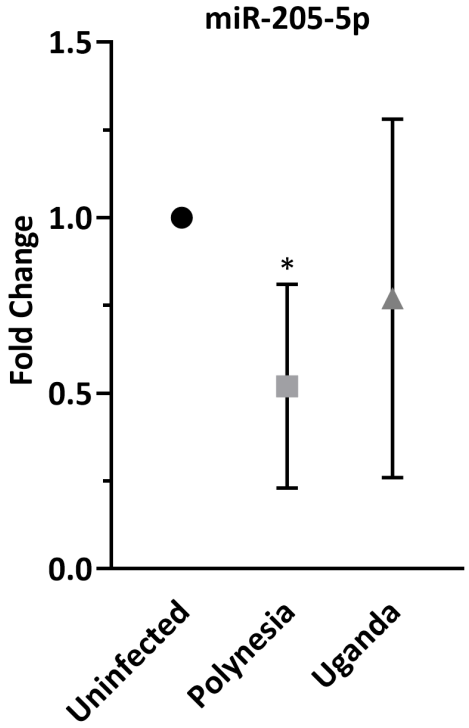

Figure 17. Dysregulation of miR-205 by ZIKV Uganda and Polynesia.
Relative miR-205 levels measured by qRT-PCR presented as fold change compared to uninfected control cells at 48 hpi at a MOI of 0.1. Error bar represents the mean ± SEM of n = 3 biological replicates; *p < 0.05 (Tabari et al. 2020).

3.5 Modulation of miRNAs in Extracellular Vesicles Following ZIKV Infection

Given the essential role of extracellular vesicle (EV)-derived miRNAs in intercellular communication, and their potential involvement in viral dissemination and pathogenesis, EV-associated miRNAs were analysed at 24, 48, and 72 hpi in lt-NES® cells infected with ZIKV Uganda and ZIKV Polynesia strains at a MOI of 1 (Gurunathan et al. 2019; Martínez-Rojas et al. 2025). Uninfected cells under the same conditions served as controls.

ZIKV Uganda infection led to a time-dependent increase in the levels of EV-associated miRNAs, while ZIKV Polynesia showed a stronger effect on EV miRNA signatures at 48 hpi (Figure 18a). A total of five miRNAs were identified with altered levels in EVs in response to both ZIKV strains (Figure 18b).

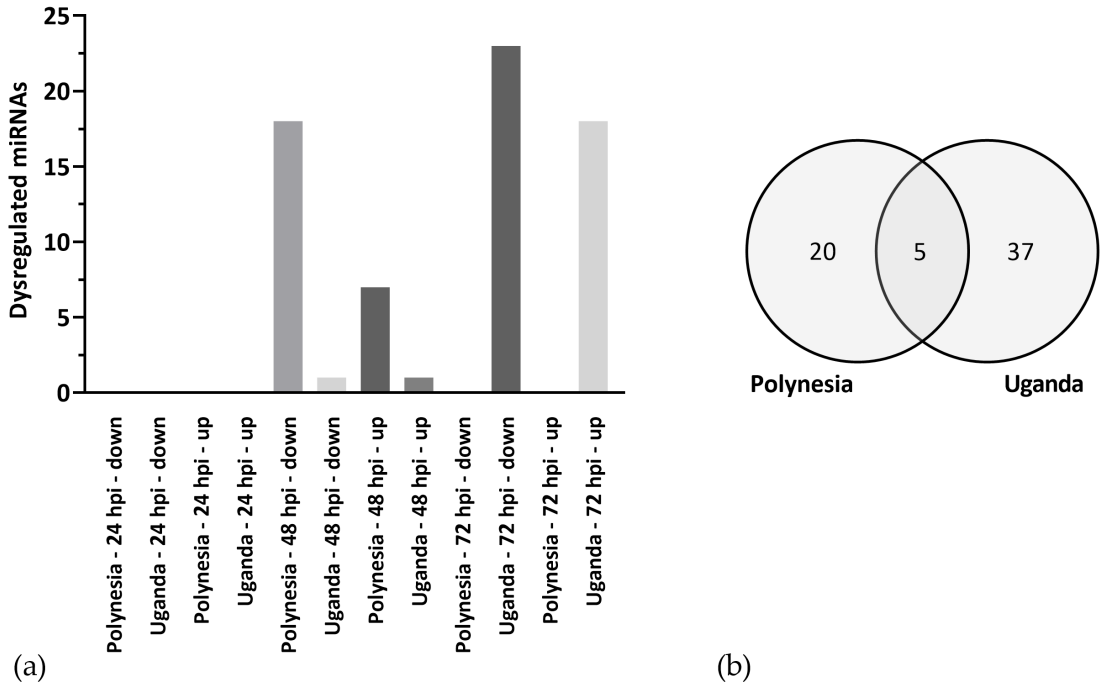

Figure 18. Altered EV-derived miRNA Levels Following ZIKV Infection.
(a) Significantly ≥ 2-fold dysregulated mature miRNAs, which were incorporated into EVs during infection of lt-NES® cells with either ZIKV Polynesia or Uganda. (b) EV-derived miRNAs with levels altered (≥ 2-fold) following infection with ZIKV Polynesia and Uganda at any time point (Tabari et al. 2020).

KEGG pathway analysis of potential targets for these altered miRNAs, performed using the Diana mirPath v3 tool, revealed significant enrichment in pathways involved in neurodevelopmental processes, including Wnt signalling, Pi3K-Akt signalling, and pluripotency regulation of stem cells (Figure 19). Both ZIKV strains also modulated EV-associated miRNAs implicated in FoxO signalling and axon guidance pathways.

One miRNA of particular interest, miR-4792, exhibited a significant increase in EVs following infection with both ZIKV Polynesia (1.4-fold) and ZIKV Uganda (2.9-fold) at 48 hpi. Additionally, intracellular levels of miR-4792 were upregulated by both strains at various time points, and this upregulation was validated using RT-qPCR (Figure 20). Gene Ontology analysis of predicted miR-4792 targets, based on experimentally validated data from the Tarbase database, indicated that these targets are involved in processes such as in utero embryonic development and negative regulation of oxidoreductase activity (Table 10).

Previous studies have demonstrated interactions between miR-4792 and forkhead box C1 (*FOXC1*) in various cell lines (Y. Li and Chen 2015; Liu et al. 2019). To explore this in the context of ZIKV infection, *FOXC1* mRNA expression was analysed in lt-NES® cells, revealing slight downregulation after infection with both ZIKV strains (Figure 21). However, further research is required to determine whether this downregulation is directly mediated by the upregulation of miR-4792 in response to ZIKV infection in lt-NES® cells.

In summary, ZIKV infection alters the secretion of host miRNAs in extracellular vesicles, particularly miR-4792, which is linked to oxidative and neurodevelopmental pathways. These changes suggest a potential role for EV-associated miRNAs in ZIKV-induced neuropathogenesis.

Table 10. miR-4792: Diana mirPath v3 Gene Ontology Analysis

GO Category	p-value	#genes
gene expression	2.49E-05	12
cellular nitrogen compound metabolic process	0.00013	37
macromolecular complex assembly	0.00162	13
protein complex assembly	0.01012	11
cellular component assembly	0.01986	14
biosynthetic process	0.02673	28
biological process	0.02901	90
negative regulation of oxidoreductase activity	0.03821	2
in utero embryonic development	0.03821	7

Biological processes, in which potential targets of miR-4792 are involved, as predicted by TarBase.

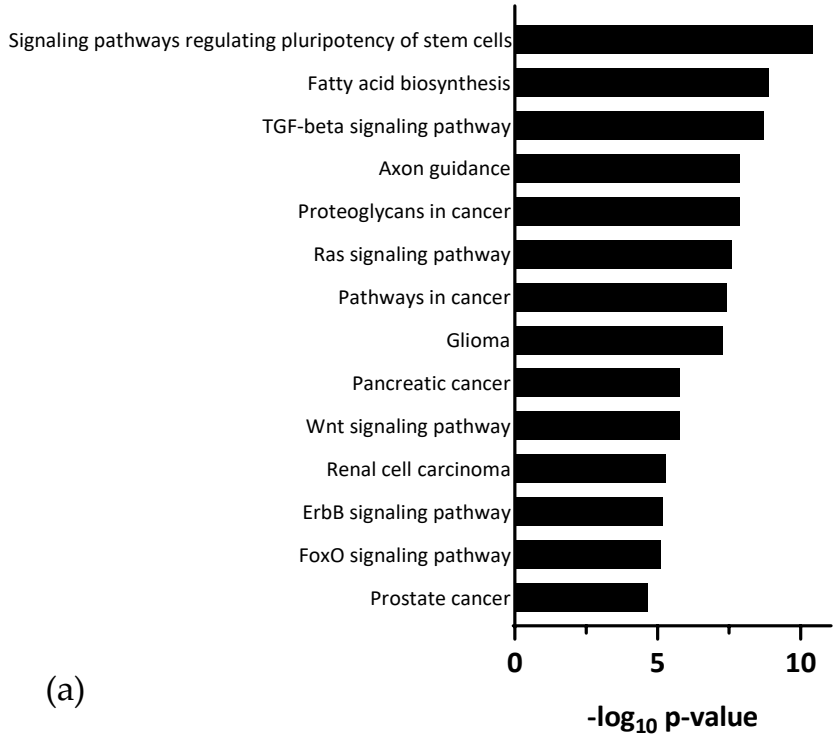

(a)

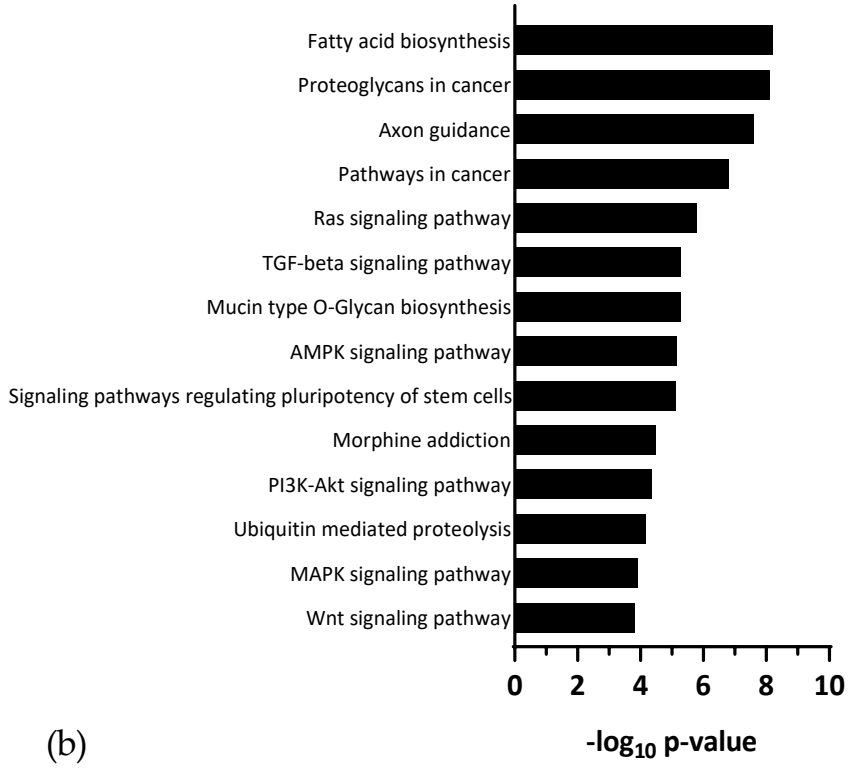

(b)

Figure 19. KEGG Pathway Enrichment of Predicted Targets of EV-Derived miRNAs. KEGG Pathway analysis of potential targets of EV-derived miRNAs that were differentially incorporated following infection with (a) ZIKV Polynesia and (b) ZIKV Uganda (Tabari et al. 2020).

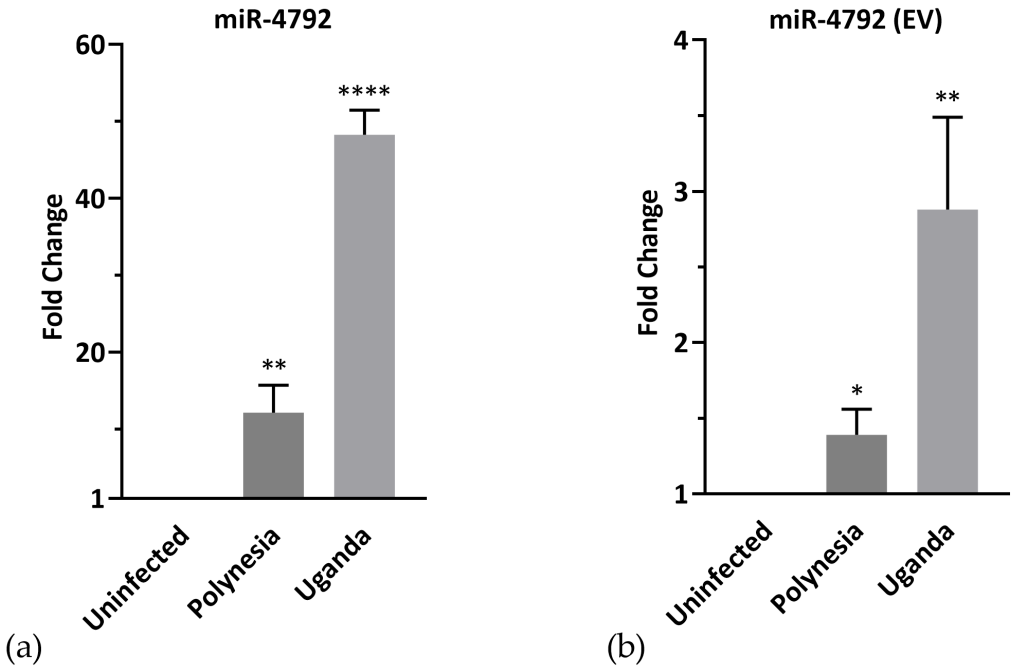

Figure 20: Dysregulation of miR-4792 by ZIKV Uganda and Polynesia.
(a) Relative intracellular miR-4792 levels measured by qRT-PCR presented as fold change compared to uninfected control cells at 72 hpi at MOI of 0.1. Error bar represents the mean ± SEM of n = 3 biological replicates; **p < 0.01; ****p < 0.0001. (b) Relative EV-derived miR-4792 levels measured by qRT-PCR presented as fold change compared to uninfected control cells at 48 hpi at MOI of 1. Error bar represents the mean ± SEM of n = 3 biological replicates; *p < 0.05; **p < 0.01 (Tabari et al. 2020).

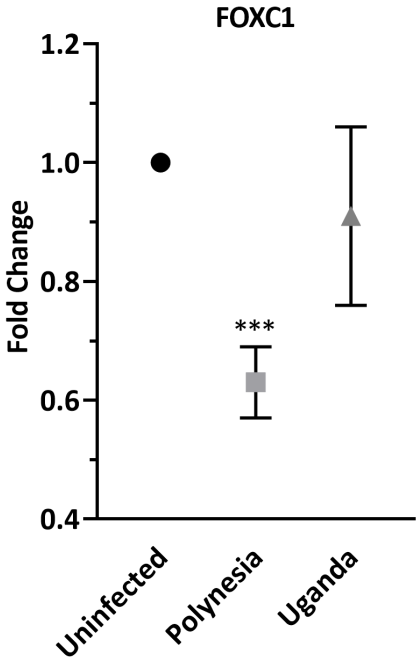

Figure 21. Dysregulation of *FOXC1* by ZIKV Uganda and Polynesia.
Relative *FOXC1* mRNA levels measured by qRT-PCR presented as fold change compared to uninfected control cells at 72 hpi at MOI of 0.1. Error bar represents the mean ± SEM of n = 3 biological replicates; ***p < 0.001 (Tabari et al. 2020).

3.6 Regulation of Oxidative Stress in ZIKV-Infected Cells

Previous studies have linked ER stress and increased ROS to *Flaviviridae* pathogenesis and to the induction of autophagy, which can facilitate viral morphogenesis (Bender and Hildt 2019; Medvedev et al. 2017). In this context, the effect of ZIKV infection on miRNA-dependent regulation of genes related to oxidative and ER stress was investigated. To evaluate whether ZIKV induces oxidative stress, the carbonylation of proteins by ROS was quantified using oxyblots. ZIKV Uganda and ZIKV Polynesia infections significantly increased the levels of oxidative modified proteins compared to uninfected cells at 48 and 72 hpi, indicating the induction of oxidative stress during ZIKV infection (Figure 22, Figure 23).

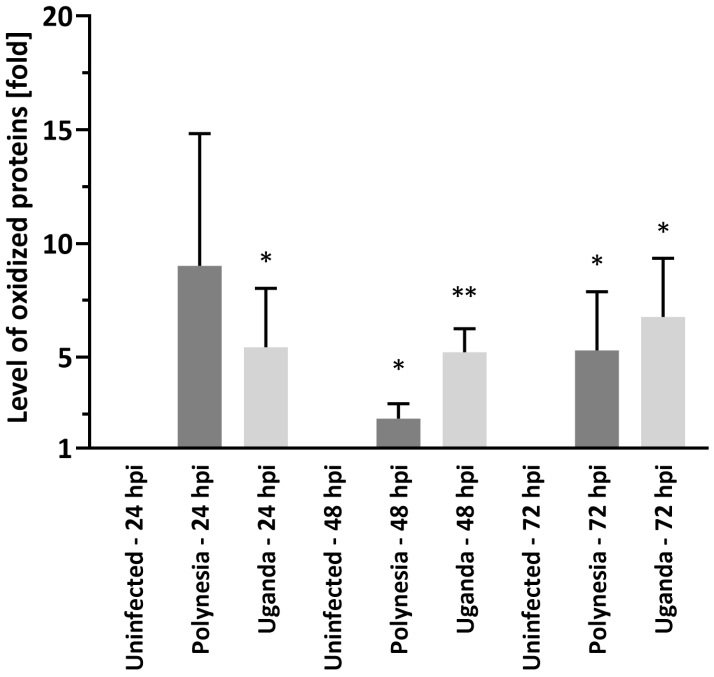

Figure 22. Increased Protein Oxidation in ZIKV-Infected It-NES® Cells.
Oxyblot analysis of lysates derived from uninfected It-NES® cells and It-NES® cells, which were infected with ZIKV Uganda and ZIKV Polynesia at MOI of 1 at 24, 48, 72 hpi. Protein oxidation was analysed by incubation with 2,4,-dinitrophenylhydrazine (DNPH) for covalent modification of oxidative modified proteins. Error bar represents the mean ± SEM of n = 3 biological replicates; *p < 0.05; **p < 0.01 (Tabari et al. 2020).

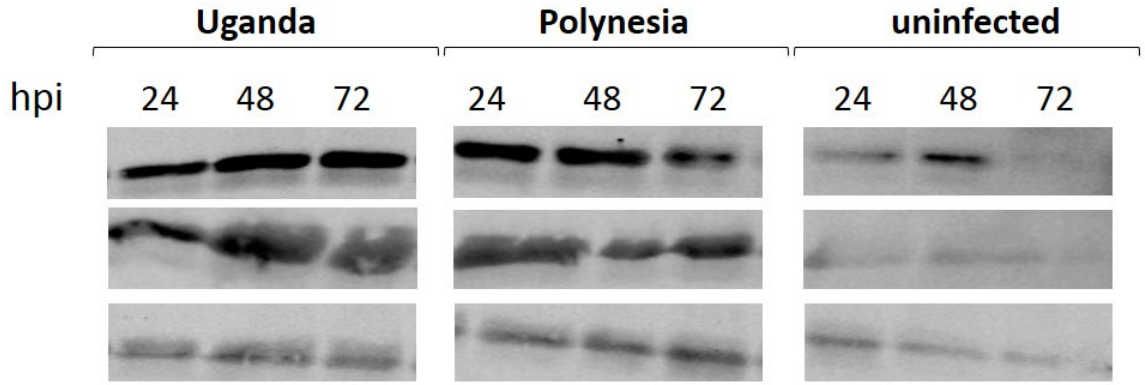

Figure 23. OxyBlot of Oxidized Proteins in ZIKV-Infected It-NES® Cells.
Oxyblot analysis of lysates derived from It-NES® cells, which were infected with ZIKV Polynesia and Uganda at MOI of 1 and from uninfected It-NES® cells. Protein oxidation was analysed by incubation with 2,4,-dinitrophenylhydrazine (DNPH) for covalent modification of oxidative modified proteins (Tabari et al. 2020).

Next, the impact of ZIKV on the Nrf2/ARE-regulated antioxidant response was investigated. As Nrf2 requires nuclear small musculoaponeurotic fibrosarcoma (sMaf) proteins to drive antioxidant gene expression, their localization was analysed to assess whether ZIKV perturbs this interaction (Yamamoto et al. 2018). Immunofluorescence analysis showed colocalization of ZIKV Uganda and Polynesia envelope proteins with sMaf, along with an enrichment of sMaf in perinuclear regions post-infection (Figure 24).

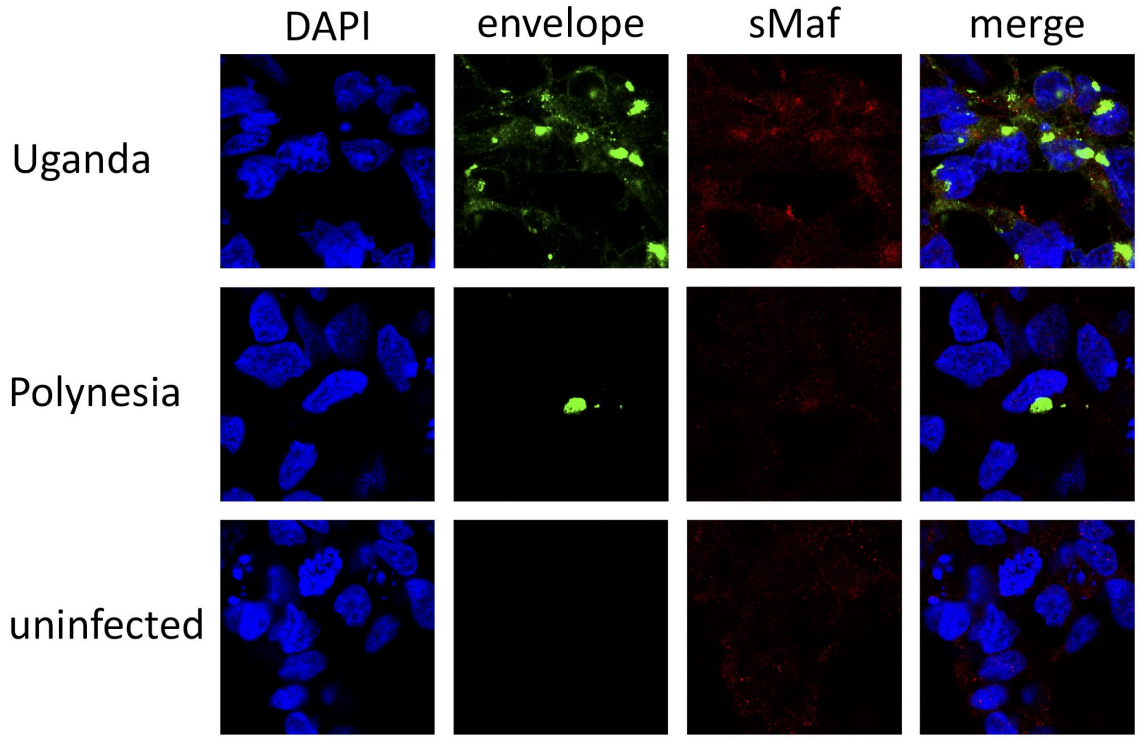

Figure 24. Increased Amount of sMaf Proteins in ZIKV Infected Cells.
Confocal immunofluorescence microscopy of ZIKV-positive cells (ZIKV Uganda at 48 hpi and ZIKV Polynesia at 24 hpi) or negative control cells (24 hpi). The immunofluorescence staining was performed using the polyclonal sMaf-specific serum and an envelope specific antibody. Nuclei were stained with DAPI (Tabari et al. 2020).

Additionally, RT-qPCR revealed a significant upregulation of the antioxidant gene Sestrin 2 (*SESN2*, Figure 25a). Notably, a significant downregulation of miR-182-5p was observed during ZIKV infection (Figure 25b), and this miRNA is predicted to target *SESN2*, a gene involved in antioxidant regulation, as reported by Lin et al. (Lin et al. 2018).

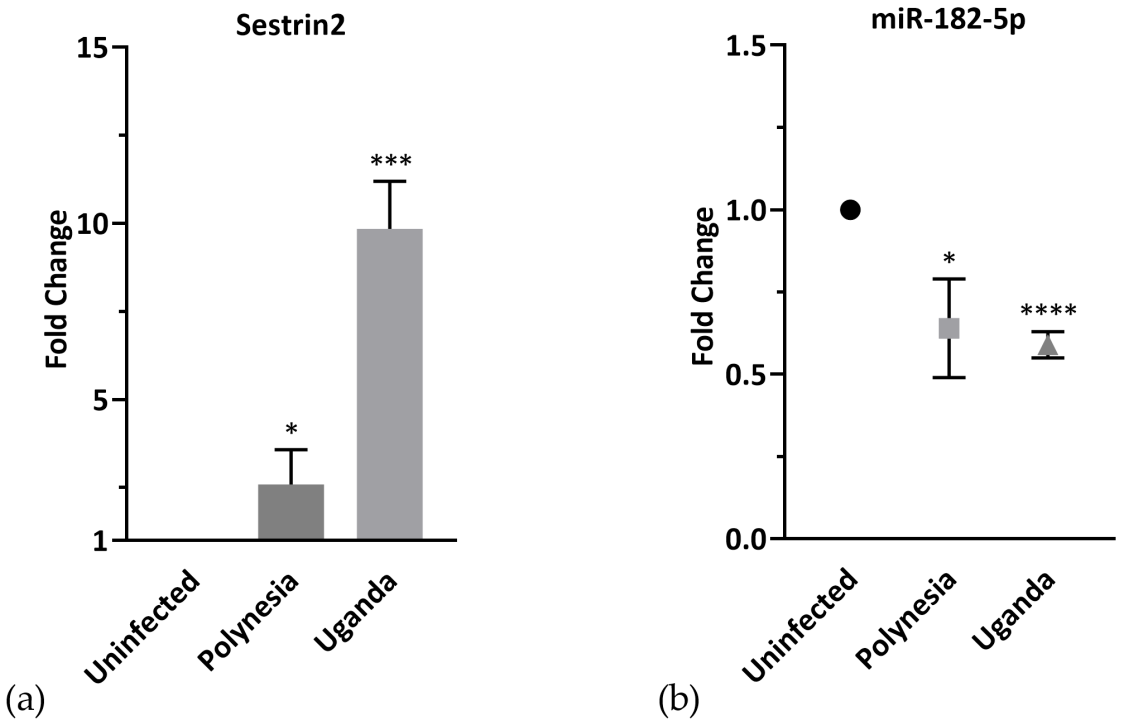

Figure 25. Dysregulation of Sestrin2 and miR-182 by ZIKV Uganda and Polynesia. (a) Relative *SESN2* mRNA levels measured by qRT-PCR presented as fold change compared to uninfected control cells at 72 hpi at MOI of 0.1. Error bar represents the mean ± SEM of n = 3 biological replicates; *p < 0.05; ***p < 0.001. (b) Relative miR-182-5p levels measured by qRT-PCR presented as fold change compared to uninfected control cells at 72 hpi at MOI of 0.1. Error bar represents the mean ± SEM of n = 3 biological replicates; *p < 0.05; ****p < 0.0001 (Tabari et al. 2020).

Gene Ontology analysis was conducted to identify differentially expressed genes in ZIKV Polynesia-infected cells associated with oxidative stress and ER stress. Nineteen upregulated genes were identified, including *DDIT3* (DNA-damage-inducible transcript 3), XBP1 (X-box binding protein 1), and *EIF2AK2* (eukaryotic translation initiation factor 2-alpha kinase 2) (Table 11, Table 12). To assess potential miRNA regulation of these genes, an integrative analysis using Tarbase was performed, revealing that miR-205-5p, downregulated at the intracellular level, could potentially target activating transcription factor 3 (*ATF3*) in addition to *ASNS*. Furthermore, several EV-associated miRNAs were found to have decreased levels following infection with ZIKV Polynesia, potentially regulating the same mRNA targets involved in oxidative and ER stress pathways (Table 13).

Taken together, ZIKV infection induces oxidative stress and modulates potential miRNA-mRNA interactions related to oxidative and ER stress. These differentially regulated miRNAs may contribute to the pathogenesis of ZIKV by influencing stress-related pathways.

Table 11. DEGs During Infection with ZIKV Polynesia at 72 hpi, Which Were Annotated to GO-term 'Response to Oxidative Stress'.

DEG	Fold Change ZIKV Polynesia
PNPT1	3.36
FOS	5.18
XBP1	2.06
PPARGC1A	2.06
KLF4	6.28
PML	3.76
TNFAIP3	4.96
STAT1	17.09
SLC7A11	2.11
JUN	2.10

Table 12. DEGs During Infection with ZIKV Polynesia at 72 hpi, Which Were Annotated to GO-term 'Response to Endoplasmic Reticulum Stress'.

DEG	Fold Change ZIKV Polynesia
XBP1	2.06
EIF2AK2	4.72
ASNS	2.13
TRIB3	2.84
DDIT3	5.17
ATF3	5.56
HERPUD1	2.48
PPP1R15A	2.31
FBXO6	2.33
CHAC1	4.46

Table 13. EV Associated miRNAs with Reduced Levels and Their Potential mRNA Targets.

miRNA ID	Gene Targets (ID)
hsa-miR-26b-5p	*TRIB3, FOS, HERPUD1, TNFAIP3, JUN, ASNS, CHAC1, ATF3*
hsa-let-7g-5p	*TRIB3, FBXO6, CHAC1*
hsa-miR-17-5p	*FOS, TNFAIP3, JUN, KLF4*
hsa-miR-221-3p	*FOS, PPP1R15A*
hsa-miR-16-5p	*HERPUD1, PML, EIF2AK2, JUN, ASNS, PPP1R15A, CHAC1, STAT1*
hsa-miR-106b-5p	*TNFAIP3*
hsa-miR-374a-5p	*TNFAIP3, EIF2AK2*
hsa-miR-93-5p	*TNFAIP3, JUN*
hsa-miR-20a-5p	*TNFAIP3*
hsa-miR-186-5p	*EIF2AK2, JUN, ASNS, CHAC1*
hsa-miR-32-5p	*JUN, KLF4*
hsa-miR-218-5p	*CHAC1*
hsa-miR-340-5p	*PPARGC1A*

4. Discussion

4.1 Antiviral Responses and Immune Evasion in ZIKV-Infected HaCaT Cells

ZIKV infection has been linked to severe neurodevelopmental disorders, yet the mechanisms underlying its pathogenesis remain incompletely understood. Characterising ZIKV-induced molecular alterations may not only advance our understanding of key pathogenic processes but also highlight candidate signatures that could support biomarker discovery and guide therapeutic intervention. This study investigated molecular pathways and cellular processes affected by ZIKV infection in two distinct cell types: HaCaT keratinocytes, representing the primary site of viral entry, and lt-NES® cells, a model for studying neurodevelopmental effects.

ZIKV infection of HaCaT keratinocytes elicited a robust innate immune response, characterised by significant upregulation of interferon-stimulated genes (ISGs), including IFI44L and MX2, which are key mediators of the antiviral response (Reikine et al. 2014). However, treatment with fibroblast growth factor 7 (FGF7) markedly attenuated this ISG response, indicating that FGF7 exerts a suppressive effect on the innate immune response. This finding is particularly relevant in the context of tissue repair, as FGF7 is known to be upregulated at sites of skin injury, such as those resulting from mosquito bites (Maddaluno et al. 2017). The observed suppression of ISG expression is consistent with previous evidence that FGF signalling interferes with type I interferon (IFN) pathways predominantly via FGFR2b, with a minor contribution from FGFR1b, in a kinase-dependent manner that involves proteasomal degradation, independent of direct interactions with IFN receptors (Maddaluno et al. 2020). Maddaluno et al. demonstrated that FGFs suppress ISG transcription, and that inhibition of FGFR signalling restores ISG expression while reducing viral replication. Their findings also showed that this suppression enhances the replication of several viruses, including ZIKV, highlighting the importance of FGF-mediated modulation of the antiviral response (Maddaluno et al. 2020). In the context of ZIKV infection, elevated FGF7 levels at mosquito bite sites may alter the local immune environment by reducing ISG responses, thereby facilitating the initial establishment of viral infection. While FGF7 supports wound healing and promotes tissue regeneration, its ability to suppress the innate immune response suggests a dual role that

could favour viral replication (Finch and Rubin 2004). The therapeutic potential of FGFR inhibitors, which have been shown to counteract FGF-mediated ISG suppression and reduce viral replication, may offer a promising approach for enhancing antiviral immunity in the skin (Maddaluno et al. 2020).

Microarray analysis identified bone marrow stromal antigen 2 (*BST2*), which encodes the restriction factor tetherin, as significantly upregulated in both ZIKV-infected HaCaT and lt-NES® cells. Tetherin is an interferon-stimulated protein known to restrict the release of enveloped viruses by tethering budding virions to the cell membrane, thus inhibiting their spread (Kaletsky et al. 2009; Le Tortorec et al. 2011; Neil et al. 2008; Sakuma et al. 2009). The upregulation of *BST2* in the microarray analysis suggested a potential role for tetherin in the host response to ZIKV infection.

To explore this further, Herrlein et al. performed additional experiments and investigated the interaction between ZIKV and tetherin (Herrlein et al. 2022). In their study, ZIKV infection strongly induced *BST2* mRNA expression, consistent with its role as an interferon-stimulated gene. However, this transcriptional upregulation did not result in an increase in tetherin protein levels. Instead, tetherin protein levels were reduced due to accelerated lysosomal degradation, highlighting a viral strategy to evade restriction. This degradation was independent of early autophagic processes but relied on components of the endo-lysosomal system. These results support the hypothesis that the upregulation of *BST2* observed in the microarray analysis represents an antiviral response to ZIKV infection. However, the virus effectively counteracts this defence mechanism. By manipulating the degradation process, Herrlein et al. demonstrated that stabilizing tetherin - either by inhibiting lysosomal acidification or depleting the ESCRT-0 protein HRS (endosomal sorting complexes required for transport-0 protein hepatocyte growth factor-regulated tyrosine kinase substrate) - led to a marked reduction in ZIKV release. These findings suggest that HRS could be a potential target for antiviral treatments. Immunofluorescence studies performed by Herrlein et al. further revealed that ZIKV virions were trapped in tetherin-positive compartments, suggesting that tetherin inhibits the release of ZIKV by retaining virions within intracellular vesicular structures. These results underscore tetherin's role as a restriction factor that directly impacts the ZIKV life cycle (Herrlein et al. 2022).

4.2 Mechanisms of ZIKV Pathogenesis in lt-NES® Cells and Neurodevelopmental Implications

Despite the important role of miRNAs in the pathogenesis of *Flavivirus* infections (Lowey et al. 2019; Zhu et al. 2014), the way in which ZIKV alters global miRNA regulation and contributes to pathogenesis and microcephaly has not yet been fully elucidated (Azouz et al. 2019; J. W. Dang et al. 2019; Kozak et al. 2017). In this study, transcriptomic and miRNA analyses were performed in ZIKV-infected lt-NES® cells and their extracellular vesicles, revealing key alterations that may contribute to disrupted neurogenesis and ZIKV pathogenesis.

Global miRNA transcriptome analyses showed substantial overlap in intracellular miRNA profiles altered by the ZIKV strains Uganda and French Polynesia. However, ZIKV Uganda induced more pronounced mRNA and miRNA dysregulation, likely due to its higher infection level (J. W. Dang et al. 2019). Both ZIKV strains induced dysregulation in multiple pathways associated with neurodevelopment and cell cycle control, suggesting a potential role in the development of the microcephaly phenotype. Notably, infection with ZIKV Uganda resulted in differential expression of several genes, including *COL4A1*, *MIR17HG*, *TUBA1A*, *SLC2A1* and *STAMBP*, which have been linked to microcephaly based on data from the Comparative Toxicogenomics Database (Davis et al. 2017).

These findings highlight the potential of ZIKV to disrupt critical neurodevelopmental pathways but also raise questions about the differences in pathogenic mechanisms between ZIKV lineages. While ZIKV was first associated with microcephaly in 2013, which involved the Asian lineage, accumulating evidence suggests that African ZIKV strains can induce neuronal damage comparable to or exceeding that caused by Asian lineages (Jaeger et al. 2019a; Nutt and Adams 2017). The findings of this study support the hypothesis that the ZIKV Uganda strain may also affect neurodevelopment, and that clinical cases may have gone undetected prior to 2013 due to limited diagnostic capacity in Africa (Meda et al. 2016; Simonin et al. 2016). Both African and Asian lineages have been shown to cross the placental barrier and induce congenital defects (Jaeger et al. 2019b; Vermillion et al. 2017). A key distinction between the two lineages appears to be their cytopathic effects and overall pathogenic potential. African strains generally show higher viral fitness and replication efficiency, with higher mosquito transmissibility and

increased lethality in immunocompromised adult mice, suggesting a more virulent phenotype (F. Aubry et al. 2021). In contrast, Asian lineage strains appear less cytotoxic, potentially enabling persistent infection within the central nervous system rather than inducing rapid cell death (Anfasa et al. 2017; Sheridan et al. 2018; Simonin et al. 2017). These differences may influence disease outcomes, with African strains potentially leading to early pregnancy loss, while Asian strains may allow foetal survival but increase the risk of congenital abnormalities. Consistent with this, increased cell death was observed in ZIKV Uganda-infected It-NES® cells in this study, further supporting the idea that African strains may induce stronger cytopathic effects. ZIKV Uganda exerted broader and more pronounced influence on host gene expression compared to the French Polynesia strain. This greater impact on host regulatory networks was consistent with the higher number of infectious particles produced by ZIKV Uganda at early stages of infection. These findings indicate that the Uganda strain replicated more efficiently and induced a stronger host response, whereas the Polynesia strain exerted a comparatively moderate effect, potentially favouring longer-term persistence and secondary spread.
It has been proposed that, over time, Asian lineage strains underwent attenuation, shifting from high foetal mortality to a greater incidence of Congenital Zika Syndrome (CZS). This evolutionary change could explain the absence of documented CZS cases associated with African ZIKV strains (Jaeger et al. 2019b). The re-emergence of ZIKV in outbreak regions was likely not driven by viral adaptation alone, but rather by a combination of epidemiological factors, including increased global travel, high vector densities, and immunologically naive populations (F. Aubry et al. 2021; Weaver 2017). These conditions may have facilitated the spread of ZIKV, contributing to large-scale outbreaks in susceptible populations.

Moving from the broader implications of ZIKV lineage differences, this study also identified specific genes and miRNAs that may play a critical role in ZIKV-induced neurodevelopmental disruption.
The gene *ASNS* was identified as differentially expressed by both strains and has been previously linked to developmental disorders, including microcephaly (Lomelino et al. 2017; Schleinitz et al. 2018). *ASNS* encodes the protein asparagine synthetase, a metabolic enzyme that catalyses the ATP-dependent conversion of aspartate and

glutamine into asparagine and glutamate (Richards and Kilberg 2006). Dysregulation of the balance of amino acid in the brain induced by ZIKV may contribute to the microcephaly phenotype (Lomelino et al. 2017; Schleinitz et al. 2018). The overexpression of *ASNS* following ZIKV infection may be linked to the downregulation of miR-205-5p, which is predicted to target *ASNS*, although further experiments should be performed to study this interaction in lt-NES® cells.

In addition to miR-205-5p, other miRNAs were found to be dysregulated that could play antiviral roles, suggesting a complex interplay between ZIKV and host defence mechanisms.

In this study, miR-3614-5p was found to be upregulated at the intracellular level in lt-NES® cells at 72 hpi by both ZIKV Uganda and Polynesia strains. This finding aligns with previous research on Dengue virus (DENV), where miR-3614-5p was upregulated in macrophages exposed to DENV and identified as an antiviral factor that restricts viral replication. Interestingly, miR-3614-5p was also shown to inhibit West Nile virus (WNV), suggesting that it may act as a broad antiviral regulator against flaviviruses (Diosa-Toro et al. 2017).

The observed upregulation of miR-3614-5p in ZIKV-infected lt-NES® cells suggests that ZIKV may induce an antiviral response similar to DENV, potentially through a shared immune strategy aimed at limiting viral replication. However, further investigation is needed to assess whether miR-3614-5p plays a functional role in controlling viral replication in neural stem cells. This could provide insight into a common antiviral miRNA-mediated defence strategy against flaviviruses (Diosa-Toro et al. 2017).

While some miRNAs appear to act as antiviral factors, others may be downregulated by ZIKV as part of its strategy to evade host defences.

In this study, miR-431-5p was found to be downregulated in lt-NES® cells following infection with ZIKV Uganda. Interestingly, recent work by Yuan et al. has identified miR-431-5p as an antiviral factor in mesenchymal stem cell-derived extracellular vesicles (EVs), where its overexpression significantly reduced ZIKV replication by targeting Cluster of differentiation 95 (CD95) and enhancing nuclear factor kappa-light-chain-enhancer of activated B cells (NF-κB)-mediated antiviral responses (Yuan et al. 2024). The observed

downregulation of miR-431-5p in ZIKV-infected lt-NES® cells may indicate a viral strategy to evade host antiviral defences, potentially allowing the virus to suppress immune signalling pathways that would otherwise limit replication.
Further supporting this, a recent study by Bagasra et al. on chronically ZIKV-infected neuroblastoma cells also reported miR-431-5p downregulation and identified a sequence homology between miR-431-5p and the ZIKV nucleocapsid gene (Bagasra et al. 2021). Given its role in modulating antiviral immunity, further research is needed to determine whether miR-431-5p downregulation in neural cells contributes to a weakened host response or other ZIKV-associated pathogenic effects in the central nervous system (CNS).

In addition, miR-4497 was found to be upregulated following infection of lt-NES® cells by ZIKV Polynesia at 48 hpi and 72 hpi, as well as by ZIKV Uganda at the same time points. Bagasra et al. similarly observed miR-4497 upregulation following ZIKV infection of neuroblastoma cells and identified a sequence homology between miR-4497 and the ZIKV NS1 gene (Bagasra et al. 2021). This suggests a potential virus-host interaction mechanism, where ZIKV may modulate miR-4497 regulation to influence cellular pathways relevant to infection. Further research is needed to clarify the implications of these interactions and their role in ZIKV pathogenesis.

Beyond intracellular miRNA changes, ZIKV infection also alters the miRNA content of extracellular vesicles, which may play a role in intercellular communication and pathogenesis. Viruses are known to exploit EV pathways by packaging viral proteins or genomes into vesicles and by redistributing host cargo, thereby facilitating dissemination, immune evasion, and modulation of host responses (Chahar et al. 2015). Although EV-associated miRNAs have been implicated in several viral infections, their alteration during ZIKV infection remains poorly characterised (Mao et al. 2023; Slonchak et al. 2019; Yoshikawa et al. 2019). In this study, ZIKV infection of lt-NES® cells was found to modify the profile of EV-associated miRNAs. The differentially incorporated miRNAs in EVs produced in response to ZIKV infection were linked to biological processes related to neural and embryonic development, including axon guidance and FoxO signalling pathways.

Among these changes, miR-103a-3p was significantly enriched in EVs at 72 hpi following infection with ZIKV Uganda, while otubain deubiquitinase 4 (*OTUD4*) was notably downregulated in infected lt-NES® cells at this time point. These findings are consistent with the study by Ye et al. (2022), which demonstrated that miR-103a-3p enhances ZIKV replication in human alveolar basal epithelial cells (A549) by targeting *OTUD4*, a negative regulator of the p38 mitogen-activated protein kinase (MAPK) signalling pathway. The MAPK pathway plays a crucial role in cellular stress responses and has been linked to increased viral replication when activated. While Ye et al. observed intracellular upregulation of miR-103a-3p, the present study found that ZIKV infection leads to miR-103a-3p enrichment in EVs, rather than intracellular accumulation. This suggests that ZIKV may regulate miRNA distribution as part of its interaction with host cells, potentially influencing signalling pathways in both infected and recipient cells (H. Ye et al. 2022). EVs may act as vehicles for both redistribution of host miRNAs and viral dissemination, thereby modulating key cellular pathways in infected and neighbouring cells.

Another miRNA of interest, miR-4792, was found to be enriched in EVs secreted from ZIKV-infected cells and exhibited significant upregulation at the intracellular level in response to both ZIKV strains.

Previous studies by other groups have reported that miR-4792 overexpression suppresses nasopharyngeal tumour growth in mice, induces cell cycle arrest, and promotes apoptosis in A459 cells (Y. Li and Chen 2015; Liu et al. 2019). The observed upregulation of miR-4792 following ZIKV infection may contribute to cell death in neural stem cells, with potential transmission via EVs affecting neighbouring uninfected cells, thereby representing a possible mechanism underlying impaired brain development.

Additionally, miR-4792 has been identified as a direct regulator of the transcription factor forkhead box C1 (*FOXC1*) in both nasopharyngeal carcinoma and A549 cells (Y. Li and Chen 2015; Liu et al. 2019). *FOXC1* is essential for normal cerebellar development, and its dysfunction has been implicated in Dandy-Walker syndrome (Aldinger et al. 2009, p. 1; Haldipur et al. 2017), a brain malformation associated with ZIKV infection (Pool et al. 2019). Given that *FOXC1* was downregulated in lt-NES® cells following ZIKV infection, its suppression may play a role in the pathogenesis of congenital ZIKV syndrome.

FOXC1 is also involved in the oxidative stress response, whereby reduced *FOXC1* mRNA and protein levels have been observed in HTM cells subjected to oxidative stress (Ito et al. 2014, p. 1).

Oxidative stress is implicated in numerous neurodegenerative diseases (Singh et al. 2019), and several members of the *Flaviviridae* family are known to trigger reactive oxygen species (ROS) accumulation while disrupting antioxidant defence mechanisms, thereby influencing both viral replication and cellular metabolism (Medvedev et al. 2017; Olagnier et al. 2014). Hepatitis C virus (HCV) suppresses the nuclear factor erythroid 2-related factor 2 (Nrf2) mediated antioxidant response, which in turn favours the release of viral particles. In HCV-infected cells, small musculoaponeurotic fibrosarcoma proteins (sMafs) are bound to the non-structural protein NS3 and are delocalized from the nucleus to the replicon surface, sequestering Nrf2 and preventing its entry into the nucleus (Bender and Hildt 2019; Carvajal-Yepes et al. 2011; Medvedev et al. 2017). This impairment of Nrf2/ARE signalling leads to elevated ROS levels, which in turn activate autophagy, a pathway commonly exploited by positive-strand RNA viruses to enhance replication and release. The crosstalk between oxidative stress and autophagy can further support exosome-mediated viral particle release, as both processes involve membrane trafficking and are functionally interconnected (Choi et al. 2018; Dreux and Chisari 2010; Medvedev et al. 2017; Tabari et al. 2020).

In this study, a significant increase in oxidatively modified proteins was observed following ZIKV infection, indicating oxidative stress induction. Immunofluorescence analysis revealed colocalization of sMaf proteins with the envelope proteins of both ZIKV Uganda and ZIKV Polynesia strains, along with sMaf accumulation in perinuclear regions. Similar to HCV, ZIKV may interfere with sMafs to suppress ARE-dependent gene expression. Notably, key Nrf2 target genes, including *HO-1*, *NQO1*, *GCL*, *GST* remained unaffected despite oxidative stress induction, suggesting potential regulatory interference by ZIKV; (Itoh et al. 1997; Rushworth et al. 2008; Vasiliou et al. 2006). Unlike HCV, where sMafs interact with non-structural proteins such as NS3, the present study investigated the colocalization of sMafs with ZIKV structural envelope proteins. Previous work by other groups has similarly shown that ZIKV suppresses Nrf2 activity, leading to impaired antioxidant responses. A study by Almeida et al. demonstrated that ZIKV infection significantly reduces ARE-driven transcription and decreases antioxidant enzyme activity

in neuronal and hepatic cells, suggesting an active viral mechanism to disrupt oxidative homeostasis. Their findings also indicated increased oxidative stress markers in ZIKV-infected brain and liver tissues in vivo, highlighting the potential role of oxidative imbalance in ZIKV-induced pathology (Almeida et al. 2020).

In line with these observations, recent transcriptomic analyses by da Silva et al. have shown that ZIKV infection activates activator protein 1 (AP-1) signalling, with upregulation of Jun proto-oncogene (*JUN*) and Fos proto-oncogene (*FOS*) observed in both infected cells and multiple sclerosis (MS) patient samples. Da Silva et al. identified *JUN* and *FOS* as key regulatory factors in both ZIKV infection and MS, suggesting a shared molecular signature between viral-induced oxidative stress and inflammatory demyelination (da Silva et al. 2023). Consistent with these findings, *JUN* and *FOS* were also upregulated in the present study following infection of lt-NES® cells by both ZIKV strains, further supporting the idea that ZIKV-induced oxidative stress may drive inflammatory pathways linked to neuropathology. These results indicate that oxidative imbalance, combined with AP-1 activation, could be a key factor in the long-term neurological consequences of ZIKV infection (da Silva et al. 2023).

While in the present study oxidative stress-related cytoprotective genes were not significantly altered, expression of the antioxidant gene Sestrin 2 (*SESN2*) was significantly upregulated following ZIKV infection. *SESN2* expression can be induced in response to ER stress by the transcription factors ATF4 (Activating Transcription Factor 4) or ATF6 (Activating Transcription Factor 6) and via the Nrf2/ARE pathway (Ding et al. 2016; Jegal et al. 2017; Shin et al. 2012; Tabari et al. 2020). Consistent with these findings, Carr et al. recently reported *SESN2* upregulation following infection with Japanese encephalitis virus and ZIKV Uganda in neuroblastoma cells (Carr et al. 2019). *SESN2* plays a crucial role in ROS regulation and autophagy activation through mechanistic target of rapamycin complex 1 (mTORC1) inhibition, making it a potential biomarker and therapeutic target in various diseases. Altered *SESN2* levels have been observed in patients with neurodegenerative disorders, where its plasma concentrations correlate with disease severity (Soontornniyomkij et al. 2012; Xiao et al. 2019; J. Ye et al. 2017). Additionally, suppression of miR-182-5p has been shown to induce *SESN2* expression in glioma and adenocarcinoma cell lines (Lin et al. 2018). Notably, miR-182-

5p was downregulated in lt-NES® cells following ZIKV infection, potentially contributing to the observed *SESN2* upregulation. However, further gain- and loss-of-function studies are necessary to assess the interaction between miRNAs and mRNAs.
Overall, multiple dysregulated host miRNAs and mRNAs were identified in response to ZIKV infection, particularly those involved in neurodevelopment and oxidative stress, which may contribute to a better understanding of the neurodegenerative phenotype induced by ZIKV infection.

4.3 Conclusion

In conclusion, this study provides critical insights into the molecular and cellular mechanisms underlying ZIKV infection and its impact on neural development. By investigating two distinct cell types - HaCaT keratinocytes and lt-NES® cells - key pathways through which ZIKV modulates host responses were identified, including innate immunity, miRNA regulation, and oxidative stress. In HaCaT cells, ZIKV infection elicited a robust innate immune response, characterised by the upregulation of ISGs. The upregulation of *BST2* in both cell types indicated an antiviral response, but this defence was counteracted by ZIKV by promoting tetherin degradation, underscoring the virus's ability to evade host immunity. In lt-NES® cells, ZIKV infection disrupted neurodevelopmental pathways, with differential expression of genes and miRNAs linked to microcephaly and other neurodevelopmental disorders. Notably, African and Asian ZIKV lineages exhibited distinct pathogenic profiles, with African strains inducing stronger cytopathic effects, underscoring the need for further research into their differential impact on neurodevelopmental outcomes. The dysregulation of miRNAs, including miR-205-5p, miR-3614-5p, miR-431-5p, miR-103a-3p, and miR-4792, highlighted the complex interplay between ZIKV and host defence mechanisms, with some miRNAs acting as potential antiviral factors while others were suppressed to potentially facilitate viral replication. Additionally, ZIKV-induced oxidative stress and the modulation of antioxidant pathways, including the upregulation of *SESN2*, suggested a role for oxidative imbalance in ZIKV-associated neuropathology. These findings advance the current understanding of ZIKV pathogenesis and highlight potential therapeutic targets that may mitigate viral replication and neurodevelopmental damage. Future investigations are needed to elucidate the functional roles of dysregulated miRNAs and oxidative stress pathways in

ZIKV infection, as well as the broader implications of lineage-specific differences in viral pathogenicity. Collectively, these findings enhance the growing body of knowledge about ZIKV, highlighting molecular signatures that may inform future biomarker and therapeutic development.

5. Abstract

Zika virus (ZIKV) is a mosquito-borne *Flavivirus* capable of causing severe neurological complications, including congenital Zika syndrome (CZS) in newborns and Guillain-Barré syndrome (GBS) in adults. Although incidence has declined following the 2015–2016 epidemic in the Americas, ZIKV continues to circulate at low levels and poses a persistent health concern, particularly in regions where *Aedes* mosquito vectors are endemic or expanding due to climate change.

While the clinical consequences of ZIKV infection are well recognized, the underlying molecular mechanisms driving impact on host development remain poorly understood. Given the emerging roles of microRNAs (miRNAs) and extracellular vesicles (EVs) in gene regulation and intercellular communication, this study primarily investigated how ZIKV modulates host miRNA and mRNA expression in biologically relevant human cell models. Transcriptomic and miRNA profiling were conducted in long-term neuroepithelial-like stem cells (lt-NES®), representing early neural development. In parallel, gene expression changes were analysed in HaCaT keratinocytes, which model the skin epithelium as the likely initial site of viral entry. Cells were infected with ZIKV strains from the African (Uganda) and Asian (French Polynesia) lineages. The Asian strain is linked to microcephaly, whereas the neuroteratogenic potential of the African strain remains unclear. Host mRNA responses were assessed by microarray, and intracellular as well as EV-associated miRNAs were profiled by next-generation sequencing. Integrative analyses were conducted to identify regulatory networks and molecular signatures associated with infection.

ZIKV infection resulted in widespread and strain-specific dysregulation of host transcripts and miRNAs. In lt-NES® cells, infection altered genes and miRNAs involved in neurodevelopmental and oxidative stress pathways, with the African strain inducing stronger cytopathic effects and broader gene expression changes than the Asian strain. Key dysregulated miRNAs, including miR-205-5p, miR-4792, and miR-431-5p, were linked to neuronal differentiation, antiviral defence, and redox regulation. ZIKV infection induced oxidative stress, as indicated by Sestrin 2 (*SESN2*) upregulation and increased protein carbonylation. In HaCaT cells, a robust induction of interferon-stimulated genes

was observed, including *BST2* (tetherin), which was modulated by fibroblast growth factor 7 (FGF7) treatment.

These findings provide new insights into the molecular mechanisms of ZIKV pathogenesis, revealing transcriptional and post-transcriptional host responses across relevant human cell types. The identification of lineage-specific molecular profiles and regulatory networks enhances the understanding of ZIKV-induced neuropathology and provides candidate molecular signatures that could guide future biomarker discovery and the development of targeted antiviral strategies.

6. List of Figures

7. List of Tables

8. References

Acosta-Ampudia, Y., Monsalve, D. M., Castillo-Medina, L. F., Rodríguez, Y., Pacheco, Y., Halstead, S., et al. (2018). Autoimmune Neurological Conditions Associated With Zika Virus Infection. *Frontiers in Molecular Neuroscience*, *11*, 116. https://doi.org/10.3389/fnmol.2018.00116

Agarwal, V., Bell, G. W., Nam, J.-W., & Bartel, D. P. (2015). Predicting effective microRNA target sites in mammalian mRNAs. *eLife*, *4*. https://doi.org/10.7554/eLife.05005

Aldinger, K. A., Lehmann, O. J., Hudgins, L., Chizhikov, V. V., Bassuk, A. G., Ades, L. C., et al. (2009). FOXC1 is required for normal cerebellar development and is a major contributor to chromosome 6p25.3 Dandy-Walker malformation. *Nature Genetics*, *41*(9), 1037–1042. https://doi.org/10.1038/ng.422

Alera, M. T., Hermann, L., Tac-An, I. A., Klungthong, C., Rutvisuttinunt, W., Manasatienkij, W., et al. (2015). Zika Virus Infection, Philippines, 2012. *Emerging Infectious Diseases*, *21*(4), 722–724. https://doi.org/10.3201/eid2104.141707

Almeida, L. T., Ferraz, A. C., da Silva Caetano, C. C., da Silva Menegatto, M. B., dos Santos Pereira Andrade, A. C., Lima, R. L. S., et al. (2020). Zika virus induces oxidative stress and decreases antioxidant enzyme activities *in vitro* and *in vivo*. *Virus Research*, *286*, 198084. https://doi.org/10.1016/j.virusres.2020.198084

Alves-Leon, S. V., Fontes-Dantas, F. L., & Rueda-Lopes, F. C. (2021). Chapter 18 - Neurological manifestations similar to multiple sclerosis in adults after Zika virus infection. In C. R. Martin, C. J. H. Martin, V. R. Preedy, & R. Rajendram (Eds.), *Zika Virus Biology, Transmission, and Pathology* (pp. 199–207). Academic Press. https://doi.org/10.1016/B978-0-12-820268-5.00018-3

Alves-Leon, S. V., Lima, M. da R., Nunes, P. C. G., Chimelli, L. M. C., Rabelo, K., Nogueira, R. M. R., et al. (2019). Zika virus found in brain tissue of a multiple sclerosis patient undergoing an acute disseminated encephalomyelitis-like episode. *Multiple Sclerosis (Houndmills, Basingstoke, England)*, *25*(3), 427–430. https://doi.org/10.1177/1352458518781992

Anfasa, F., Siegers, J. Y., van der Kroeg, M., Mumtaz, N., Stalin Raj, V., de Vrij, F. M. S., et al. (2017). Phenotypic Differences between Asian and African Lineage Zika Viruses in Human Neural Progenitor Cells. *mSphere*, *2*(4), mSphere.00292-17, e00292-17. https://doi.org/10.1128/mSphere.00292-17

Aubry, F., Jacobs, S., Darmuzey, M., Lequime, S., Delang, L., Fontaine, A., et al. (2021). Recent African strains of Zika virus display higher transmissibility and fetal pathogenicity than Asian strains. *Nature Communications*, *12*(1), 916. https://doi.org/10.1038/s41467-021-21199-z

Aubry, M., Finke, J., Teissier, A., Roche, C., Broult, J., Paulous, S., et al. (2015). Seroprevalence of arboviruses among blood donors in French Polynesia, 2011–2013. *International Journal of Infectious Diseases*, *41*, 11–12. https://doi.org/10.1016/j.ijid.2015.10.005

Azar, S. R., & Weaver, S. C. (2019). Vector Competence: What Has Zika Virus Taught Us? *Viruses*, *11*(9), 867. https://doi.org/10.3390/v11090867

Azevedo, R. S. S., Araujo, M. T., Martins Filho, A. J., Oliveira, C. S., Nunes, B. T. D., Cruz, A. C. R., et al. (2016). Zika virus epidemic in Brazil. I. Fatal disease in adults: Clinical and laboratorial aspects. *Journal of Clinical Virology*, *85*, 56–64. https://doi.org/10.1016/j.jcv.2016.10.024

Azouz, F., Arora, K., Krause, K., Nerurkar, V., & Kumar, M. (2019). Integrated MicroRNA and mRNA Profiling in Zika Virus-Infected Neurons. *Viruses*, *11*(2), 162. https://doi.org/10.3390/v11020162

Bagasra, O., Shamabadi, N. S., Pandey, P., Desoky, A., & McLean, E. (2021). Differential expression of miRNAs in a human developing neuronal cell line chronically infected with Zika virus. *The Libyan Journal of Medicine*, *16*(1), 1909902. https://doi.org/10.1080/19932820.2021.1909902

Baldwin, W. R., Livengood, J. A., Giebler, H. A., Stovall, J. L., Boroughs, K. L., Sonnberg, S., et al. (2018). Purified Inactivated Zika Vaccine Candidates Afford Protection against Lethal Challenge in Mice. *Scientific Reports*, *8*(1), 16509. https://doi.org/10.1038/s41598-018-34735-7

Barbu, M. G., Condrat, C. E., Thompson, D. C., Bugnar, O. L., Cretoiu, D., Toader, O. D., et al. (2020). MicroRNA Involvement in Signaling Pathways During Viral Infection. *Frontiers in Cell and Developmental Biology*, *8*, 143. https://doi.org/10.3389/fcell.2020.00143

Barnard, T. R., Abram, Q. H., Lin, Q. F., Wang, A. B., & Sagan, S. M. (2021). Molecular Determinants of Flavivirus Virion Assembly. *Trends in Biochemical Sciences*, *46*(5), 378–390. https://doi.org/10.1016/j.tibs.2020.12.007

Barrows, N. J., Anglero-Rodriguez, Y., Kim, B., Jamison, S. F., Le Sommer, C., McGee, C. E., et al. (2019). Dual roles for the ER membrane protein complex in flavivirus infection: viral entry and protein biogenesis. *Scientific Reports*, *9*(1), 9711. https://doi.org/10.1038/s41598-019-45910-9

Bartel, D. P. (2018). Metazoan MicroRNAs. *Cell*, *173*(1), 20–51. https://doi.org/10.1016/j.cell.2018.03.006

Barzon, L., Pacenti, M., Franchin, E., Lavezzo, E., Trevisan, M., Sgarabotto, D., & Palù, G. (2016). Infection dynamics in a traveller with persistent shedding of Zika virus RNA in semen for six months after returning from Haiti to Italy, January 2016. *Euro Surveillance: Bulletin Europeen Sur Les Maladies Transmissibles = European Communicable Disease Bulletin*, *21*(32), 30316. https://doi.org/10.2807/1560-7917.ES.2016.21.32.30316

Baud, D., Gubler, D. J., Schaub, B., Lanteri, M. C., & Musso, D. (2017). An update on Zika virus infection. *The Lancet*, *390*(10107), 2099–2109. https://doi.org/10.1016/S0140-6736(17)31450-2

Bebelman, M. P., Smit, M. J., Pegtel, D. M., & Baglio, S. R. (2018). Biogenesis and function of extracellular vesicles in cancer. *Pharmacology & Therapeutics*, *188*, 1–11. https://doi.org/10.1016/j.pharmthera.2018.02.013

Bender & Hildt. (2019). Effect of Hepatitis Viruses on the Nrf2/Keap1-Signaling Pathway and Its Impact on Viral Replication and Pathogenesis. *International Journal of Molecular Sciences*, *20*(18), 4659. https://doi.org/10.3390/ijms20184659

Bollman, B., Nunna, N., Bahl, K., Hsiao, C. J., Bennett, H., Butler, S., et al. (2023). An optimized messenger RNA vaccine candidate protects non-human primates from Zika virus infection. *npj Vaccines*, *8*(1), 1–10. https://doi.org/10.1038/s41541-023-00656-4

Borges, F. T., Reis, L. A., & Schor, N. (2013). Extracellular vesicles: structure, function, and potential clinical uses in renal diseases. *Brazilian Journal of Medical and Biological Research*, *46*, 824–830. https://doi.org/10.1590/1414-431X20132964

Brasil, P., Pereira, J. P., Moreira, M. E., Nogueira, R. M. R., Damasceno, L., Wakimoto, M., et al. (2016). Zika Virus Infection in Pregnant Women in Rio de Janeiro. *New England Journal of Medicine*, *375*(24), 2321–2334. https://doi.org/10.1056/NEJMoa1602412

Caby, M.-P., Lankar, D., Vincendeau-Scherrer, C., Raposo, G., & Bonnerot, C. (2005). Exosomal-like vesicles are present in human blood plasma. *International Immunology*, *17*(7), 879–887. https://doi.org/10.1093/intimm/dxh267

Calvet, G., Aguiar, R. S., Melo, A. S. O., Sampaio, S. A., de Filippis, I., Fabri, A., et al. (2016). Detection and sequencing of Zika virus from amniotic fluid of fetuses with microcephaly in Brazil: a case study. *The Lancet. Infectious Diseases*, *16*(6), 653–660. https://doi.org/10.1016/S1473-3099(16)00095-5

Canada. (2023a). Zika virus: Latest travel health advice. https://www.canada.ca/en/public-health/services/diseases/zika-virus/latest-travel-health-advice.html. Accessed 16 July 2025

Canada, P. H. A. of. (2023b, June 23). Zika virus: For health professionals. education and awareness. https://www.canada.ca/en/public-health/services/diseases/zika-virus/health-professionals.html. Accessed 9 October 2024

Cao-Lormeau, V.-M., Blake, A., Mons, S., Lastère, S., Roche, C., Vanhomwegen, J., et al. (2016). Guillain-Barré Syndrome outbreak associated with Zika virus infection in French Polynesia: a case-control study. *Lancet (London, England)*, *387*(10027), 1531–1539. https://doi.org/10.1016/S0140-6736(16)00562-6

Cao-Lormeau, V.-M., Roche, C., Teissier, A., Robin, E., Berry, A.-L., Mallet, H.-P., et al. (2014). Zika Virus, French Polynesia, South Pacific, 2013. *Emerging Infectious Diseases*, *20*(6), 1085. https://doi.org/10.3201/eid2006.140138

Carr, M., Gonzalez, G., Martinelli, A., Wastika, C. E., Ito, K., Orba, Y., et al. (2019). Upregulated expression of the antioxidant sestrin 2 identified by transcriptomic analysis of Japanese encephalitis virus-infected SH-SY5Y neuroblastoma cells. *Virus Genes*, *55*(5), 630–642. https://doi.org/10.1007/s11262-019-01683-x

Carteaux, G., Maquart, M., Bedet, A., Contou, D., Brugières, P., Fourati, S., et al. (2016). Zika Virus Associated with Meningoencephalitis. *New England Journal of Medicine*, *374*(16), 1595–1596. https://doi.org/10.1056/NEJMc1602964

Carvajal-Yepes, M., Himmelsbach, K., Schaedler, S., Ploen, D., Krause, J., Ludwig, L., et al. (2011). Hepatitis C Virus Impairs the Induction of Cytoprotective Nrf2 Target Genes by Delocalization of Small Maf Proteins. *Journal of Biological Chemistry*, *286*(11), 8941–8951. https://doi.org/10.1074/jbc.M110.186684

Cauchemez, S., Besnard, M., Bompard, P., Dub, T., Guillemette-Artur, P., Eyrolle-Guignot, D., Salje, H., Kerkhove, M. D. V., et al. (2016). Association between Zika virus and microcephaly in French Polynesia, 2013–15: a retrospective study. *The Lancet*, *387*(10033), 2125–2132. https://doi.org/10.1016/S0140-6736(16)00651-6

Cauchemez, S., Besnard, M., Bompard, P., Dub, T., Guillemette-Artur, P., Eyrolle-Guignot, D., Salje, H., Van Kerkhove, M. D., et al. (2016). Association between Zika virus and microcephaly in French Polynesia, 2013-15: a retrospective study. *Lancet (London, England)*, *387*(10033), 2125–2132. https://doi.org/10.1016/S0140-6736(16)00651-6

CDC. (2024a). Zika Cases in the United States. *Zika Virus*. https://www.cdc.gov/zika/zika-cases-us/index.html. Accessed 16 July 2025

CDC. (2024b). Zika Travel Information | Travelers' Health | CDC. https://wwwnc.cdc.gov/travel/page/zika-travel-information. Accessed 16 July 2025

CDC. (2024c, May 17). Treatment of Zika. *Zika Virus*. https://www.cdc.gov/zika/treatment/index.html. Accessed 10 October 2024

CDC. (2024d, May 31). Preventing Zika. *Zika Virus*. https://www.cdc.gov/zika/prevention/index.html. Accessed 10 October 2024

CDC. (2024e, August 14). Sexual Transmission of Zika Virus. *Zika Virus*. https://www.cdc.gov/zika/hcp/sexual-transmission/index.html. Accessed 10 October 2024

CDC. (2024f, August 23). Recommendations for Travelers and People Living Abroad. *Zika Virus*. https://www.cdc.gov/zika/travel/index.html. Accessed 9 October 2024

Chahar, H. S., Bao, X., & Casola, A. (2015). Exosomes and Their Role in the Life Cycle and Pathogenesis of RNA Viruses. *Viruses*, *7*(6), 3204. https://doi.org/10.3390/v7062770

Chiramel, A. I., & Best, S. M. (2018). Role of autophagy in Zika virus infection and pathogenesis. *Virus Research*, *254*, 34–40. https://doi.org/10.1016/j.virusres.2017.09.006

Choi, Y., Bowman, J. W., & Jung, J. U. (2018). Autophagy during viral infection — a double-edged sword. *Nature Reviews Microbiology*, *16*(6), 341–354. https://doi.org/10.1038/s41579-018-0003-6

Chouin-Carneiro, T., Vega-Rua, A., Vazeille, M., Yebakima, A., Girod, R., Goindin, D., et al. (2016). Differential Susceptibilities of Aedes aegypti and Aedes albopictus from the Americas to Zika Virus. *PLOS Neglected Tropical Diseases*, *10*(3), e0004543. https://doi.org/10.1371/journal.pntd.0004543

Cortese, M., Goellner, S., Acosta, E. G., Neufeldt, C. J., Oleksiuk, O., Lampe, M., et al. (2017). Ultrastructural Characterization of Zika Virus Replication Factories. *Cell Reports*, *18*(9), 2113–2123. https://doi.org/10.1016/j.celrep.2017.02.014

Croft, D., Mundo, A. F., Haw, R., Milacic, M., Weiser, J., Wu, G., et al. (2014). The Reactome pathway knowledgebase. *Nucleic Acids Research*, *42*(D1), D472–D477. https://doi.org/10.1093/nar/gkt1102

Cugola, F. R., Fernandes, I. R., Russo, F. B., Freitas, B. C., Dias, J. L. M., Guimarães, K. P., et al. (2016). The Brazilian Zika virus strain causes birth defects in experimental models. *Nature*, *534*(7606), 267–271. https://doi.org/10.1038/nature18296

da Conceição, P. J. P., de Carvalho, L. R., de Godoy, B. L. V., Nogueira, M. L., Terzian, A. C. B., de Godoy, M. F., et al. (2022). Detection of Zika virus in urine from randomly tested individuals in Mirassol, Brazil. *Infection*, *50*(1), 149–156. https://doi.org/10.1007/s15010-021-01667-w

da Silva, E. V., Fontes-Dantas, F. L., Dantas, T. V., Dutra, A., Nascimento, O. J. M., & Alves-Leon, S. V. (2023). Shared Molecular Signatures Across Zika Virus Infection and Multiple Sclerosis Highlight AP-1 Transcription Factor as a Potential Player in Post-ZIKV MS-Like Phenotypes. *Molecular Neurobiology*, *60*(8), 4184–4205. https://doi.org/10.1007/s12035-023-03305-y

Dai, L., Wang, Q., Qi, J., Shi, Y., Yan, J., & Gao, G. F. (2016). Molecular basis of antibody-mediated neutralization and protection against flavivirus. *IUBMB life*, *68*(10), 783–791. https://doi.org/10.1002/iub.1556

Dang, J., Tiwari, S. K., Lichinchi, G., Qin, Y., Patil, V. S., Eroshkin, A. M., & Rana, T. M. (2016). Zika Virus Depletes Neural Progenitors in Human Cerebral Organoids through Activation of the Innate Immune Receptor TLR3. *Cell Stem Cell*, *19*(2), 258–265. https://doi.org/10.1016/j.stem.2016.04.014

Dang, J. W., Tiwari, S. K., Qin, Y., & Rana, T. M. (2019). Genome-wide Integrative Analysis of Zika-Virus-Infected Neuronal Stem Cells Reveals Roles for MicroRNAs in Cell Cycle and Stemness. *Cell Reports*, *27*(12), 3618-3628.e5. https://doi.org/10.1016/j.celrep.2019.05.059

Davis, A. P., Grondin, C. J., Johnson, R. J., Sciaky, D., King, B. L., McMorran, R., et al. (2017). The Comparative Toxicogenomics Database: update 2017. *Nucleic Acids Research*, *45*(D1), D972–D978. https://doi.org/10.1093/nar/gkw838

De Smet, B., Van den Bossche, D., van de Werve, C., Mairesse, J., Schmidt-Chanasit, J., Michiels, J., et al. (2016). Confirmed Zika virus infection in a Belgian traveler returning from Guatemala, and the diagnostic challenges of imported cases into Europe. *Journal of Clinical Virology: The Official Publication of the Pan American Society for Clinical Virology*, *80*, 8–11. https://doi.org/10.1016/j.jcv.2016.04.009

Díaz-Menéndez, M., de la Calle-Prieto, F., Montero, D., Antolín, E., Vazquez, A., Arsuaga, M., et al. (2018). Initial experience with imported Zika virus infection in Spain. *Enfermedades Infecciosas Y Microbiologia Clinica (English Ed.)*, *36*(1), 4–8. https://doi.org/10.1016/j.eimc.2016.08.003

Dick, G. W. (1953). Epidemiological notes on some viruses isolated in Uganda; Yellow fever, Rift Valley fever, Bwamba fever, West Nile, Mengo, Semliki forest, Bunyamwera, Ntaya, Uganda S and Zika viruses. *Transactions of the Royal Society of Tropical Medicine and Hygiene*, *47*(1), 13–48. https://doi.org/10.1016/0035-9203(53)90021-2

Dick, G. W. A., Kitchen, S. F., & Haddow, A. J. (1952). Zika Virus (I). Isolations and serological specificity. *Transactions of the Royal Society of Tropical Medicine and Hygiene*, *46*(5), 509–520. https://doi.org/10.1016/0035-9203(52)90042-4

Ding, B., Parmigiani, A., Divakaruni, A. S., Archer, K., Murphy, A. N., & Budanov, A. V. (2016). Sestrin2 is induced by glucose starvation via the unfolded protein response and protects cells from non-canonical necroptotic cell death. *Scientific Reports*, *6*(1), 22538. https://doi.org/10.1038/srep22538

Diosa-Toro, M., Echavarría-Consuegra, L., Flipse, J., Fernández, G. J., Kluiver, J., van den Berg, A., et al. (2017). MicroRNA profiling of human primary macrophages exposed to dengue virus identifies

miRNA-3614-5p as antiviral and regulator of ADAR1 expression. *PLoS neglected tropical diseases*, *11*(10), e0005981. https://doi.org/10.1371/journal.pntd.0005981

D'Ortenzio, E., Matheron, S., Lamballerie, X. de, Hubert, B., Piorkowski, G., Maquart, M., et al. (2016). Evidence of Sexual Transmission of Zika Virus. *New England Journal of Medicine*, *374*(22), 2195–2198. https://doi.org/10.1056/NEJMc1604449

Dreux, M., & Chisari, F. V. (2010). Viruses and the autophagy machinery. *Cell Cycle*, *9*(7), 1295–1307. https://doi.org/10.4161/cc.9.7.11109

Driggers, R. W., Ho, C.-Y., Korhonen, E. M., Kuivanen, S., Jääskeläinen, A. J., Smura, T., et al. (2016). Zika Virus Infection with Prolonged Maternal Viremia and Fetal Brain Abnormalities. *The New England Journal of Medicine*, *374*(22), 2142–2151. https://doi.org/10.1056/NEJMoa1601824

Duffy, M. R., Chen, T.-H., Hancock, W. T., Powers, A. M., Kool, J. L., Lanciotti, R. S., et al. (2009). Zika virus outbreak on Yap Island, Federated States of Micronesia. *The New England Journal of Medicine*, *360*(24), 2536–2543. https://doi.org/10.1056/NEJMoa0805715

Duijster, J. W., Goorhuis, A., van Genderen, P. J. J., Visser, L. G., Koopmans, M. P., Reimerink, J. H., et al. (2016). Zika virus infection in 18 travellers returning from Surinam and the Dominican Republic, The Netherlands, November 2015–March 2016. *Infection*, *44*(6), 797–802. https://doi.org/10.1007/s15010-016-0906-y

Dupont-Rouzeyrol, M., Biron, A., O'Connor, O., Huguon, E., & Descloux, E. (2016). Infectious Zika viral particles in breastmilk. *The Lancet*, *387*(10023), 1051. https://doi.org/10.1016/S0140-6736(16)00624-3

ECDC. (2015). Rapid risk assessment: Zika virus epidemic in the Americas: potential association with microcephaly and Guillain-Barré syndrome - 4th update, 10 December 2015. https://www.ecdc.europa.eu/en/publications-data/rapid-risk-assessment-zika-virus-epidemic-americas-potential-association. Accessed 16 July 2025

Erasmus, J. H., Archer, J., Fuerte-Stone, J., Khandhar, A. P., Voigt, E., Granger, B., et al. (2020). Intramuscular Delivery of Replicon RNA Encoding ZIKV-117 Human Monoclonal Antibody Protects against Zika Virus Infection. *Molecular Therapy. Methods & Clinical Development*, *18*, 402–414. https://doi.org/10.1016/j.omtm.2020.06.011

Falk, A., Koch, P., Kesavan, J., Takashima, Y., Ladewig, J., Alexander, M., et al. (2012). Capture of Neuroepithelial-Like Stem Cells from Pluripotent Stem Cells Provides a Versatile System for In Vitro Production of Human Neurons. *PLOS ONE*, *7*(1), e29597. https://doi.org/10.1371/journal.pone.0029597

Faria, N. R., Azevedo, R. do S. da S., Kraemer, M. U. G., Souza, R., Cunha, M. S., Hill, S. C., et al. (2016). Zika virus in the Americas: Early epidemiological and genetic findings. *Science*, *352*(6283), 345–349. https://doi.org/10.1126/science.aaf5036

Faye, O., Freire, C. C. M., Iamarino, A., Faye, O., de Oliveira, J. V. C., Diallo, M., et al. (2014). Molecular Evolution of Zika Virus during Its Emergence in the 20th Century. *PLoS Neglected Tropical Diseases*, *8*(1), e2636. https://doi.org/10.1371/journal.pntd.0002636

Finch, P. W., & Rubin, J. S. (2004). Keratinocyte growth factor/fibroblast growth factor 7, a homeostatic factor with therapeutic potential for epithelial protection and repair. *Advances in Cancer Research*, *91*, 69–136. https://doi.org/10.1016/S0065-230X(04)91003-2

Fleiss, C. (2021). India Reported 1.77 Lakh Dengue, 237 Zika Virus Cases in 2021, Says Report. *Medindia*. https://www.medindia.net/news/india-reported-177-lakh-dengue-237-zika-virus-cases-in-2021-says-report-204661-1.htm. Accessed 16 July 2025

Freitas, D. A., Souza-Santos, R., Carvalho, L. M. A., Barros, W. B., Neves, L. M., Brasil, P., & Wakimoto, M. D. (2020). Congenital Zika syndrome: A systematic review. *PLOS ONE*, *15*(12), e0242367. https://doi.org/10.1371/journal.pone.0242367

Friedman, R. C., Farh, K. K.-H., Burge, C. B., & Bartel, D. P. (2009). Most mammalian mRNAs are conserved targets of microRNAs. *Genome Research*, *19*(1), 92–105. https://doi.org/10.1101/gr.082701.108

Fu, G., Brkić, J., Hayder, H., & Peng, C. (2013). MicroRNAs in Human Placental Development and Pregnancy Complications. *International Journal of Molecular Sciences*, *14*(3), 5519–5544. https://doi.org/10.3390/ijms14035519

Gallian, P., Cabié, A., Richard, P., Paturel, L., Charrel, R. N., Pastorino, B., et al. (2017). Zika virus in asymptomatic blood donors in Martinique. *Blood*, *129*(2), 263–266. https://doi.org/10.1182/blood-2016-09-737981

Garcez, P. P., Loiola, E. C., Madeiro da Costa, R., Higa, L. M., Trindade, P., Delvecchio, R., et al. (2016). Zika virus impairs growth in human neurospheres and brain organoids. *Science (New York, N.Y.)*, *352*(6287), 816–818. https://doi.org/10.1126/science.aaf6116

Geiszt, M., & Leto, T. L. (2004). The Nox Family of NAD(P)H Oxidases: Host Defense and Beyond *. *Journal of Biological Chemistry*, *279*(50), 51715–51718. https://doi.org/10.1074/jbc.R400024200

Gregory, R. I., Chendrimada, T. P., Cooch, N., & Shiekhattar, R. (2005). Human RISC couples microRNA biogenesis and posttranscriptional gene silencing. *Cell*, *123*(4), 631–640. https://doi.org/10.1016/j.cell.2005.10.022

Gregory, R. I., Yan, K., Amuthan, G., Chendrimada, T., Doratotaj, B., Cooch, N., & Shiekhattar, R. (2004). The Microprocessor complex mediates the genesis of microRNAs. *Nature*, *432*(7014), 235–240. https://doi.org/10.1038/nature03120

Grigor'eva, A. E., Tamkovich, S. N., Eremina, A. V., Tupikin, A. E., Kabilov, M. R., Chernykh, V. V., et al. (2016). Exosomes in tears of healthy individuals: Isolation, identification, and characterization. *Biochemistry (Moscow) Supplement Series B: Biomedical Chemistry*, *10*(2), 165–172. https://doi.org/10.1134/S1990750816020049

Grubaugh, N. D., Saraf, S., Gangavarapu, K., Watts, A., Tan, A. L., Oidtman, R. J., et al. (2019). Travel Surveillance and Genomics Uncover a Hidden Zika Outbreak during the Waning Epidemic. *Cell*, *178*(5), 1057-1071.e11. https://doi.org/10.1016/j.cell.2019.07.018

Gurunathan, S., Kang, M.-H., Jeyaraj, M., Qasim, M., & Kim, J.-H. (2019). Review of the Isolation, Characterization, Biological Function, and Multifarious Therapeutic Approaches of Exosomes. *Cells*, *8*(4). https://doi.org/10.3390/cells8040307

Gutiérrez-Bugallo, G., Piedra, L. A., Rodriguez, M., Bisset, J. A., Lourenço-de-Oliveira, R., Weaver, S. C., et al. (2019). Vector-borne transmission and evolution of Zika virus. *Nature Ecology & Evolution*, *3*(4), 561–569. https://doi.org/10.1038/s41559-019-0836-z

Haddow, A. D., Schuh, A. J., Yasuda, C. Y., Kasper, M. R., Heang, V., Huy, R., et al. (2012). Genetic characterization of Zika virus strains: geographic expansion of the Asian lineage. *PLoS neglected tropical diseases*, *6*(2), e1477. https://doi.org/10.1371/journal.pntd.0001477

Halani, S., Tombindo, P. E., O'Reilly, R., Miranda, R. N., Erdman, L. K., Whitehead, C., et al. (2021). Clinical manifestations and health outcomes associated with Zika virus infections in adults: A systematic review. *PLoS neglected tropical diseases*, *15*(7), e0009516. https://doi.org/10.1371/journal.pntd.0009516

Haldipur, P., Dang, D., Aldinger, K. A., Janson, O. K., Guimiot, F., Adle-Biasette, H., et al. (2017). Phenotypic outcomes in Mouse and Human Foxc1 dependent Dandy-Walker cerebellar malformation suggest shared mechanisms. *eLife*, *6*, e20898. https://doi.org/10.7554/eLife.20898

Halliwell, B., & Cross, C. E. (1994). Oxygen-Derived Species: Their Relation to Human Disease and Environmental Stress. *Environmental Health Perspectives*, *102*, 5–12. https://doi.org/10.2307/3432205

Halstead, S. B., & O'Rourke, E. J. (1977). Dengue viruses and mononuclear phagocytes. I. Infection enhancement by non-neutralizing antibody. *The Journal of Experimental Medicine*, *146*(1), 201–217. https://doi.org/10.1084/jem.146.1.201

Hamel, R., Dejarnac, O., Wichit, S., Ekchariyawat, P., Neyret, A., Luplertlop, N., et al. (2015a). Biology of Zika Virus Infection in Human Skin Cells. *Journal of Virology*, *89*(17), 8880. https://doi.org/10.1128/JVI.00354-15

Hamel, R., Dejarnac, O., Wichit, S., Ekchariyawat, P., Neyret, A., Luplertlop, N., et al. (2015b). Biology of Zika Virus Infection in Human Skin Cells. *Journal of Virology*, *89*(17), 8880–8896. https://doi.org/10.1128/JVI.00354-15

Han, H.-H., Diaz, C., Acosta, C. J., Liu, M., & Borkowski, A. (2021). Safety and immunogenicity of a purified inactivated Zika virus vaccine candidate in healthy adults: an observer-blind, randomised, phase 1 trial. *The Lancet. Infectious Diseases*, *21*(9), 1282–1292. https://doi.org/10.1016/S1473-3099(20)30733-7

Hastings, A. K., Yockey, L. J., Jagger, B. W., Hwang, J., Uraki, R., Gaitsch, H. F., et al. (2017). TAM receptors are not required for Zika virus infection in mice. *Cell reports*, *19*(3), 558. https://doi.org/10.1016/j.celrep.2017.03.058

Heinz, F. X., & Stiasny, K. (2017). The Antigenic Structure of Zika Virus and Its Relation to Other Flaviviruses: Implications for Infection and Immunoprophylaxis. *Microbiology and molecular biology reviews: MMBR*, *81*(1), e00055-16. https://doi.org/10.1128/MMBR.00055-16

Herrlein, M.-L., Schmanke, P., Elgner, F., Sabino, C., Akhras, S., Bender, D., et al. (2022). Catch Me if You Can: the Crosstalk of Zika Virus and the Restriction Factor Tetherin. *Journal of Virology*, *96*(4), e0211721. https://doi.org/10.1128/jvi.02117-21

Heymann, D. L., Hodgson, A., Sall, A. A., Freedman, D. O., Staples, J. E., Althabe, F., et al. (2016). Zika virus and microcephaly: why is this situation a PHEIC? *Lancet (London, England)*, *387*(10020), 719–721. https://doi.org/10.1016/S0140-6736(16)00320-2

Hill, S. C., Vasconcelos, J., Neto, Z., Jandondo, D., Zé-Zé, L., Aguiar, R. S., et al. (2019). Emergence of the Asian lineage of Zika virus in Angola: an outbreak investigation. *The Lancet Infectious Diseases*, *19*(10), 1138–1147. https://doi.org/10.1016/S1473-3099(19)30293-2

Hornick, N. I., Huan, J., Doron, B., Goloviznina, N. A., Lapidus, J., Chang, B. H., & Kurre, P. (2015). Serum Exosome MicroRNA as a Minimally-Invasive Early Biomarker of AML. *Scientific Reports*, *5*, 11295. https://doi.org/10.1038/srep11295

Ito, Y. A., Goping, I. S., Berry, F., & Walter, M. A. (2014). Dysfunction of the stress-responsive FOXC1 transcription factor contributes to the earlier-onset glaucoma observed in Axenfeld-Rieger syndrome patients. *Cell Death & Disease*, *5*(2), e1069–e1069. https://doi.org/10.1038/cddis.2014.8

Itoh, K., Chiba, T., Takahashi, S., Ishii, T., Igarashi, K., Katoh, Y., et al. (1997). An Nrf2/small Maf heterodimer mediates the induction of phase II detoxifying enzyme genes through antioxidant response elements. *Biochemical and Biophysical Research Communications*, *236*(2), 313–322. https://doi.org/10.1006/bbrc.1997.6943

Jaeger, A. S., Murrieta, R. A., Goren, L. R., Crooks, C. M., Moriarty, R. V., Weiler, A. M., et al. (2019a). Zika viruses of African and Asian lineages cause fetal harm in a mouse model of vertical transmission. *PLOS Neglected Tropical Diseases*, *13*(4), e0007343. https://doi.org/10.1371/journal.pntd.0007343

Jaeger, A. S., Murrieta, R. A., Goren, L. R., Crooks, C. M., Moriarty, R. V., Weiler, A. M., et al. (2019b). Zika viruses of African and Asian lineages cause fetal harm in a mouse model of vertical transmission. *PLoS neglected tropical diseases*, *13*(4), e0007343. https://doi.org/10.1371/journal.pntd.0007343

Jaiswal, A. K. (2004). Nrf2 signaling in coordinated activation of antioxidant gene expression. *Free Radical Biology and Medicine*, *36*(10), 1199–1207. https://doi.org/10.1016/j.freeradbiomed.2004.02.074

Jamrozik, E., & Selgelid, M. J. (2018). Ethics, health policy, and Zika: From emergency to global epidemic? *Journal of Medical Ethics*, *44*(5), 343–348.

Jegal, K. H., Park, S. M., Cho, S. S., Byun, S. H., Ku, S. K., Kim, S. C., et al. (2017). Activating transcription factor 6-dependent sestrin 2 induction ameliorates ER stress-mediated liver injury. *Biochimica et*

Biophysica Acta (BBA) - Molecular Cell Research, *1864*(7), 1295–1307. https://doi.org/10.1016/j.bbamcr.2017.04.010

Jorge, F. A., Thomazella, M. V., de Castro Moreira, D., Lopes, L. D. G., Teixeira, J. J. V., & Bertolini, D. A. (2020). Evolutions and upcoming on Zika virus diagnosis through an outbreak: A systematic review. *Reviews in Medical Virology*, *30*(3), e2105. https://doi.org/10.1002/rmv.2105

Kaletsky, R. L., Francica, J. R., Agrawal-Gamse, C., & Bates, P. (2009). Tetherin-mediated restriction of filovirus budding is antagonized by the Ebola glycoprotein. *Proceedings of the National Academy of Sciences of the United States of America*, *106*(8), 2886–2891. https://doi.org/10.1073/pnas.0811014106

Kanehisa, M., & Goto, S. (2000). KEGG: kyoto encyclopedia of genes and genomes. *Nucleic Acids Research*, *28*(1), 27–30. https://doi.org/10.1093/nar/28.1.27

Kaufmann, B., & Rossmann, M. G. (2010). Molecular mechanisms involved in the early steps of flavivirus cell entry. *Microbes and infection / Institut Pasteur*, *13*(1), 1. https://doi.org/10.1016/j.micinf.2010.09.005

Kim, J.-A., Seong, R.-K., Son, S. W., & Shin, O. S. (2019). Insights into ZIKV-Mediated Innate Immune Responses in Human Dermal Fibroblasts and Epidermal Keratinocytes. *Journal of Investigative Dermatology*, *139*(2), 391–399. https://doi.org/10.1016/j.jid.2018.07.038

Kobayashi, M., Li, L., Iwamoto, N., Nakajima-Takagi, Y., Kaneko, H., Nakayama, Y., et al. (2009). The Antioxidant Defense System Keap1-Nrf2 Comprises a Multiple Sensing Mechanism for Responding to a Wide Range of Chemical Compounds. *Molecular and Cellular Biology*, *29*(2), 493–502. https://doi.org/10.1128/MCB.01080-08

Kobayashi, M., & Yamamoto, M. (2005). Molecular mechanisms activating the Nrf2-Keap1 pathway of antioxidant gene regulation. *Antioxidants & Redox Signaling*, *7*(3–4), 385–394. https://doi.org/10.1089/ars.2005.7.385

Koch, P., Opitz, T., Steinbeck, J. A., Ladewig, J., & Brustle, O. (2009). A rosette-type, self-renewing human ES cell-derived neural stem cell with potential for in vitro instruction and synaptic integration. *Proceedings of the National Academy of Sciences*, *106*(9), 3225–3230. https://doi.org/10.1073/pnas.0808387106

Komatsu, M., Kurokawa, H., Waguri, S., Taguchi, K., Kobayashi, A., Ichimura, Y., et al. (2010). The selective autophagy substrate p62 activates the stress responsive transcription factor Nrf2 through inactivation of Keap1. *Nature Cell Biology*, *12*(3), 213–223. https://doi.org/10.1038/ncb2021

Kozak, R., Majer, A., Biondi, M., Medina, S., Goneau, L., Sajesh, B., et al. (2017). MicroRNA and mRNA Dysregulation in Astrocytes Infected with Zika Virus. *Viruses*, *9*(10), 297. https://doi.org/10.3390/v9100297

Kraemer, M. U., Sinka, M. E., Duda, K. A., Mylne, A. Q., Shearer, F. M., Barker, C. M., et al. (2015). The global distribution of the arbovirus vectors Aedes aegypti and Ae. albopictus. *eLife*, *4*, e08347. https://doi.org/10.7554/eLife.08347

Kramer, L. D., & Ciota, A. T. (2015). Dissecting vectorial capacity for mosquito-borne viruses. *Current Opinion in Virology*, *15*, 112–118. https://doi.org/10.1016/j.coviro.2015.10.003

Krek, A., Grün, D., Poy, M. N., Wolf, R., Rosenberg, L., Epstein, E. J., et al. (2005). Combinatorial microRNA target predictions. *Nature Genetics*, *37*(5), 495–500. https://doi.org/10.1038/ng1536

Kutsuna, S. (2017). Zika virus infection: Clinical overview with a summary of Japanese cases. *Clinical and Experimental Neuroimmunology*, *8*(3), 192–198. https://doi.org/10.1111/cen3.12408

Lanciotti, R. S., Kosoy, O. L., Laven, J. J., Velez, J. O., Lambert, A. J., Johnson, A. J., et al. (2008). Genetic and Serologic Properties of Zika Virus Associated with an Epidemic, Yap State, Micronesia, 2007. *Emerging Infectious Diseases*, *14*(8), 1232–1239. https://doi.org/10.3201/eid1408.080287

Lanciotti, R. S., Lambert, A. J., Holodniy, M., Saavedra, S., & Signor, L. del C. C. (2016). Phylogeny of Zika Virus in Western Hemisphere, 2015. *Emerging Infectious Diseases*, *22*(5), 933–935. https://doi.org/10.3201/eid2205.160065

Le Tortorec, A., Willey, S., & Neil, S. J. D. (2011). Antiviral Inhibition of Enveloped Virus Release by Tetherin/BST-2: Action and Counteraction. *Viruses*, *3*(5), 520–540. https://doi.org/10.3390/v3050520

Lei, Z., Gu, Y., Liu, Y., Liu, H., Lu, X., Chen, W., et al. (2025). Identification of antiviral RNAi regulators, ILF3/DHX9, recruit at ZIKV stem loop B to protect against ZIKV induced microcephaly. *Nature Communications*, *16*(1), 1991. https://doi.org/10.1038/s41467-025-56859-x

Li, L., Lok, S.-M., Yu, I.-M., Zhang, Y., Kuhn, R. J., Chen, J., & Rossmann, M. G. (2008). The flavivirus precursor membrane-envelope protein complex: structure and maturation. *Science (New York, N.Y.)*, *319*(5871), 1830–1834. https://doi.org/10.1126/science.1153263

Li, S., Lei, Z., & Sun, T. (2022). The role of microRNAs in neurodegenerative diseases: a review. *Cell Biology and Toxicology*, *39*(1), 53. https://doi.org/10.1007/s10565-022-09761-x

Li, Y., & Chen, X. (2015). miR-4792 inhibits epithelial–mesenchymal transition and invasion in nasopharyngeal carcinoma by targeting FOXC1. *Biochemical and Biophysical Research Communications*, *468*(4), 863–869. https://doi.org/10.1016/j.bbrc.2015.11.045

Lin, L.-T., Liu, S.-Y., Leu, J.-D., Chang, C.-Y., Chiou, S.-H., Lee, T.-C., & Lee, Y.-J. (2018). Arsenic trioxide-mediated suppression of miR-182-5p is associated with potent anti-oxidant effects through up-regulation of SESN2. *Oncotarget*, *9*(22), 16028–16042. https://doi.org/10.18632/oncotarget.24678

Littaua, R., Kurane, I., & Ennis, F. A. (1990). Human IgG Fc receptor II mediates antibody-dependent enhancement of dengue virus infection. *Journal of Immunology (Baltimore, Md.: 1950)*, *144*(8), 3183–3186.

Liu, P., Pu, J., Zhang, J., Chen, Z., Wei, K., & Shi, L. (2019). Bioinformatic analysis of miR-4792 regulates Radix Tetrastigma hemsleyani flavone to inhibit proliferation, invasion, and induce apoptosis of A549 cells. *OncoTargets and Therapy*, *Volume 12*, 1401–1412. https://doi.org/10.2147/OTT.S182525

Lomelino, C. L., Andring, J. T., McKenna, R., & Kilberg, M. S. (2017). Asparagine synthetase: Function, structure, and role in disease. *Journal of Biological Chemistry*, *292*(49), 19952–19958. https://doi.org/10.1074/jbc.R117.819060

López-Medina, E., Rojas, C. A., Calle-Giraldo, J. P., Alexander, N., Hurtado, I. C., Dávalos, D. M., et al. (2021). Risks of Adverse Childhood Outcomes According to Prenatal Time of Exposure to Zika Virus: Assessment in a Cohort Exposed to Zika During an Outbreak in Colombia. *Journal of the Pediatric Infectious Diseases Society*, *10*(3), 337–340. https://doi.org/10.1093/jpids/piaa042

Lowey, B., Hertz, L., Chiu, S., Valdez, K., Li, Q., & Liang, T. J. (2019). Hepatitis C Virus Infection Induces Hepatic Expression of NF-□B-Inducing Kinase and Lipogenesis by Downregulating miR-122, *10*(4), 19.

Maddaluno, L., Urwyler, C., Rauschendorfer, T., Meyer, M., Stefanova, D., Spörri, R., et al. (2020). Antagonism of interferon signaling by fibroblast growth factors promotes viral replication. *EMBO Molecular Medicine*, *12*(9), e11793. https://doi.org/10.15252/emmm.201911793

Maddaluno, L., Urwyler, C., & Werner, S. (2017). Fibroblast growth factors: key players in regeneration and tissue repair. *Development (Cambridge, England)*, *144*(22), 4047–4060. https://doi.org/10.1242/dev.152587

Mansuy, J. M., Suberbielle, E., Chapuy-Regaud, S., Mengelle, C., Bujan, L., Marchou, B., et al. (2016). Zika virus in semen and spermatozoa. *The Lancet Infectious Diseases*, *16*(10), 1106–1107. https://doi.org/10.1016/S1473-3099(16)30336-X

Mao, L., Chen, Y., Gu, J., Zhao, Y., & Chen, Q. (2023). Roles and mechanisms of exosomal microRNAs in viral infections. *Archives of Virology*, *168*(4), 121. https://doi.org/10.1007/s00705-023-05744-3

mapchart.net. (2025). Mapchart. *MapChart*. https://mapchart.net/world.html. Accessed 16 July 2025

Maria, A. T., Maquart, M., Makinson, A., Flusin, O., Segondy, M., Leparc-Goffart, I., et al. (2016). Zika virus infections in three travellers returning from South America and the Caribbean respectively, to Montpellier, France, December 2015 to January 2016. *Eurosurveillance*, *21*(6), 30131. https://doi.org/10.2807/1560-7917.ES.2016.21.6.30131

Martínez-Rojas, P. P., Monroy-Martínez, V., & Ruiz-Ordaz, B. H. (2025). Role of extracellular vesicles in the pathogenesis of mosquito-borne flaviviruses that impact public health. *Journal of Biomedical Science*, *32*(1), 4. https://doi.org/10.1186/s12929-024-01096-5

Meaney-Delman, D., Hills, S. L., Williams, C., Galang, R. R., Iyengar, P., Hennenfent, A. K., et al. (2016). Zika Virus Infection Among U.S. Pregnant Travelers - August 2015-February 2016. *MMWR. Morbidity and mortality weekly report*, *65*(8), 211–214. https://doi.org/10.15585/mmwr.mm6508e1

Mécharles, S., Herrmann, C., Poullain, P., Tran, T.-H., Deschamps, N., Mathon, G., et al. (2016). Acute myelitis due to Zika virus infection. *Lancet (London, England)*, *387*(10026), 1481. https://doi.org/10.1016/S0140-6736(16)00644-9

Meda, N., Salinas, S., Kagoné, T., Simonin, Y., & Van de Perre, P. (2016). Zika virus epidemic: Africa should not be neglected. *The Lancet*, *388*(10042), 337–338. https://doi.org/10.1016/S0140-6736(16)31103-5

Medvedev, R., Ploen, D., Spengler, C., Elgner, F., Ren, H., Bunten, S., & Hildt, E. (2017). HCV-induced oxidative stress by inhibition of Nrf2 triggers autophagy and favors release of viral particles. *Free Radical Biology and Medicine*, *110*, 300–315. https://doi.org/10.1016/j.freeradbiomed.2017.06.021

Meertens, L., Labeau, A., Dejarnac, O., Cipriani, S., Sinigaglia, L., Bonnet-Madin, L., et al. (2017). Axl Mediates ZIKA Virus Entry in Human Glial Cells and Modulates Innate Immune Responses. *Cell Reports*, *18*(2), 324–333. https://doi.org/10.1016/j.celrep.2016.12.045

Mendell, J. T. (2005). MicroRNAs: critical regulators of development, cellular physiology and malignancy. *Cell Cycle (Georgetown, Tex.)*, *4*(9), 1179–1184. https://doi.org/10.4161/cc.4.9.2032

Miner, J. J., & Diamond, M. S. (2017a). Zika Virus Pathogenesis and Tissue Tropism. *Cell Host & Microbe*, *21*(2), 134–142. https://doi.org/10.1016/j.chom.2017.01.004

Miner, J. J., & Diamond, M. S. (2017b). Dengue Antibodies, then Zika: A Fatal Sequence in Mice. *Immunity*, *46*(5), 771–773. https://doi.org/10.1016/j.immuni.2017.04.023

Miner, J. J., Sene, A., Richner, J. M., Smith, A. M., Santeford, A., Ban, N., et al. (2016). Zika virus infection in mice causes pan-uveitis with shedding of virus in tears. *Cell reports*, *16*(12), 3208. https://doi.org/10.1016/j.celrep.2016.08.079

Mlakar, J., Korva, M., Tul, N., Popović, M., Poljšak-Prijatelj, M., Mraz, J., et al. (2016). Zika Virus Associated with Microcephaly. *The New England Journal of Medicine*, *374*(10), 951–958. https://doi.org/10.1056/NEJMoa1600651

Mousavi, M. J., Arefinia, N., Azarsa, M., Hoseinnezhad, T., & Behboudi, E. (2024). MicroRNA profiles in Zika virus infection: Insights from diverse sources. *Indian Journal of Medical Microbiology*, *51*, 100697. https://doi.org/10.1016/j.ijmmb.2024.100697

Musso, D., & Gubler, D. J. (2016). Zika Virus. *Clinical Microbiology Reviews*, *29*(3), 487–524. https://doi.org/10.1128/cmr.00072-15

Neil, S. J. D., Zang, T., & Bieniasz, P. D. (2008). Tetherin inhibits retrovirus release and is antagonized by HIV-1 Vpu. *Nature*, *451*(7177), 425–430. https://doi.org/10.1038/nature06553

Nicastri, E., Castilletti, C., Liuzzi, G., Iannetta, M., Capobianchi, M. R., & Ippolito, G. (2016). Persistent detection of Zika virus RNA in semen for six months after symptom onset in a traveller returning from Haiti to Italy, February 2016. *Eurosurveillance*, *21*(32), 30314. https://doi.org/10.2807/1560-7917.ES.2016.21.32.30314

Nicastri, E., Pisapia, R., Corpolongo, A., Fusco, F. M., Cicalini, S., Scognamiglio, P., et al. (2016). Three cases of Zika virus imported in Italy: need for a clinical awareness and evidence-based knowledge. *BMC infectious diseases*, *16*(1), 669. https://doi.org/10.1186/s12879-016-1973-5

Nkolola, J. P., Hope, D., Guan, R., Colarusso, A., Aid, M., Weiss, D., et al. (2024). Protective threshold of a potent neutralizing Zika virus monoclonal antibody in rhesus macaques. *Journal of Virology*, *98*(12), e01429-24. https://doi.org/10.1128/jvi.01429-24

Nogueira, M. L., Estofolete, C. F., Terzian, A. C. B., Mascarin do Vale, E. P. B., da Silva, R. C. M. A., da Silva, R. F., et al. (2017). Zika Virus Infection and Solid Organ Transplantation: A New Challenge. *American Journal of Transplantation: Official Journal of the American Society of Transplantation and the American Society of Transplant Surgeons*, *17*(3), 791–795. https://doi.org/10.1111/ajt.14047

Nutt, C., & Adams, P. (2017). Zika in Africa—the invisible epidemic? *The Lancet*, *389*(10079), 1595–1596. https://doi.org/10.1016/S0140-6736(17)31051-6

Oehler, E., Watrin, L., Larre, P., Leparc-Goffart, I., Lastere, S., Valour, F., et al. (2014). Zika virus infection complicated by Guillain-Barre syndrome--case report, French Polynesia, December 2013. *Euro Surveillance: Bulletin Europeen Sur Les Maladies Transmissibles = European Communicable Disease Bulletin*, *19*(9). https://doi.org/10.2807/1560-7917.es2014.19.9.20720

Olagnier, D., Peri, S., Steel, C., van Montfoort, N., Chiang, C., Beljanski, V., et al. (2014). Cellular Oxidative Stress Response Controls the Antiviral and Apoptotic Programs in Dengue Virus-Infected Dendritic Cells. *PLoS Pathogens*, *10*(12), e1004566. https://doi.org/10.1371/journal.ppat.1004566

Oliveira Melo, A. S., Malinger, G., Ximenes, R., Szejnfeld, P. O., Alves Sampaio, S., & Bispo de Filippis, A. M. (2016). Zika virus intrauterine infection causes fetal brain abnormality and microcephaly: tip of the iceberg? *Ultrasound in Obstetrics & Gynecology: The Official Journal of the International*

Society of Ultrasound in Obstetrics and Gynecology, *47*(1), 6–7. https://doi.org/10.1002/uog.15831

Owczarek, K., Chykunova, Y., Jassoy, C., Maksym, B., Rajfur, Z., & Pyrc, K. (2019). Zika virus: mapping and reprogramming the entry. *Cell Communication and Signaling*, *17*(1), 41. https://doi.org/10.1186/s12964-019-0349-z

Paniz-Mondolfi, A. E., Rodriguez-Morales, A. J., Blohm, G., Marquez, M., & Villamil-Gomez, W. E. (2016). ChikDenMaZika Syndrome: the challenge of diagnosing arboviral infections in the midst of concurrent epidemics. *Annals of Clinical Microbiology and Antimicrobials*, *15*(1), 42. https://doi.org/10.1186/s12941-016-0157-x

Parra, B., Lizarazo, J., Jiménez-Arango, J. A., Zea-Vera, A. F., González-Manrique, G., Vargas, J., et al. (2016). Guillain–Barré Syndrome Associated with Zika Virus Infection in Colombia. *New England Journal of Medicine*, *375*(16), 1513–1523. https://doi.org/10.1056/NEJMoa1605564

Passemard, S., Kaindl, A. M., & Verloes, A. (2013). Microcephaly. *Handbook of Clinical Neurology*, *111*, 129–141. https://doi.org/10.1016/B978-0-444-52891-9.00013-0

Paz-Bailey, G., Rosenberg, E. S., Doyle, K., Munoz-Jordan, J., Santiago, G. A., Klein, L., et al. (2018). Persistence of Zika Virus in Body Fluids — Final Report. *New England Journal of Medicine*, *379*(13), 1234–1243. https://doi.org/10.1056/NEJMoa1613108

Persaud, M., Martinez-Lopez, A., Buffone, C., Porcelli, S. A., & Diaz-Griffero, F. (2018). Infection by Zika viruses requires the transmembrane protein AXL, endocytosis and low pH. *Virology*, *518*, 301–312. https://doi.org/10.1016/j.virol.2018.03.009

Pierson, T. C., & Diamond, M. S. (2018). The emergence of Zika virus and its new clinical syndromes. *Nature*, *560*(7720), 573–581. https://doi.org/10.1038/s41586-018-0446-y

Pizzino, G., Irrera, N., Cucinotta, M., Pallio, G., Mannino, F., Arcoraci, V., et al. (2017). Oxidative Stress: Harms and Benefits for Human Health. *Oxidative Medicine and Cellular Longevity*, *2017*(1), 8416763. https://doi.org/10.1155/2017/8416763

Pool, K.-L., Adachi, K., Karnezis, S., Salamon, N., Romero, T., Nielsen-Saines, K., et al. (2019). Association Between Neonatal Neuroimaging and Clinical Outcomes in Zika-Exposed Infants From Rio de Janeiro, Brazil. *JAMA Network Open*, *2*(7), e198124. https://doi.org/10.1001/jamanetworkopen.2019.8124

Pyke, A. T., Moore, P. R., Hall-Mendelin, S., McMahon, J. L., Harrower, B. J., Constantino, T. R., & van den Hurk, A. F. (2016). Isolation of Zika Virus Imported from Tonga into Australia. *PLoS Currents*, *8*, ecurrents.outbreaks.849adc0ad16beec4536695281707f785. https://doi.org/10.1371/currents.outbreaks.849adc0ad16beec4536695281707f785

Raposo, G., & Stoorvogel, W. (2013). Extracellular vesicles: Exosomes, microvesicles, and friends. *Journal of Cell Biology*, *200*(4), 373–383. https://doi.org/10.1083/jcb.201211138

Reczko, M., Maragkakis, M., Alexiou, P., Grosse, I., & Hatzigeorgiou, A. G. (2012). Functional microRNA targets in protein coding sequences. *Bioinformatics (Oxford, England)*, *28*(6), 771–776. https://doi.org/10.1093/bioinformatics/bts043

Rehbach, K., Kesavan, J., Hauser, S., Ritzenhofen, S., Jungverdorben, J., Schüle, R., et al. (2019). Multiparametric rapid screening of neuronal process pathology for drug target identification in HSP patient-specific neurons. *Scientific Reports*, *9*. https://doi.org/10.1038/s41598-019-45246-4

Reid, D. W., Campos, R. K., Child, J. R., Zheng, T., Chan, K. W. K., Bradrick, S. S., et al. (2018). Dengue Virus Selectively Annexes Endoplasmic Reticulum-Associated Translation Machinery as a Strategy for Co-opting Host Cell Protein Synthesis. *Journal of Virology*, *92*(7), e01766-17. https://doi.org/10.1128/JVI.01766-17

Reikine, S., Nguyen, J. B., & Modis, Y. (2014). Pattern Recognition and Signaling Mechanisms of RIG-I and MDA5. *Frontiers in Immunology*, *5*. https://doi.org/10.3389/fimmu.2014.00342

Richard, A. S., Shim, B.-S., Kwon, Y.-C., Zhang, R., Otsuka, Y., Schmitt, K., et al. (2017). AXL-dependent infection of human fetal endothelial cells distinguishes Zika virus from other pathogenic

flaviviruses. *Proceedings of the National Academy of Sciences of the United States of America*, *114*(8), 2024–2029. https://doi.org/10.1073/pnas.1620558114

Richards, N. G. J., & Kilberg, M. S. (2006). Asparagine Synthetase Chemotherapy. *Annual review of biochemistry*, *75*, 629–654. https://doi.org/10.1146/annurev.biochem.75.103004.142520

Rodrigo, W. W. S. I., Jin, X., Blackley, S. D., Rose, R. C., & Schlesinger, J. J. (2006). Differential enhancement of dengue virus immune complex infectivity mediated by signaling-competent and signaling-incompetent human Fcgamma RIA (CD64) or FcgammaRIIA (CD32). *Journal of Virology*, *80*(20), 10128–10138. https://doi.org/10.1128/JVI.00792-06

Rodriguez-Morales, A. J. (2015). Zika: the new arbovirus threat for Latin America. *The Journal of Infection in Developing Countries*, *9*(06), 684–685. https://doi.org/10.3855/jidc.7230

Rushworth, S. A., MacEwan, D. J., & O'Connell, M. A. (2008). Lipopolysaccharide-Induced Expression of NAD(P)H:Quinone Oxidoreductase 1 and Heme Oxygenase-1 Protects against Excessive Inflammatory Responses in Human Monocytes. *The Journal of Immunology*, *181*(10), 6730–6737. https://doi.org/10.4049/jimmunol.181.10.6730

Sabino, C., Bender, D., Herrlein, M.-L., & Hildt, E. (2021). The Epidermal Growth Factor Receptor Is a Relevant Host Factor in the Early Stages of The Zika Virus Life Cycle In Vitro. *Journal of Virology*, *95*(20), e0119521. https://doi.org/10.1128/JVI.01195-21

Sager, G., Gabaglio, S., Sztul, E., & Belov, G. A. (2018). Role of Host Cell Secretory Machinery in Zika Virus Life Cycle. *Viruses*, *10*(10), 559. https://doi.org/10.3390/v10100559

Sakuma, T., Noda, T., Urata, S., Kawaoka, Y., & Yasuda, J. (2009). Inhibition of Lassa and Marburg virus production by tetherin. *Journal of Virology*, *83*(5), 2382–2385. https://doi.org/10.1128/JVI.01607-08

Salomon, C., Kobayashi, M., Ashman, K., Sobrevia, L., Mitchell, M. D., & Rice, G. E. (2013). Hypoxia-Induced Changes in the Bioactivity of Cytotrophoblast-Derived Exosomes. *PLOS ONE*, *8*(11), e79636. https://doi.org/10.1371/journal.pone.0079636

Sarkar, S., & Gardner, L. (2016). Zika: the cost of neglect. *Palgrave Communications*, *2*(1), 1–6. https://doi.org/10.1057/palcomms.2016.60

Schleinitz, D., Seidel, A., Stassart, R., Klammt, J., Hirrlinger, P. G., Winkler, U., et al. (2018). Novel Mutations in the Asparagine Synthetase Gene (ASNS) Associated With Microcephaly. *Frontiers in Genetics*, *9*, 245. https://doi.org/10.3389/fgene.2018.00245

Schmittgen, T. D., & Livak, K. J. (2008). Analyzing real-time PCR data by the comparative C T method. *Nature Protocols*, *3*(6), 1101–1108. https://doi.org/10.1038/nprot.2008.73

Schuler-Faccini, L., Ribeiro, E. M., Feitosa, I. M. L., Horovitz, D. D. G., Cavalcanti, D. P., Pessoa, A., et al. (2016). Possible Association Between Zika Virus Infection and Microcephaly - Brazil, 2015. *MMWR. Morbidity and mortality weekly report*, *65*(3), 59–62. https://doi.org/10.15585/mmwr.mm6503e2

SETHUPATHY, P., CORDA, B., & HATZIGEORGIOU, A. G. (2006). TarBase: A comprehensive database of experimentally supported animal microRNA targets. *RNA*, *12*(2), 192–197. https://doi.org/10.1261/rna.2239606

Sheridan, M. A., Balaraman, V., Schust, D. J., Ezashi, T., Roberts, R. M., & Franz, A. W. E. (2018). African and Asian strains of Zika virus differ in their ability to infect and lyse primitive human placental trophoblast. *PLOS ONE*, *13*(7), e0200086. https://doi.org/10.1371/journal.pone.0200086

Shin, B. Y., Jin, S. H., Cho, I. J., & Ki, S. H. (2012). Nrf2-ARE pathway regulates induction of Sestrin-2 expression. *Free Radical Biology & Medicine*, *53*(4), 834–841. https://doi.org/10.1016/j.freeradbiomed.2012.06.026

Sies, H. (2015). Oxidative stress: a concept in redox biology and medicine. *Redox Biology*, *4*, 180–183. https://doi.org/10.1016/j.redox.2015.01.002

Simmonds, P., Becher, P., Bukh, J., Gould, E. A., Meyers, G., Monath, T., et al. (2017). ICTV Virus Taxonomy Profile: Flaviviridae. *The Journal of General Virology*, *98*(1), 2–3. https://doi.org/10.1099/jgv.0.000672

Simonin, Y., Loustalot, F., Desmetz, C., Foulongne, V., Constant, O., Fournier-Wirth, C., et al. (2016). Zika Virus Strains Potentially Display Different Infectious Profiles in Human Neural Cells. *EBioMedicine*, *12*, 161–169. https://doi.org/10.1016/j.ebiom.2016.09.020

Simonin, Y., van Riel, D., Van de Perre, P., Rockx, B., & Salinas, S. (2017). Differential virulence between Asian and African lineages of Zika virus. *PLoS Neglected Tropical Diseases*, *11*(9). https://doi.org/10.1371/journal.pntd.0005821

Simons, M., & Raposo, G. (2009). Exosomes – vesicular carriers for intercellular communication. *Current Opinion in Cell Biology*, *21*(4), 575–581. https://doi.org/10.1016/j.ceb.2009.03.007

Singh, A., Kukreti, R., Saso, L., & Kukreti, S. (2019). Oxidative Stress: A Key Modulator in Neurodegenerative Diseases. *Molecules*, *24*(8), 1583. https://doi.org/10.3390/molecules24081583

Sirohi, D., Chen, Z., Sun, L., Klose, T., Pierson, T. C., Rossmann, M. G., & Kuhn, R. J. (2016). The 3.8 Å resolution cryo-EM structure of Zika virus. *Science*, *352*(6284), 467–470. https://doi.org/10.1126/science.aaf5316

Sirohi, D., & Kuhn, R. J. (2017). Zika Virus Structure, Maturation, and Receptors. *The Journal of Infectious Diseases*, *216*(suppl_10), S935–S944. https://doi.org/10.1093/infdis/jix515

Slonchak, A., Clarke, B., Mackenzie, J., Amarilla, A. A., Setoh, Y. X., & Khromykh, A. A. (2019). West Nile virus infection and interferon alpha treatment alter the spectrum and the levels of coding and noncoding host RNAs secreted in extracellular vesicles. *BMC Genomics*, *20*(1), 474. https://doi.org/10.1186/s12864-019-5835-6

Soontornniyomkij, V., Soontornniyomkij, B., Moore, D. J., Gouaux, B., Masliah, E., Tung, S., et al. (2012). Antioxidant Sestrin-2 Redistribution to Neuronal Soma in Human Immunodeficiency Virus-Associated Neurocognitive Disorders. *Journal of Neuroimmune Pharmacology*, *7*(3), 579–590. https://doi.org/10.1007/s11481-012-9357-0

Staples, J. E., Dziuban, E. J., Fischer, M., Cragan, J. D., Rasmussen, S. A., Cannon, M. J., et al. (2016). Interim Guidelines for the Evaluation and Testing of Infants with Possible Congenital Zika Virus Infection - United States, 2016. *MMWR. Morbidity and mortality weekly report*, *65*(3), 63–67. https://doi.org/10.15585/mmwr.mm6503e3

Street, J. M., Barran, P. E., Mackay, C. L., Weidt, S., Balmforth, C., Walsh, T. S., et al. (2012). Identification and proteomic profiling of exosomes in human cerebrospinal fluid. *Journal of Translational Medicine*, *10*(1), 5. https://doi.org/10.1186/1479-5876-10-5

Tabari, D., Scholl, C., Steffens, M., Weickhardt, S., Elgner, F., Bender, D., et al. (2020). Impact of Zika Virus Infection on Human Neural Stem Cell MicroRNA Signatures. *Viruses*, *12*(11). https://doi.org/10.3390/v12111219

Tang, H., Hammack, C., Ogden, S. C., Wen, Z., Qian, X., Li, Y., et al. (2016). Zika Virus Infects Human Cortical Neural Progenitors and Attenuates Their Growth. *Cell Stem Cell*, *18*(5), 587–590. https://doi.org/10.1016/j.stem.2016.02.016

tenOever, B. R. (2013). RNA viruses and the host microRNA machinery. *Nature Reviews Microbiology*, *11*(3), 169–180. https://doi.org/10.1038/nrmicro2971

Valadão, A. L. C., Aguiar, R. S., & de Arruda, L. B. (2016). Interplay between Inflammation and Cellular Stress Triggered by Flaviviridae Viruses. *Frontiers in Microbiology*, *7*, 1233. https://doi.org/10.3389/fmicb.2016.01233

Vasiliou, V., Ross, D., & Nebert, D. W. (2006). Update of the NAD(P)H:quinone oxidoreductase (NQO) gene family. *Human Genomics*, *2*(5), 329. https://doi.org/10.1186/1479-7364-2-5-329

Vazeille, M., Madec, Y., Mousson, L., Bellone, R., Barré-Cardi, H., Sousa, C. A., et al. (2019). Zika virus threshold determines transmission by European Aedes albopictus mosquitoes. *Emerging Microbes & Infections*, *8*(1), 1668. https://doi.org/10.1080/22221751.2019.1689797

Ventura, C. V., Maia, M., Dias, N., Ventura, L. O., & Belfort, R. (2016). Zika: neurological and ocular findings in infant without microcephaly. *Lancet (London, England)*, *387*(10037), 2502. https://doi.org/10.1016/S0140-6736(16)30776-0

Vermillion, M. S., Lei, J., Shabi, Y., Baxter, V. K., Crilly, N. P., McLane, M., et al. (2017). Intrauterine Zika virus infection of pregnant immunocompetent mice models transplacental transmission and adverse perinatal outcomes. *Nature Communications*, *8*, 14575. https://doi.org/10.1038/ncomms14575

Vlachos, I. S., Zagganas, K., Paraskevopoulou, M. D., Georgakilas, G., Karagkouni, D., Vergoulis, T., et al. (2015). DIANA-miRPath v3.0: deciphering microRNA function with experimental support. *Nucleic Acids Research*, *43*(W1), W460–W466. https://doi.org/10.1093/nar/gkv403

Vojtech, L., Woo, S., Hughes, S., Levy, C., Ballweber, L., Sauteraud, R. P., et al. (2014). Exosomes in human semen carry a distinctive repertoire of small non-coding RNAs with potential regulatory functions. *Nucleic Acids Research*, *42*(11), 7290–7304. https://doi.org/10.1093/nar/gku347

von der Hagen, M., Pivarcsi, M., Liebe, J., von Bernuth, H., Didonato, N., Hennermann, J. B., et al. (2014). Diagnostic approach to microcephaly in childhood: a two-center study and review of the literature. *Developmental Medicine and Child Neurology*, *56*(8), 732–741. https://doi.org/10.1111/dmcn.12425

Vora, A., Zhou, W., Londono-Renteria, B., Woodson, M., Sherman, M. B., Colpitts, T. M., et al. (2018). Arthropod EVs mediate dengue virus transmission through interaction with a tetraspanin domain containing glycoprotein Tsp29Fb. *Proceedings of the National Academy of Sciences of the United States of America*, *115*(28), E6604–E6613. https://doi.org/10.1073/pnas.1720125115

Wang, X. (2008). miRDB: A microRNA target prediction and functional annotation database with a wiki interface. *RNA*, *14*(6), 1012–1017. https://doi.org/10.1261/rna.965408

Wang, Z.-Y., Wang, Z., Zhen, Z.-D., Feng, K.-H., Guo, J., Gao, N., et al. (2017). Axl is not an indispensable factor for Zika virus infection in mice. *The Journal of General Virology*, *98*(8), 2061. https://doi.org/10.1099/jgv.0.000886

Weaver, S. C. (2017). Emergence of Epidemic Zika Virus Transmission and Congenital Zika Syndrome: Are Recently Evolved Traits to Blame? *mBio*, *8*(1), e02063-16. https://doi.org/10.1128/mBio.02063-16

Weaver, S. C., Costa, F., Garcia-Blanco, M. A., Ko, A. I., Ribeiro, G. S., Saade, G., et al. (2016). Zika virus: History, emergence, biology, and prospects for control. *Antiviral Research*, *130*, 69–80. https://doi.org/10.1016/j.antiviral.2016.03.010

WHO. (2016). Fifth meeting of the Emergency Committee under the International Health Regulations (2005) regarding microcephaly, other neurological disorders and Zika virus. https://www.who.int/news/item/18-11-2016-fifth-meeting-of-the-emergency-committee-under-the-international-health-regulations-(2005)-regarding-microcephaly-other-neurological-disorders-and-zika-virus. Accessed 16 July 2025

WHO. (2022). Zika epidemiology update - February 2022. https://www.who.int/publications/m/item/zika-epidemiology-update---february-2022. Accessed 16 July 2025

WHO. (2024). Zika epidemiology update - May 2024. https://www.who.int/publications/m/item/zika-epidemiology-update-may-2024. Accessed 16 July 2025

Wikan, N., & Smith, D. R. (2016). Zika virus: history of a newly emerging arbovirus. *The Lancet. Infectious Diseases*, *16*(7), e119–e126. https://doi.org/10.1016/S1473-3099(16)30010-X

Woodson, S. E., & Morabito, K. M. (2024). Continuing development of vaccines and monoclonal antibodies against Zika virus. *npj Vaccines*, *9*(1), 1–8. https://doi.org/10.1038/s41541-024-00889-x

Xiao, T., Zhang, L., Huang, Y., Shi, Y., Wang, J., Ji, Q., et al. (2019). Sestrin2 increases in aortas and plasma from aortic dissection patients and alleviates angiotensin II-induced smooth muscle cell apoptosis via the Nrf2 pathway. *Life Sciences*, *218*, 132–138. https://doi.org/10.1016/j.lfs.2018.12.043

Yamamoto, M., Kensler, T. W., & Motohashi, H. (2018). The KEAP1-NRF2 System: a Thiol-Based Sensor-Effector Apparatus for Maintaining Redox Homeostasis. *Physiological Reviews*, *98*(3), 1169–1203. https://doi.org/10.1152/physrev.00023.2017

Yáñez-Mó, M., Siljander, P. R.-M., Andreu, Z., Zavec, A. B., Borràs, F. E., Buzas, E. I., et al. (2015). Biological properties of extracellular vesicles and their physiological functions. *Journal of Extracellular Vesicles*, *4*, 27066. https://doi.org/10.3402/jev.v4.27066

Yao, S. (2016). MicroRNA biogenesis and their functions in regulating stem cell potency and differentiation. *Biological Procedures Online*, *18*, 8. https://doi.org/10.1186/s12575-016-0037-y

Ye, H., Kang, L., Yan, X., Li, S., Huang, Y., Mu, R., et al. (2022). MiR-103a-3p Promotes Zika Virus Replication by Targeting OTU Deubiquitinase 4 to Activate p38 Mitogen-Activated Protein Kinase Signaling Pathway. *Frontiers in Microbiology*, *13*, 862580. https://doi.org/10.3389/fmicb.2022.862580

Ye, J., Wang, M., Xu, Y., Liu, J., Jiang, H., Wang, Z., et al. (2017). Sestrins increase in patients with coronary artery disease and associate with the severity of coronary stenosis. *Clinica Chimica Acta; International Journal of Clinical Chemistry*, *472*, 51–57. https://doi.org/10.1016/j.cca.2017.07.020

Yin, Y., Xu, Y., Su, L., Zhu, X., Chen, M., Zhu, W., et al. (2016). Epidemiologic investigation of a family cluster of imported ZIKV cases in Guangdong, China: probable human-to-human transmission. *Emerging Microbes & Infections*, *5*(1), 1–7. https://doi.org/10.1038/emi.2016.100

Yoshikawa, F. S. Y., Teixeira, F. M. E., Sato, M. N., & Oliveira, L. M. da S. (2019). Delivery of microRNAs by Extracellular Vesicles in Viral Infections: Could the News be Packaged? *Cells*, *8*(6), 611. https://doi.org/10.3390/cells8060611

Yuan, M., Tian, X., Ma, W., Zhang, R., Zou, X., Jin, Y., et al. (2024). miRNA-431-5p enriched in EVs derived from IFN-β stimulated MSCs potently inhibited ZIKV through CD95 downregulation. *Stem Cell Research & Therapy*, *15*(1), 435. https://doi.org/10.1186/s13287-024-04040-4

Zaborowski, M. P., Balaj, L., Breakefield, X. O., & Lai, C. P. (2015). Extracellular Vesicles: Composition, Biological Relevance, and Methods of Study. *BioScience*, *65*(8), 783–797. https://doi.org/10.1093/biosci/biv084

Zanluca, C., Melo, V. C. A. de, Mosimann, A. L. P., Santos, G. I. V. dos, Santos, C. N. D. dos, Luz, K., et al. (2015). First report of autochthonous transmission of Zika virus in Brazil. *Memórias do Instituto Oswaldo Cruz*, *110*(4), 569–572. https://doi.org/10.1590/0074-02760150192

Zeng, J., Dong, S., Luo, Z., Xie, X., Fu, B., Li, P., et al. (2020). The Zika Virus Capsid Disrupts Corticogenesis by Suppressing Dicer Activity and miRNA Biogenesis. *Cell Stem Cell*, *27*(4), 618-632.e9. https://doi.org/10.1016/j.stem.2020.07.012

Zé-Zé, L., Prata, M. B., Teixeira, T., Marques, N., Mondragão, A., Fernandes, R., et al. (2016). Zika virus infections imported from Brazil to Portugal, 2015. *IDCases*, *4*, 46–49. https://doi.org/10.1016/j.idcr.2016.03.004

Zhang, Q., Sun, K., Chinazzi, M., Pastore Y Piontti, A., Dean, N. E., Rojas, D. P., et al. (2017). Spread of Zika virus in the Americas. *Proceedings of the National Academy of Sciences of the United States of America*, *114*(22), E4334–E4343. https://doi.org/10.1073/pnas.1620161114

Zhang, X., Xie, X., Xia, H., Zou, J., Huang, L., Popov, V. L., et al. (2019). Zika Virus NS2A-Mediated Virion Assembly. *mBio*, *10*(5), e02375-19. https://doi.org/10.1128/mBio.02375-19

Zhang, Z., Rong, L., & Li, Y.-P. (2019). Flaviviridae Viruses and Oxidative Stress: Implications for Viral Pathogenesis. *Oxidative Medicine and Cellular Longevity*, *2019*(1), 1409582. https://doi.org/10.1155/2019/1409582

Zhu, X., He, Z., Hu, Y., Wen, W., Lin, C., Yu, J., et al. (2014). MicroRNA-30e* Suppresses Dengue Virus Replication by Promoting NF-κB–Dependent IFN Production. *PLoS Neglected Tropical Diseases*, *8*(8), e3088. https://doi.org/10.1371/journal.pntd.0003088

9. Statement on Own Contribution

This work was carried out at the Federal Institute for Drugs and Medical Devices (BfArM, Bonn) under the supervision of Prof. Dr. Julia Stingl. The overall framework and scientific objectives of the project were defined in consultation with Prof. Dr. Julia Stingl and Prof. Dr. Eberhard Hildt. The lt-NES® cells used in this study were generated and maintained by the research group of Prof. Dr. Oliver Brüstle at the Life & Brain Center (Bonn). Stocks of ZIKV Uganda and French Polynesia strains, as well as HaCaT cell infections and corresponding RNA extractions, were provided by the research group of Prof. Dr. Eberhard Hildt at the Paul-Ehrlich-Institut (Langen). The following experimental work was conducted by me: infections of lt-NES® cells, RNA extractions from lt-NES® and EV samples, miRNA sequencing and downstream analyses, microarray-based gene expression profiling, RT-qPCR, oxyblot assays, immunofluorescence microscopy, as well as the associated data processing and bioinformatic analyses. Statistical evaluation of the miRNA sequencing data using DESeq was performed by Dr. Michael Steffens at BfArM. The evaluation and interpretation of the results were carried out by me in consultation with Prof. Dr. Julia Stingl and Prof. Dr. Eberhard Hildt. In preparing this work, I used ChatGPT and DeepL to improve the readability and language of the manuscript. After using these tools, I reviewed the relevant passages and take full responsibility for the content of the published dissertation. I confirm that I have written this thesis independently and have not used any sources or aids other than those specified by me. I hereby confirm that my thesis complies with the Statement by the Executive Committee of the Deutsche Forschungsgemeinschaft (DFG, German Research Foundation) on the Influence of Generative Models of Text and Image Creation on Science and the Humanities and on the DFG’s Funding Activities.

10. Acknowledgements

First of all, I would like to sincerely thank Prof. Julia Stingl, my supervisor, for her guidance, trust, and continuous support throughout this work. Beyond research, I especially appreciated her thoughtful involvement and remain grateful for the opportunity she gave me to also speak about a topic of societal importance that I deeply care about.

I am very grateful to Prof. Eberhard Hildt, whose expert insights in virology and dedicated support of our projects at the Paul-Ehrlich-Institut enriched this research in many ways. His advice was always generous and truly helpful. Many thanks as well to Prof. Ulrich Jaehde, my second supervisor, for his steady support throughout this process. I would also like to thank Prof. Oliver Brüstle for his valuable contribution to this work and for agreeing to be part of my dissertation committee.

Special thanks go to Dr. Catharina Scholl for her guidance and advice during the laboratory and writing phases, and to Dr. Michael Steffens for carefully performing the statistical analyses.

I warmly thank my friends and colleagues from the BfArM research division, among them Sarah, Sabrina, and Tina, as well as many others, for the shared moments inside and outside of work. Thanks also go to my colleagues at the Paul-Ehrlich-Institut for providing such a welcoming and collegial working environment. I am especially grateful to Marie-Luise, Daniela, Fabian, Mirco, and Tobias for their kindness and support. To my current team, with Swapna and George, and all the wonderful colleagues I am working with and learning from, thank you for constantly motivating me to keep going.

I am truly grateful to Markus for the many ways he supported me, from reviewing presentations and staying up late to help, to providing steady support through critical stages of this journey.

To my dear friends Aysan and Shagha, thank you for your thoughtful care, and for always being there.

Finally, my deepest thanks go to my family. Parvin, Amir, and Omid, your guidance and encouragement have been with me throughout. I am especially grateful to my parents, whose efforts and sacrifices opened doors for me that I know are not to be taken for granted. And to Lukas, thank you for helping me grow, and for being by my side.